

THE HYDRAULIC ROUGHNESS OF AN IRRIGATION
CHANNEL WITH DECREASING SPATIALLY
VARIED FLOW

By

JOHN MARBROOKS SWEETEN, JR.

Bachelor of Science

Texas Technological College

Lubbock, Texas

1965

Submitted to the faculty of the Graduate College
of the Oklahoma State University
in partial fulfillment of the requirements
for the degree of
MASTER OF SCIENCE
May, 1967

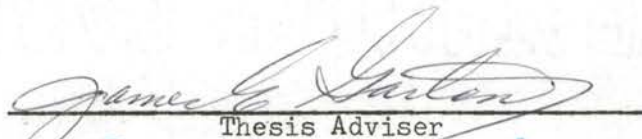
THIRD
1927
SOUTH
PAGE 2

OKLAHOMA
STATE UNIVERSITY
LIBRARY

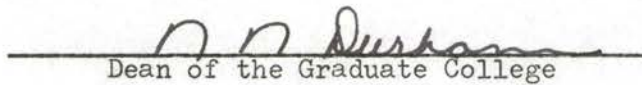
JAN 18 1968

THE HYDRAULIC ROUGHNESS OF AN IRRIGATION
CHANNEL WITH DECREASING SPATIALLY
VARIED FLOW

Thesis Approved:


Thesis Adviser




Dean of the Graduate College

660201

ACKNOWLEDGMENTS

The research reported in this thesis was financed in part by the United States Department of the Interior as authorized by the Water Resources Research Act of 1964, Public Law 88-379. The research project, entitled "Reduction of Water Application Losses Through Improved Distribution Channel Design," was funded as Project Number A-004-OKLAHOMA of the Oklahoma Water Resources Research Institute.

The author is grateful to the Department of Agricultural Engineering, headed by Professor E. W. Schroeder, and to the Oklahoma Agricultural Experiment Station for furnishing assistantships which made the work possible.

A deep expression of thankfulness is extended to the author's adviser Dr. James E. Garton for contributing ideas, competent guidance, and genuine enthusiasm during every phase of this research project.

The design and installation of the concrete channel and development of experimental techniques resulted primarily from the efforts of Dr. Albert L. Mink, whose research project preceded that of the author. Sincere appreciation is given to Dr. Mink for the use of data, computer programs, and helpful suggestions.

My thanks are extended to Mr. W. O. Ree, Engineer in Charge of the Outdoor Hydraulic Laboratory, Agricultural Research Service of the United States Department of Agriculture, for granting access to the experimental facilities. Certain other members of the Outdoor Hydraulic

Laboratory staff - Mr. W. R. Gwinn, Dr. Don K. McCool, Mr. George Hebaus, and Mr. John Pierce - are thanked for their cooperation. Draftsmen Jack Fryrear and Don McCrackin are acknowledged for their excellent work in preparing illustrative materials. Mr. Clyde Skoch and Mr. Norvil Cole of the Agricultural Engineering Research Laboratory were helpful in supplying necessary equipment.

The useful comments and suggestions supplied by fellow graduate students were appreciated. Special thanks are offered to Charles F. Cromwell, Jr. with whom the author satisfactorily shared certain instruments.

The assistance furnished by undergraduate Larry Hada throughout the study was valued and is hereby recognized.

Finally, sincere appreciation is extended to Mrs. Creasia Stone for her conscientious typing of the thesis.

TABLE OF CONTENTS

Chapter	Page
I. INTRODUCTION	1
The Problem	1
Objectives	3
II. REVIEW OF LITERATURE	5
Manning's Formula	6
Gradually Varied Flow	7
The Energy Equation	8
The Momentum Equation	9
Gradually Varied Flow in Concrete Channels	10
Spatially Varied Flow	15
Increasing Spatially Varied Flow	15
Decreasing Spatially Varied Flow	18
Siphon Tubes	24
III. THEORY	28
Gradually Varied Steady Flow	28
Decreasing Spatially Varied Steady Flow	29
Calculation of Adjusted \bar{n}	31
Calculation of n_e	32
Calculation of Flow Profiles	33
Relationship Between \bar{n} and n_e	36
IV. EQUIPMENT AND PROCEDURE	39
Experimental System	39
The Channel	39
Siphon Tubes	43
Accessory Equipment	45
Experimental Procedure	47
Channel Properties	48
Brass Plug Elevations	48
Gage Zeros	50
Testing Procedure	52
V. PRESENTATION AND ANALYSIS OF DATA	54
Gradually Varied Flow	54
Channel Roughness Without Siphon Tubes	54

Chapter	Page
Channel Roughness With Siphon Tubes	57
Spatially Varied Flow	57
Error Criteria For Selecting Experiments	57
Adjusted \bar{n}	60
Effective n	62
Presentation of Roughness Coefficients	63
Experimental Relation of \bar{n} and n	63
Comparison of Manning's n With \bar{n}^e and n_e	69
Multivariable Response Surfaces	71
Water-Surface Profiles in Decreasing Spatially	
Varied Flow	75
Flow Profiles Using Entering Velocity	75
Depth Required For Level Water Surface	83
Graphical Solution to Flow Profiles	85
Uniformity of Siphon Tube Discharge	90
Profiles Calculated With \bar{n}	90
The Effect of Roughness	90
Unrestrained Siphon Tubes	94
Gradually Varied Flow	94
Spatially Varied Flow	97
 VI. SUMMARY AND CONCLUSIONS	 100
Summary	100
Conclusions	101
Suggestions For Future Research	103
 BIBLIOGRAPHY	 104
 APPENDIX A	 107
 APPENDIX B	 111
 APPENDIX C	 114
 APPENDIX D	 117

LIST OF TABLES

Table	Page
I. Manning's n for Concrete-Lined Channels	11
II. Tube Diameters, Coefficients, and Exponents for Calculating Discharge From Plastic Siphon Tubes . . .	26
III. Constants for Equations of Channel Geometry	49
IV. Channel Roughness Without Siphon Tubes ($\alpha = 1.00$) . . .	56
V. Experimental Conditions and Manning's n for Gradually Varied Flow With Siphon Tubes ($\alpha = 1.00$) . .	58
VI. Roughness Coefficients From All Restrained Tube Spatially Varied Flow Experiments	66
VII. Change in Water-Surface Elevations and Roughness Coefficients for Various Siphon Tube Spacings, Diameters, Channel Discharges and Depths ($\delta \cong 0.30$)	67
VIII. Change in Water-Surface Elevations and Roughness Coefficients for Various Siphon Tube Spacings, Diameters, Channel Discharges and Depths ($\delta \cong 0.50$)	68
IX. Experimental Coefficients, Standard Deviations, and Correlation Coefficients of Multivariable Equations for Computing \bar{n} and n_e	73
X. Per Cent Variation in Tube Discharge, Based on the Upstream Siphon Tube, for Flow Profiles Calculated With \bar{n}	91
XI. Experimental and Calculated n Values From GVF Experiments Using Unrestrained Siphon Tubes	96
XII. Roughness Coefficients From SVF Experiments Using Unrestrained Siphon Tubes	98

LIST OF FIGURES

Figure	Page
1. General View of the Experimental Channel	40
2. Water Supply System Showing the Control Valves and Orifice Flanges	41
3. View of the Orifice Flanges, Manometer Pressure Taps, and Air Discharge Valves	42
4. The Check Dam With Cable and Winch Used for Accurate Depth Control	42
5. Gage Well, Point Gage, and Electrical Outlet at Station 2 + 40	44
6. Siphon Tube Outlets Placed at the Reference Elevation, With Wind Panels Installed in the Background	44
7. Interior View of Channel Showing Restrained Siphon Tubes	46
8. Rotation of Unrestrained Siphon Tubes Due to Channel Current	46
9. Comparison of n_{eI} With n_{eII}	64
10. Comparison of n_{eI} With n_{eIII}	65
11. Relationship Between \bar{n} and n_e ($\delta \cong 0.30$)	70
12. Multivariable Response Surface, Equation (26), Showing the Effects of Siphon Tube Spacing, Diameter, and Submergence on n_e	76
13. Observed and Calculated Flow Profiles for Experiments Using 1.5 and 2 Inch Siphon Tubes at 20 Inch Spacing . .	77
14. Observed and Calculated Flow Profiles for Experiments Using 1.5 Inch Siphon Tubes at 20 and 40 Inch Spacings	78
15. Observed and Calculated Flow Profiles for Experiments Using 1.5 and 2 Inch Siphon Tubes at 60 Inch Spacing, and 2 Inch Tubes at 80 Inch Spacing	79

Figure	Page
16. Observed and Calculated Flow Profiles for Experiments Using 3 Inch Siphon Tubes at 40 Inch Spacing	80
17. Comparison of Observed Water-Surface Elevations to Velocity Head Recoveries , Friction Losses, and Resultant Flow Profiles	82
18. Depth for Level Water Surface as a Function of Roughness and Length of Horizontal Irrigation Bay	84
19. Nomograph for Finding Velocity Head Recovery	86
20. Nomograph for Finding Friction Head Loss	87
21. Depth Versus $A R^{\frac{4}{3}}$ for a Trapezoidal Channel With 1 Foot Bottom and 1:1 Side Slopes	87
22. Flow Profiles Calculated From Equation (20) for 0, ± 10 , and ± 25 Per Cent Variation in Roughness	93

CHAPTER I

INTRODUCTION

The Problem

Siphon tube irrigation from concrete-lined channels is an established method of surface irrigation. Concrete irrigation channels offer several advantages as compared to earthen ditches; among these are (10)* :

1. less water waste due to seepage
2. larger discharge capacity for the same cross-sectional area
3. minimum weed growth and silt deposition.

Properly designed concrete channels can provide for the uniform discharge of regulated amounts of irrigation water into furrows.

When furrows being irrigated simultaneously receive water at different rates, the waste of water is inevitable. The furrows with the highest flow rates receive excessive amounts of water resulting in runoff losses before the lesser furrow streams have advanced to the downstream field boundary. Much of the water applied percolates beyond the root zone. Deep percolation losses can occur at any point along the furrow but they are most likely to occur near the head ditch or at the downstream end of the furrow. Resulting from these losses, the water

* Number in parentheses refers to the "Selected Bibliography."

application efficiency of the average farm is well below the efficiencies attained with the same surface irrigation method by the superior farmers and researchers (12). Design and management of irrigation systems aimed at acquiring the maximum uniformity of water application will result in higher efficiencies.

The uniform discharge of water through siphon tubes of the same diameter requires that the tubes have the same head, i.e. the same potential energy causing flow. The position and profile of the water surface in the channel directly affect the head on each siphon tube. The water-surface elevation at any cross-section is related to the entering flow and the channel roughness.

The discharge of water from an irrigation distribution bay is a form of spatially varied flow with decreasing discharge (hereinafter called decreasing spatially varied flow). The energy losses in channels with decreasing spatially varied flow comprise an ill-defined area of hydraulic and irrigation knowledge. Roughness coefficients from gradually varied flow are usually applied to calculations involving decreasing spatially varied flow.

Mink (16) conducted an extensive series of experiments to evaluate the roughness of a concrete channel with siphon tubes. Both gradually varied flow and decreasing spatially varied flow conditions were studied. The conclusion was reached that the roughness coefficients obtained in gradually varied flow were not adequate to predict the flow profiles observed in decreasing spatially varied flow. For all these experiments a siphon tube spacing of 40 inches was utilized.

Based on the work of Mink (16), hydraulic experiments were designed to determine the effect of siphon tube spacing on the hydraulic

roughness of a concrete irrigation channel. These experiments involved tube spacings of 20, 60, and 80 inches, and the data of Mink (40 inch spacing) was incorporated where appropriate. The chosen spacings covered the range expected to be encountered in siphon tube irrigation. The tube diameters represented the range of siphon tube sizes commonly used.

The experiments were confined in scope to steady flow in an essentially horizontal channel. For the spatially varied flow experiments, all the entering flow was discharged through the siphon tubes, whose outlets were placed at the same elevation.

The law of conservation of energy was applied to both gradually varied flow and decreasing spatially varied flow phenomena. The Manning formula was the basis for expressing channel roughness.

Objectives

The objectives of the research project reported in this thesis were:

1. To determine the influence of siphon tube spacing on the hydraulic roughness of a horizontal concrete-lined irrigation channel.
2. To determine if the roughness coefficients obtained from non-uniform steady flow experiments could be used to accurately predict spatially varied flow profiles.
3. To determine, if necessary, new roughness coefficients to satisfy the spatially varied flow conditions.
4. To develop procedures to predict the rise or fall of flow profiles under conditions of decreasing spatially varied flow in

a horizontal channel.

5. To conduct a limited number of experiments to determine if restrained siphon tubes (where the tubes were secured to the channel wall) and unrestrained siphon tubes produce roughness coefficients of similar magnitudes.

CHAPTER II

REVIEW OF LITERATURE

This chapter contains basic hydraulic theory pertinent to open-channel flow, such as that encountered in surface irrigation systems. The material deals primarily with boundary roughness and water-surface features. A discussion of the Manning formula precedes an analysis of gradually varied flow and spatially varied flow. Both increasing and decreasing spatially varied flow are considered. Recent research concerning the discharge capacity of siphon tubes is presented.

The objective of surface irrigation is (8):

To distribute water over the land in such a way that it will enter the soil and be stored uniformly within the potential root zone.

The uniformity of water application is partly influenced by the hydraulic characteristics of the distribution channel. The boundary roughness of a channel, because it affects the water-surface position, is an important hydraulic characteristic. According to some irrigation engineers (21), the following questions pertaining to hydraulic roughness need answering:

1. What is hydraulic roughness?
2. How can it be defined?
3. What are the factors which affect roughness?
4. How can roughness be measured?

5. How can it be expressed?

Hansen (8) declared that the major need in irrigation is the evaluation of a roughness coefficient which best describes the open-channel flow encountered.

Manning's Formula

The ASCE Task Force on Friction Factors in Open Channels (2)

stated:

... Manning's formula (or Strickler's as it is called in Europe) is used around the world and is quite satisfactory for most purposes. Chow's book (27) appears to be the best published source of information on the value of n .

Also, Chow (3) reported:

... Despite many new proposals for a formula having a theoretical background, the Manning formula still holds its indisputable top position in the field of practical applications.

Flamant in 1891 proposed the formula,

$$V = \frac{R^{2/3} S^{1/2}}{n}$$

which he called the Manning formula (2). Buckley in 1911 deduced the coefficient 1.486 for the English system of units (2) making:

$$V = \frac{1.486}{n} R^{2/3} S^{1/2} \quad (1)$$

Some hydraulicians write the Manning equation using a variable exponent for R , the hydraulic radius (3). Pavlovsky wrote in 1925 (3),

$$C = \frac{R^y}{n}$$

where R is measured in meters, C is Chezy's resistance factor, and

$$y = 2.5 \sqrt{n} - 0.13 - 0.75 \sqrt{R} (\sqrt{n} - 0.10)$$

This cumbersome equation may be approximated by (2, 3):

$$y = 1.5 \sqrt{n} \quad \text{for } R < 1 \text{ meter}$$

$$y = 1.3 \sqrt{n} \quad \text{for } R > 1 \text{ meter}$$

The Manning equation with constant n is applicable to the fully rough zone of turbulent flow (2). The Reynolds number R_n is the usual criterion for identifying the fully rough regime. For sufficiently high Reynolds numbers, Manning's n (and Chezy's C) is nearly constant, varying with roughness alone (2, 25). The fully rough regime encompasses this region of constant n .

Vennard (25) presented a plot of absolute roughness height K versus n for hydraulic radii of 1.0 to 10.0 feet. This graph showed that $n = 0.0225$ is independent of hydraulic radius and is thus a true measurement of roughness. At both higher and lower n values, n varies increasingly with R at constant values of K . However, Vennard's diagram revealed that for $R < 1.00$, n would not be appreciably affected by R .

Gradually Varied Flow

Gradually varied flow is amenable to solution by two approaches: the law of energy conservation and the law of momentum conservation. According to Chow (3), the energy and momentum concepts produce practically identical results for gradually varied flow. On page 51, Chow states (3):

... The inherent distinction between the two principles lies in the fact that energy is a scalar quantity whereas momentum is a vector quantity; also, the energy equation contains a term for internal losses, whereas the momentum equation contains a term for external resistance.

The Energy Equation

The Bernoulli energy equation can be written for gradually varied flow in open channels as (3):

$$z_1 + d_1 \cos \theta + \alpha_1 \frac{V_1^2}{2g} = z_2 + d_2 \cos \theta + \alpha_2 \frac{V_2^2}{2g} + h_f \quad (2)$$

For channel cross-sections 1 and 2, z is the bottom elevation, d is the depth perpendicular to the bottom, θ is the bottom angle of inclination, and the mean velocity is V . Also, the Coriolis velocity distribution coefficient (also called the energy coefficient) is α , h_f denotes the internal energy dissipation in the reach, and g is the acceleration of gravity.

The differential energy equation of gradually varied flow can be derived from the total energy concept, where H signifies the total energy. For a channel of large slope (3),

$$H = z + d \cos \theta + \alpha \frac{V^2}{2g} \quad (3)$$

If α and θ are constants,

$$\frac{dH}{dx} = \frac{dz}{dx} + \cos \theta \frac{dd}{dx} + \alpha \frac{d}{dx} \left(\frac{V^2}{2g} \right)$$

from which

$$\frac{dH}{dx} = \frac{dz}{dx} + \frac{dd}{dx} \left[\cos \theta + \alpha \frac{d}{dd} \left(\frac{V^2}{2g} \right) \right]$$

The friction loss dH is always negative (3) so that the friction slope

$S_f = -\frac{dH}{dx}$. The bottom slope, negative for a descending bottom, can be expressed as $S_o = -\frac{dz}{dx}$. Therefore,

$$\frac{dd}{dx} = \frac{S_o - S_f}{\cos \theta + \alpha \frac{d}{dd} \left(\frac{V^2}{2g} \right)} \quad (4)$$

Equation (4) is the general differential equation of gradually varied flow (3).

The Momentum Equation

The momentum principle is based on Newton's Second Law of Motion (3). In a given unit of time, the momentum change of a flowing body of fluid equals the sum of the external forces acting on that flow segment. For open-channel flow, these forces are pressure, gravity, and boundary shear.

The derivation of a Bernoulli-type momentum equation for gradually varied flow is found in various sources (3, 15, 16). The basic force equation is:

$$\Sigma F_x = \frac{dM}{dt} = F_{px} + F_{gx} - F_{sx} \quad (5)$$

where the subscript x refers to the direction parallel to the channel bottom in the direction of flow. The resultant pressure force on a body of fluid enclosed between two sections is F_p . The gravitational force on the enclosed fluid is F_g , while F_s is the total external force of friction. Chow (3) assumed the pressure was hydrostatically distributed, and that the bottom slope was small. In addition, he assumed the discharge through the section equals the product of the mean velocity and average area in the section. Mink (16) assumed the difference between the momentum coefficients, β_1 and β_2 representing stations 1 and 2 respectively, is small. The Bernoulli-type momentum equation

derived from Equation (5) is (3, 15, 16):

$$z_1 + y_1 + \beta_1 \frac{V_1^2}{2g} = z_2 + y_2 + \beta_2 \frac{V_2^2}{2g} + h_f' \quad (6)$$

where $y = d \cos \theta$ for small slopes. Mink (16) and McCool (15) showed that,

$$h_f' = \frac{F_{sx}}{\gamma A_{avg}}$$

where γ is the specific weight of water. According to Chow (3), h_f' is a measure of the external head losses due to the friction force.

Gradually Varied Flow in Concrete Channels

Most fluid mechanics texts include tables of Manning's n for various channel materials. Table I contains values of Manning's n recommended for uniform and gradually varied flow in concrete-lined channels. The design values of n contained in the table range from 0.011 to 0.020.

Recent experiments reported by Tilp (24) concerned the measured roughnesses of 9 large concrete-lined canals. The trapezoidal cross-sections of the channels involved had side slopes of 1.5:1 and 1.25:1. The smallest canal had a base width of 8 feet and the design flow depth was 7.1 feet. The largest canal measured 50 and 20.7 feet in bottom width and flow depth respectively. Manning's n values between 0.0137 and 0.0152 were assumed in designing the canals. The results of 52 tests conducted in straight canal reaches revealed that resistance was higher than expected for the five largest canals, n ranging from 0.015 and 0.019. However, Tilp reported that for the four smallest canals,

TABLE I

MANNING'S N FOR CONCRETE-LINED CHANNELS

Author	Description of Surface	Value(s) of n			
		Best	Good	Fair	Bad
King and Brater (13)	Concrete-lined channels.	0.012	0.014	0.016	0.018
Chow (3)	Concrete with trowel finish.	0.011	0.013	0.015	
	Concrete with float finish.	0.013	0.015	0.016	
	Finished concrete with gravel on bottom.	0.015	0.017	0.020	
	Unfinished concrete.	0.014	0.017	0.020	
Rouse (20)	Finished concrete.	0.011	—	0.013	
	Unfinished concrete.	0.013	—	0.016	
Woodward & Posey (26)	Smooth clean concrete surface, without projections, and with straight alignment.	0.011	—	0.012	
	Smooth concrete surfaces without projections, free from algae or insect growth; straight alignment.		0.013		

TABLE I (Continued)

Author	Description of Surface	Value(s) of n
Woodward & Posey (26)	Good concrete surfaces with very small projections, with some curvature, slight algae or insect growth, or with slight gravel deposits.	0.014
	Concrete with smooth sides but roughly troweled bottom, same with smoother surface but excessive curvature.	0.015
	Concrete with heavy algae or moss growth.	0.016
Streeter (23)	Finished concrete.	0.012
	Unfinished concrete.	0.014

$$0.013 < n \text{ (calculated)} < 0.016$$

as compared to,

$$0.0141 < n \text{ (design)} < 0.0145$$

Tilp attributed the high n values in the larger canals partly to the abundance of aquatic life found in them. This aquatic growth produced a seasonal variation in n values, with the peak roughness condition occurring in August. Tilp concluded that n decreased slightly with channel size.

Mink (16) conducted an extensive set of gradually varied steady flow experiments in a concrete-lined irrigation channel. His experiments dealt with two kinds of roughness conditions: the native channel roughness and roughness with siphon tubes installed.

Mink (16) reported the results of 13 gradually varied flow experiments without siphon tubes. Manning's n was calculated from each experiment. The flow rates ranged from 0.998 to 4.454 cubic feet per second (cfs). The minimum and maximum depths were 0.628 and 1.756 feet respectively. The corresponding range of Reynolds number was

$$27,550 < R_n < 97,940$$

Manning's n for $\alpha = 1.0$ varied from 0.0104 to 0.0119, with a mean value of 0.0112. The best-fit equation that Mink calculated to predict

Manning's n was:

$$n = \frac{R_n^{1/6}}{218,500 + 86.59 R_n}$$

For gradually varied flow with siphon tubes, Mink (16) presented the results of 69 experiments. Three tube sizes 1, 1.5, and 2 inch diameters were installed with the inlet ends placed 0, 6, and 12 inches

vertically above the channel bottom. The flow rates used were 1, 3, and 4.5 cfs with three depths established for each flow. For all experiments, the siphon tube spacing was 40 inches. The prediction equation Mink found was:

$$n = (0.00487 - 0.00417 TL) TS + \frac{R_n}{204,300 + 85.61 R_n}$$

where TL = vertical distance of the siphon tubes above the channel bottom, feet

TS = nominal tube diameter, inches

The following restrictions were placed on the equation:

$$0 < TS < 3.0$$

$$TL < y \text{ (= depth of flow)}$$

$$R_n > 1.0 \times 10^4$$

Mink asserted that the effect of R is probably distributed among the various coefficients.

Mink also obtained an equation for n based on the Buckingham Pi Theorem (17). The general expression was (16):

$$\frac{n}{R^{1/6}} = f \left(\frac{Q}{gR^5}, \frac{Su}{R}, \frac{TS}{R}, \frac{VR}{v} \right)$$

in which the tube submergence $S_u = y - TL$. The prediction equation for n from gradually varied flow using siphon tubes was

$$n = 0.00510 + R^{1/6} \left[(0.00319 + 0.00821 \frac{TS}{R}) \frac{Su}{R} + \frac{0.44175 R_n}{218,500 + 85.61 R_n} \right]$$

Thus, when S_u is zero, n is a function of R and R_n ; S_u cannot be

negative.

Spatially Varied Flow

The two types of spatially varied flow are:

1. Increasing in which inflow occurs along the channel.
2. Decreasing in which outflow occurs along the channel.

Most hydraulicians apply the momentum principle to problems involving increasing spatially varied flow. The energy principle is better suited to decreasing spatially varied flow (3).

Increasing Spatially Varied Flow

King and Brater (13) developed from the momentum concept the general equation for unsteady spatially varied flow. By Newton's Second Law, the sum of all external forces in the flow direction x equals the time rate of change of momentum. King and Brater considered the forces of pressure F_p , gravity F_g , wall shear F_s , and the shear caused by moving air F_a . Therefore,

$$\sum F_x = \frac{dM}{dt} = F_p + F_g + F_s + F_a$$

In developing the right side of this equation, King and Brater assumed that the channel walls neither converged or diverged and that the channel slope was mild. In addition they assumed parallel flow in an increment of length, and they neglected the friction of air on the water surface. King and Brater computed the gravitational force using the bottom slope. The boundary shearing force they expressed using the energy slope. In developing the term $\frac{dM}{dt}$, the writers eliminated higher

order differentials and failed to consider a velocity distribution coefficient. King and Brater called their resulting equation the dynamic equation for unsteady spatially varied flow. This equation is:

$$-\frac{\partial y}{\partial x} + S_o - S_f = \frac{1}{g} \frac{\partial V}{\partial t} + \frac{V}{g} \frac{\partial V}{\partial x} + \frac{V}{gA} \frac{\partial Q}{\partial x}$$

where Q and V are discharge and mean velocity respectively for the horizontal length dx . The average area of the increment is A , y is the vertical flow depth, and t is time. For steady flow, $\frac{\partial V}{\partial t} = 0$ so that,

$$\frac{\partial y}{\partial x} = S_o - S_f - \frac{V}{g} \frac{\partial V}{\partial x} - \frac{V}{gA} \frac{\partial Q}{\partial x}$$

Li (14) investigated increasing spatially varied flow in a side channel spillway. Li discarded the energy equation for such problems since the energy loss due to impact of the entering water cannot be evaluated. He used instead the momentum equation and assumed that the flow was unidirectional, although he conceded the presence of strong lateral currents. Li assumed uniform velocity distribution and neglected the unevenness of the water surface in the spillway. Hydrostatic pressure distribution was supposed even though appreciable curvature was expected at the downstream end of the channel. Li used the wall shearing forces from gradually varied flow. Finally, he stated that when friction loss is minor, its effect can be equated to the momentum of the incoming water, causing the two terms to cancel.

In 1962, Farney and Markus (5, 6) reported on an L-crested side channel spillway designed to discharge 200,000 cfs. In applying the momentum principle, they considered Q , V , and β as variable with position down the channel. They neglected friction loss, the velocity component parallel to the channel axis, and the bottom slope. Their

general equation for the water-surface profile in the spillway channel was:

$$\frac{dy}{dx} = \frac{1}{g} \left(\frac{\beta V^2}{Q} \frac{dQ}{dx} + \beta V \frac{dV}{dx} + V^2 \frac{d\beta}{dx} \right)$$

Farney and Markus reported that β had significance where inflow occurred over the end section, for an L-crested spillway. For the special case where $\beta = 1.00$, their equation reduced to that of Julian Hinds (9) in 1926.

According to Argyropoulos (1), Henry Favre in 1933 presented a more complete equation than did Farney and Markus (5). Favre included a velocity component parallel to the channel axis and a friction term. Argyropoulos stated Favre's equation in finite difference form;

$$-\Delta y = \frac{\alpha Q_1 (V_1 + V_2)}{g (Q_1 + Q_2)} \left[\Delta V + V_2 \frac{\Delta Q}{Q_1} \right] + (S_f - S_o) \Delta x$$

In this equation, ΔQ and ΔV are, respectively, the added flow rate and the velocity change in the reach Δx . The terms V_1, Q_1 and V_2, Q_2 are the velocities and discharges at the upstream and downstream ends of the reach Δx .

McCool (15) experimented with flow over a 400 foot sharp-crested weir into a grassed channel. McCool made the following assumptions concerning the prediction of surface profiles:

1. The slope of the channel bottom was small.
2. Essentially streamline flow was present.
3. Essentially hydrostatic pressure distribution existed.

4. Approximately unidirectional flow prevailed.
5. The depth and area between two sections is distributed linearly.

For a reach of length Δx , McCool's equation for profile prediction was:

$$\Delta y = - \frac{Q_1 (V_1 + V_2)}{g (Q_1 + Q_2)} \left(\beta_2 \frac{V_2}{V_1} - \beta_1 \frac{V_1}{V_2} + \beta_2 \frac{V_2}{V_1} \frac{\Delta Q}{Q_1} \right) + (S_o - S_f) \Delta x$$

This equation differs from that of Favre (cited in 1) only in the nature of the velocity distribution coefficients that each writer chose. Also, McCool's equation is practically the same as that derived by Chow (3) except that Chow assumed uniform velocity distribution. The results of McCool indicated that the above equation accurately predicts water-surface profiles, provided that appropriate values of β and n (included in S_f) can be found.

McCool (15) computed Manning's n as an empirical function of the product of velocity and hydraulic radius (VR). The coefficient and exponent of VR were calculated from vegetation length and position along the channel axis. McCool concluded that resistance coefficients from gradually varied steady flow will predict with reasonable accuracy the water-surface profiles for increasing spatially varied steady flow.

Decreasing Spatially Varied Steady Flow

Some of the hydraulics problems which deal with decreasing spatially varied flow are side weirs, sprinkler irrigation systems, and open-channel irrigation systems. Of the latter, outflow may be accomplished by wall notches (resembling side weirs), outlet tubes (some-

times called spiles), or siphon tubes.

In 1957, Collinge (4) discussed the previous notable contributions on the discharge capacity of side weirs. Most of the early work was empirical and limited in scope. H. Engels in 1917 reported results obtained from a side weir installed in a large variable-width flume (4). A low range of velocities -1.75 to 1.90 fps- was used. Engels consistently observed that the water-surface profiles dipped to a minimum depth at the upstream end of the weir and climbed asymptotically to some depth downstream from the weir crest. Similar profiles were observed by Tyler, Carollo, and Steyskal in 1929 (4).

According to Collinge (4), G. S. Coleman and Dempster Smith published in 1923 the results of capacity tests in a side weir model. Their flume was only 6 inches deep and $4\text{-}\frac{3}{4}$ inches wide. In all instances, Coleman and Smith observed a decreasing depth along the weir crest, with an increasing depth downstream from the weir.

In 1928, a theoretical approach to side weir discharge was published by Nimmo (18). Nimmo's theory was used to design a side weir which spilled excess water from a stream-diversion system. Nimmo applied the momentum principle to the problem. He assumed a sloping trapezoidal channel of decreasing cross-section. The sum of the external forces, he reasoned, equals the change of momentum in the reach minus the momentum lost in the overflowing water. Nimmo considered the external forces of gravity, boundary shear, static pressures on the end areas, and the reaction from the projected side wall areas. For predicting water-surface slope, Nimmo developed a cumbersome equation. But, for a channel with unvarying side slopes, constant bottom width, and flow top width T , the equation reduces to:

$$\frac{dy}{dx} = \frac{S_f - S_o - \frac{Q}{gA} \frac{dQ}{dx}}{1 - \frac{Q^2 T}{gA^3}}$$

Nimmo reported the results of an experiment involving 360 cfs of inflow, of which 235 cfs was discharged over the spillway. Both the observed discharge and flow profile agreed closely with the calculated values. The water surface rose approximately 1.5 feet in a 110 foot section.

According to Collinge (4) De Marchi in 1934 made a significant contribution to the theory of side weir discharge. De Marchi explained the puzzling discrepancy between the general profile forms which previous experimenters had observed. Rising profiles, such as Engels had discovered resulted from subcritical (tranquil) flow. Declining flow profiles such as Coleman and Smith had ascertained were produced by supercritical (shooting) flow. De Marchi's deductions were based on the assumption of constant total energy along the weir (4).

Collinge (4) presented De Marchi's theory for flow profile prediction which was based on the concept of specific energy. De Marchi assumed steady flow, an infinitely long channel of constant cross-section, and a weir sill parallel to the channel bottom. In addition, he postulated the existence of uniform flow at some distance both upstream and downstream from the weir. Also, the total energy was considered constant. De Marchi differentiated the specific energy with respect to distance along the weir. Collinge concluded that the De Marchi equation is precisely the same as that of Nimmo (18) when these simplifications are applied to the latter: rectangular cross-section, constant channel

width, horizontal bottom, and negligible friction losses.

Collinge (4) proffered his results of side weir experiments conducted in a flume 13 feet in length and 5 inches in depth. The bottom width was variable up to 12 inches, and the crest length was variable as well. For Froude numbers less than 0.95, Collinge's observed water-surface profiles compared favorably with the profiles computed using the De Marchi theory. Collinge found that, owing to the presence of friction loss neglected by De Marchi, the actual upstream water surface exceeded the calculated value in subcritical flow computations. A convergence of the theoretical and observed profiles was noted at the downstream end of the weir. Collinge concluded that for channels of non-rectangular cross-section, of varying cross-section, or with excessive energy losses, the Nimmo method (18) with its generality is best adapted for computing flow profiles for side weir discharge.

Another form of decreasing spatially varied flow is siphon tube irrigation from open channels. Chow (3) used the energy equation for decreasing spatially varied flow in open channels, and Garton and Mink (7, 16) applied the energy concept to siphon tube irrigation. A Bernoulli-type energy equation is:

$$z_1 + d_1 \cos \theta + \alpha_1 \frac{V_1^2}{2g} = z_2 + d_2 \cos \theta + \alpha_2 \frac{V_2^2}{2g} + h_f \quad (2)$$

If $\theta \approx 0$ so that $d \cos \theta \approx y$,

$$S_o = \frac{z_1 - z_2}{L} \quad \text{and} \quad S_f = \frac{h_f}{L}$$

and Equation (2) can be reduced to:

$$\alpha_1 \frac{V_1^2}{2g} - \alpha_2 \frac{V_2^2}{2g} + y_1 - y_2 - L(S_f - S_o) = 0 \quad (7)$$

Using a digital computer, Mink (16) solved Equation (7) between successive siphon tubes, spaced L distance apart, by incrementing y_2 until the equation was satisfied. The energy slope S_f was calculated by the Manning formula, Equation (1), rewritten as:

$$S_f = \frac{V^2 n^2}{2.208 R^{4/3}} \quad (8)$$

When the entire inflow was discharged through the siphon tubes, initial conditions were established at the downstream end of the irrigation bay where $x = 0$, and $V = 0$. Also y_1 was measured by a point gage to ± 0.001 foot. At any point, the accumulated Q (based on head discharge relationships for siphon tubes) and the assumed area were used to compute V for that section.

Mink (16) calculated an adjusted value of Manning's n which he called \bar{n} . This roughness coefficient was obtained by incrementing n in Equation (8) and solving Equation (7) until the calculated profile and the observed profile from regression agreed to within ± 0.0001 foot at the upstream end of the primed bay. Mink concluded that \bar{n} is the roughness coefficient which will best predict the water-surface profiles for spatially varied flow. The \bar{n} values were much higher than n calculated from gradually varied flow.

Mink (16) also calculated an effective n which he called n_e . This variable was computed from the Manning equation using the flow velocity and hydraulic radius of a section just upstream from the primed reach of siphon tubes. The energy slope involved was calculated by,

$$S_f = \frac{1}{L} \left[\left(\frac{V_i^2}{2g} - \frac{V_o^2}{2g} \right) + y_i - y_o \right]$$

where

L = length of the irrigation bay

V_i = entering velocity

V_o = outflow velocity (zero)

y_i = upstream depth

y_o = downstream depth

Hence, a horizontal channel with $\alpha = 1.00$ was assumed, and intermediate profile points were not considered. Mink found the relationship between n_e and \bar{n} to be (16):

$$n_e = 0.0019 + 0.4830 \bar{n}$$

Using a digital computer, Mink (16) calculated decreasing spatially varied flow profiles in a sloping channel. He assumed bottom slopes of 0.00 per cent to 0.25 per cent. Values of \bar{n} corresponding to the channel discharges and siphon tubes used in the actual level channel tests were assumed. Two siphon tube outlet conditions were studied. In the first case, all the tubes were assumed to have the same outlet elevation. Mink obtained a maximum variation in tube discharge of 5 per cent which was considered acceptable irrigation uniformity. For the second tube outlet condition, all outlets were assumed to lie a fixed distance above the channel bottom. Gross variation in tube discharge, up to 100 per cent, resulted from this outlet condition. For both conditions of siphon tube placement, the maximum discharge variation occurred at the highest slope and the smallest Q . Mink showed that, for sloping channels, the upstream water-surface was higher than the downstream surface. This difference was larger where a fixed outlet elevation was assumed to exist.

Mink reached several conclusions (16) concerning decreasing spatially varied flow in an irrigation channel. Two of these were:

1. The n values from gradually varied flow failed to adequately predict the water-surface profiles found in spatially varied flow.
2. The correct value of \bar{n} used in the Bernoulli-type energy equation will satisfactorily predict surface profiles for siphon tube irrigation.

Siphon Tubes

Siphon tubes provide a simple means of transferring water from an irrigation ditch into a furrow. The misuse of siphon tubes can render a well-designed irrigation system inefficient and wasteful.

Israelsen and Hansen (10) stated that the orifice discharge equation applies to siphon tubes. Thus,

$$Q_t = C_d A \sqrt{2gH}$$

where

Q_t = siphon tube discharge

A = cross-sectional area

H = effective head

C_d = coefficient of discharge

The discharge coefficient C_d depends upon siphon tube length as well as entrance and exit conditions. For submerged outlets, the effective head is measured vertically from the channel water surface to the furrow water surface. For free outlet conditions, the head is the vertical distance between the channel water surface and the elevation where the hydraulic grade line pierces the plane of the outlet end of the tubes (usually assumed to be the center line).

Keflemariam (11) conducted flow rate experiments with plastic

siphon tubes of six diameters, ranging from 0.75 to 3.00 inches. The double-bend siphons were 5 feet in length. Five tubes of each size were randomly selected for experimentation, and the cross-section for each tube was accurately measured. By establishing three widely separated heads for each tube, Keflemariam calculated the following prediction equation for tube flow:

$$Q_t = K D_i^{2.14} H^{0.571}$$

in which

Q_t = tube discharge, cfs

K = coefficient of discharge

D_i = actual inside tube diameter, feet

H = head on the siphon tube (free water surface to center-line of the outlet invert), feet

The values of K for each tube size are given in Table II. Keflemariam reported that irregular tube shapes had negligible effect on the measured discharge.

Mink (16) performed a regression analysis on Keflemariam's data (11). He defined head as the distance from the water surface in the channel to the lower siphon tube mount, which had a fixed elevation. The following equation was found:

$$Q_t = 0.0245 D^{2.111} H_m^{0.6121}$$

where

D = nominal tube diameter, inches

H_m = adjusted head, feet

Mink obtained a second discharge formula which was also based on Keflemariam's data (11). The general equation was:

TABLE II
 TUBE DIAMETERS, COEFFICIENTS, AND EXPONENTS
 FOR CALCULATING DISCHARGE FROM PLASTIC
 SIPHON TUBES

Nominal Tube Diameter Inches	Average Inside Diameter Inches	Coefficient * K	Coefficient ** C	Exponent ** N
0.75	0.747	4.95	0.01292	0.60697
1.00	1.028	4.43	0.02511	0.58794
1.25	1.245	5.32	0.03986	0.60844
1.50	1.478	5.43	0.05806	0.62449
2.00	1.972	5.30	0.10639	0.65513
3.00	2.898	5.06	0.24450	0.85109

* After Keflemariam (11)

** After Mink (16)

$$Q_t = C H_m^N \quad (9)$$

Values of C and N are given in Table II. Mink used Equation (9) to predict siphon tube discharge for his spatially varied flow experiments.

CHAPTER III

THEORY

The accurate computation of water-surface profiles for uniform, gradually varied, or spatially varied flows requires a knowledge of the correct magnitude of the roughness coefficient. Conversely, the roughness coefficient which describes a boundary roughness condition can be calculated from observations of the free water surface, velocity, and hydraulic radius. The relationship between water-surface profiles and Manning's n is provided through the energy equation and Manning's formula.

Gradually Varied Steady Flow

For gradually varied flow in a channel of constant cross-section and small bottom slope, the Bernoulli-type energy equation, Equation (2), can be written:

$$\alpha_1 \frac{V_1^2}{2g} + y_1 + z_1 = \alpha_2 \frac{V_2^2}{2g} + y_2 + z_2 + h_f$$

If the alphas are assumed to be unity, the energy loss term will absorb the effects of non-uniform velocity distribution. Therefore,

$$\frac{V_1^2}{2g} + y_1 + z_1 = \frac{V_2^2}{2g} + y_2 + z_2 + h_f \quad (10)$$

and,

$$h_f = S_f L = (y_1 + z_1) - (y_2 + z_2) + \left(\frac{V_1^2}{2g} - \frac{V_2^2}{2g} \right)$$

Hence,

$$S_f = \frac{1}{L} \left[WS_1 - WS_2 + \frac{Q^2}{2g} \left(\frac{1}{A_1^2} - \frac{1}{A_2^2} \right) \right] \quad (11)$$

where Q is the constant discharge and S_f is the slope of the energy line. The distance between upstream and downstream cross-sections, denoted by subscripts 1 and 2, is L . Also, A_1 , A_2 and WS_1 , WS_2 are the areas and water-surface elevations, respectively. Manning's formula, Equation (1), can be written

$$n = \frac{1.486 A R^{2/3} S_f^{1/2}}{Q} \quad (12)$$

where A and R indicate the average area and hydraulic radius. Substituting S_f from Equation (11) into Manning's equation gives a calculated n for gradually varied flow.

Decreasing Spatially Varied Steady Flow

The differential equation of decreasing spatially varied flow can be developed from the total energy concept (3). The total energy at any cross-section in a mildly sloping channel is:

$$H = z + y + \alpha \frac{V^2}{2g} = z + y + \alpha \frac{Q^2}{2gA^2}$$

Differentiating this equation with respect to x assuming α is constant gives:

$$\frac{dH}{dx} = \frac{dz}{dx} + \frac{dy}{dx} + \frac{\alpha}{2g} \left(\frac{2Q}{A} \frac{dQ}{dx} - \frac{2Q^2}{A^3} \frac{dA}{dx} \right)$$

The slope of the energy line and the slope of the channel bottom may be defined, respectively, as:

$$\frac{dH}{dx} = -S_f \quad \text{and} \quad \frac{dz}{dx} = -S_o$$

An expansion of the area derivative by the chain rule reveals that:

$$\frac{dA}{dx} = \frac{dA}{dy} \frac{dy}{dx} = T \frac{dy}{dx}$$

where T is the top width of the flow cross-section. Also, assuming constant outflow per unit length,

$$\frac{dQ}{dx} = q$$

Substituting the above expressions into the differentiated total energy equation produces:

$$-S_f = -S_o + \frac{dy}{dx} + \frac{\alpha}{2g} \left(\frac{2Qq}{A} - \frac{2Q^2 T}{A^3} \frac{dy}{dx} \right)$$

Rearranging yields:

$$\frac{dy}{dx} = \frac{S_o - S_f - \frac{\alpha Qq}{2gA}}{1 - \frac{\alpha Q^2 T}{gA^3}} \quad (13)$$

Equation (13) is the differential equation for decreasing spatially varied flow (3, 18). The calculation of water-surface profiles by this

equation is usually accomplished by replacing the differentials dy and dx by finite increments Δy and Δx .

Calculation of Adjusted \bar{n}

The roughness coefficient \bar{n} is that value of Manning's n which, when used in conjunction with the Manning formula and the energy equation, will yield the actual water-surface profile for spatially varied flow. The Bernoulli energy equation can be written for spatially varied flow as:

$$\frac{V_2^2}{2g} + y_2 + z_2 = \frac{V_1^2}{2g} + y_1 + z_1 + S_f \Delta x \quad (14)$$

where Δx is the distance between the downstream and upstream stations 1 and 2, respectively. Equation (14) involves the same assumptions as did Equation (10), apart from the type of flow being considered. Rearranging the Manning equation and substituting it into Equation (14) gives:

$$\frac{Q_2^2}{2gA_2^2} + y_2 + z_2 = \frac{Q_1^2}{2gA_1^2} + y_1 + z_1 + \frac{Q_2^2 n^2 \Delta x}{2.208 A_{avg}^2 R_{avg}^{4/3}} \quad (15)$$

where,

$$V = \frac{Q}{A}$$

and,

$$A_{avg} = \frac{1}{2} (A_1 + A_2) \quad R_{avg} = \frac{1}{2} (R_1 + R_2)$$

An accurate water-surface profile can be calculated from Equation (15) by using a correct value of n . Also required are the channel geometry, the downstream depth, and a means of calculating the discharge of each siphon tube. Calculations should start at the downstream end of the irrigation bay where $Q = 0$, z is known, and the water-surface elevation $y + z$ is measured. Incrementing y between successive siphon tubes, with Q increasing in an upstream direction, will yield a calculated water-surface profile.

However, if n has been inaccurately chosen, the calculated water surface will not agree with the true profile. Only at the downstream point where the computations originated will the profiles be the same. The roughness coefficient n can be altered so that the computed profile fits the actual profile. If the calculated profile overpredicts the actual water surface then n must be decreased. Conversely, n must be increased if the calculated profile underpredicts the observed profile. Only one value of n will accurately predict the upstream water surface elevation using Equation (15). This correct n value is hereinafter called adjusted \bar{n} .

Calculation of n_e

Another roughness coefficient can be defined by evaluating the mean energy slope between the upstream and downstream ends of an irrigation bay. Equation (14) can be rewritten,

$$\frac{V_i^2}{2g} + y_i + z_i = \frac{V_o^2}{2g} + y_o + z_o + S_{fe}L$$

in which i and o refer to the upstream and downstream channel sections,

and L is the length of the irrigation bay. If $V_o = 0$, the effective slope of the energy line between the two end sections is:

$$S_{fe} = \frac{1}{L} \left[\frac{V_i^2}{2g} + (y_i + z_i) - (y_o + z_o) \right]$$

or

$$S_{fe} = \frac{1}{L} \left(\frac{V_i^2}{2g} + WS_i - WS_o \right) \quad (16)$$

An effective n can be calculated by substituting Equation (16) into the Manning equation, with V_i equal to Q_i/A_i ;

$$n_e = \frac{1.486 A_i R_i^{2/3}}{Q_i} \left[\frac{1}{L} \left(\frac{Q_i^2}{2gA_i^3} + WS_i - WS_o \right) \right]^{1/2} \quad (17)$$

When Q_i , WS_i , and the geometric elements A_i , R_i are known, n_e can be used to predict the downstream water-surface elevation WS_o in an irrigation bay of length L .

Calculation of Flow Profiles

The entering velocity head for an initial inflow Q_i is:

$$H_{vi} = \frac{V_i^2}{2g}$$

The velocity head becomes zero at the downstream end of the irrigation bay owing to outflow along the channel. For an ideal, or inviscid, fluid (25) a potential energy gain equal to the initial velocity head will be evidenced at the downstream cross-section. At any distance x along a level, prismatic channel in which the depth is nearly constant, the gain in potential energy ΔH_{vx} due to diminishing velocity head will be:

$$\Delta H_{vx} = H_{vi} - H_{vx}$$

where

$$H_{vx} = \text{remaining velocity head at point } x$$

or

$$H_{vx} = \frac{V_i^2}{2g} \left(\frac{L-x}{L} \right)^2$$

where L is the length of the irrigation bay. Combining the two velocity heads produces:

$$\Delta H_{vx} = \frac{V_i^2}{2g} - \frac{V_i^2}{2g} \left(\frac{L-x}{L} \right)^2$$

which reduces to:

$$\Delta H_{vx} = \frac{V_i^2}{2g} \left[\frac{2x}{L} - \frac{x^2}{L^2} \right] \quad (18)$$

In a real fluid however, the potential energy gain described by Equation (18) will be offset by internal energy losses. The energy gradient at the inflow section is:

$$S_{fi} = \frac{n^2 V_i^2}{2.208 R_i^{4/3}}$$

At any location x in the outflow reach,

$$S_{fx} = \frac{n^2}{2.208 R_x^{4/3}} \left[V_i \left(\frac{L-x}{L} \right) \right]^2$$

The mean slope of the energy line over some distance $x = x_1$ can be found by integration;

$$\bar{S}_f = \frac{1}{x_1} \int_0^{x_1} S_{fx} dx$$

Using adjusted \bar{n} and the average hydraulic radius produces:

$$\bar{S}_f = \frac{\bar{n}^2}{2.208 R^{4/3}} \frac{1}{x_1} \int_0^{x_1} V_i^2 \left(\frac{L-x}{L}\right)^2 dx$$

or

$$\bar{S}_f = \frac{\bar{n}^2 V_i^2}{2.208 R^{4/3} x_1} \int_0^{x_1} \frac{L^2 - 2Lx + x^2}{L^2} dx$$

Integrating this equation and converting it into the expression for energy loss yields:

$$H_f = \bar{S}_f x_1 = \frac{\bar{n}^2 V_i^2}{2.208 R^{4/3}} \left(x_1 - \frac{x^2}{L} + \frac{x^3}{3L^2} \right) \quad (19)$$

From Equation (19), the energy lost in the reach from 0 to x_1 can be calculated.

In a horizontal channel, only velocity head gain and friction head loss contribute to the difference in potential energy, i.e. water-surface elevation, between the inflow section and some downstream point. Thus, the energy equation reduces to,

$$\Delta WS_x = \Delta H_{vx} - H_{fx}$$

in which a positive ΔWS_x corresponds to a rising water-surface profile. The water-surface elevation difference ΔWS_x can be calculated by combining Equation (18), evaluated at $x = x_1$, with Equation (19). Therefore,

$$\Delta WS_{x_1} = \frac{V_i^2}{2g} \left(\frac{2x}{L} - \frac{x^2}{L^2} \right) - \left[\frac{\bar{n}^2 V_i^2}{2.208 R^{4/3}} \left(x_1 - \frac{x^2}{L} + \frac{x^3}{3L} \right) \right] \quad (20)$$

When $x = L$,

$$\Delta WS_L = \frac{V_i^2}{2g} - \frac{\bar{n}^2 V_i^2}{2.208 R^{4/3}} \left(\frac{L}{3} \right)$$

Simplification yields,

$$\Delta WS_L = V_i^2 \left(\frac{1}{2g} - \frac{\bar{n}^2 L}{6.624 R^{4/3}} \right) \quad (21)$$

from which the change in water-surface elevation between the ends of an irrigation bay can be predicted.

Relationship Between \bar{n} and n_e

The mean and effective energy slopes can be employed to calculate the energy loss H_f between the ends of an irrigation bay of length L .

Consequently, at $x = L$,

$$H_f = \bar{S}_f L = S_{fe} L$$

or

$$\bar{S}_f = S_{fe}$$

Evaluating Equation (19) at $x = L$ gives:

$$S_f = \frac{\bar{n}^2 V_i^2}{2.208 R^{4/3} L} \left(\frac{L}{3}\right) = \frac{\bar{n}^2 V_i^2}{2.208 R^{4/3}} \quad (3)$$

Also, rewriting Equation (17), using Equation (16) and $V_i = Q_i/A_i$, gives:

$$S_{fe} = \frac{n_e^2 V_i^2}{2.208 R_i^{4/3}}$$

The two energy slopes can be equated to produce:

$$\frac{\bar{n}^2 V_i^2}{2.208 R^{4/3}} = \frac{n_e^2 V_i^2}{2.208 R_i^{4/3}} \quad (3)$$

Assuming that $R \approx R_i$ and cancelling terms,

$$\frac{\bar{n}^2}{3} = n_e^2$$

or,

$$\bar{n} = \sqrt{3} n_e \quad (22)$$

Equation (22) expresses the theoretical relationship between \bar{n} and n_e .

The difference in water-surface elevations between the upstream and downstream ends of a horizontal channel where outflow occurs can be calculated using either Equation (20) with \bar{n} or Equations (16) and (17) using n_e . However, the water-surface elevations of intermediate points should be calculated from either Equation (15) or Equation (20). The use of n_e is only valid for predicting the water-surface elevation immediately downstream from an outflow reach. In other words, n_e cannot

be used to calculate intermediate profile points.

CHAPTER IV

EQUIPMENT AND PROCEDURE

Experimental System

The Channel

An existing experimental irrigation channel was the major apparatus employed in this series of prototype experiments. A general view of the channel is displayed in Figure 1. The system included the following components: an inflow section, a test section, and an outflow section.

Inflow to the system was accomplished through a 12 inch diameter pipe which linked the channel with its water source, Lake Carl Blackwell. Discharge regulation was effected by the 12 inch gate valve shown in the foreground of Figure 2. The flow was measured by calibrated stainless steel orifice plates. The upstream and downstream flange pressure taps shown in Figure 3 were connected to a 60 inch water-air manometer. The inflow turbulence was dissipated by two stilling devices:

1. Sheet metal and screen wire baffles with long-stemmed grass matted on the upstream face.
2. Wooden surface floats.

The straight test section of the trapezoidal concrete channel was

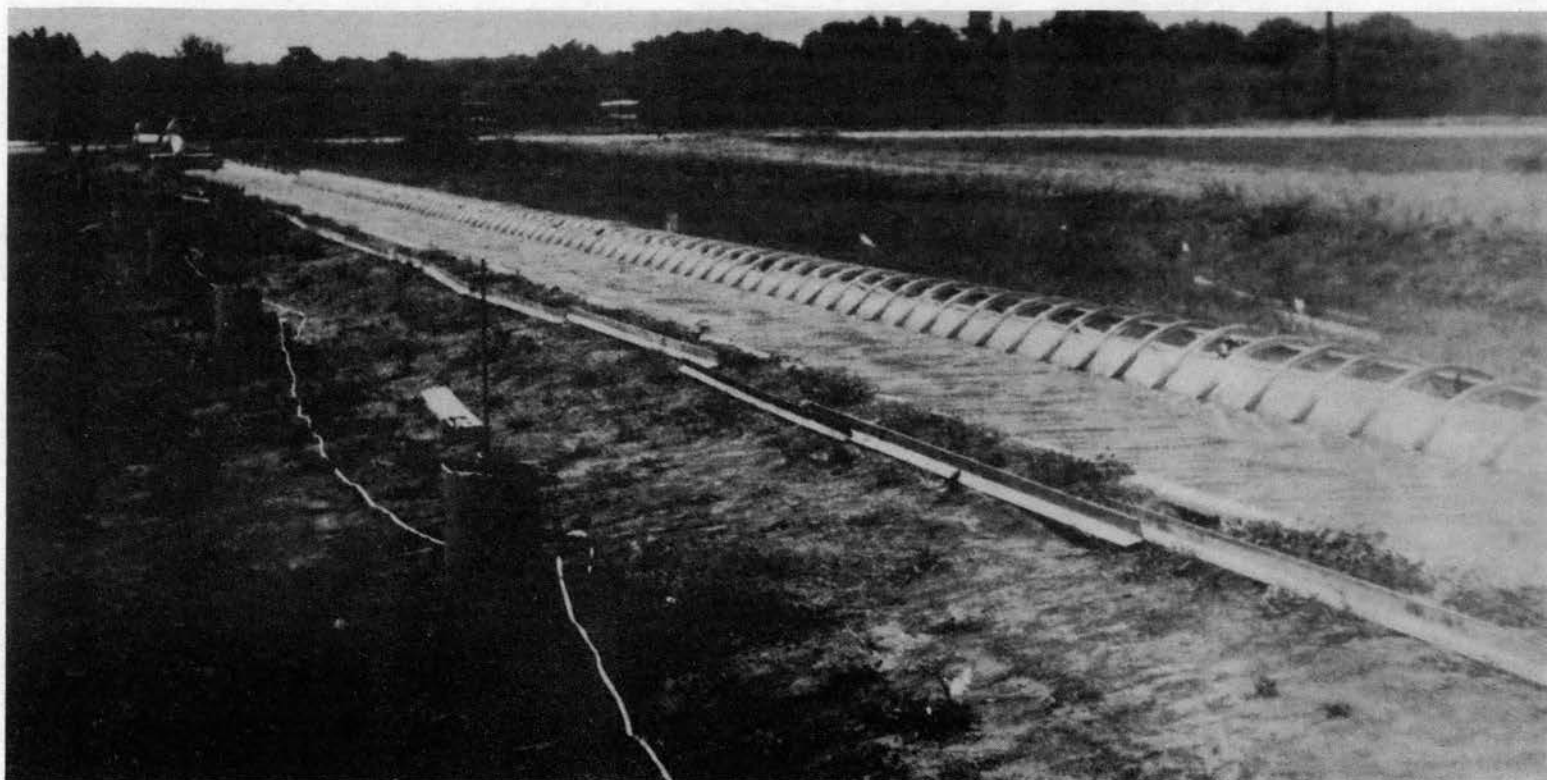


Figure 1. General View of the Experimental Channel.

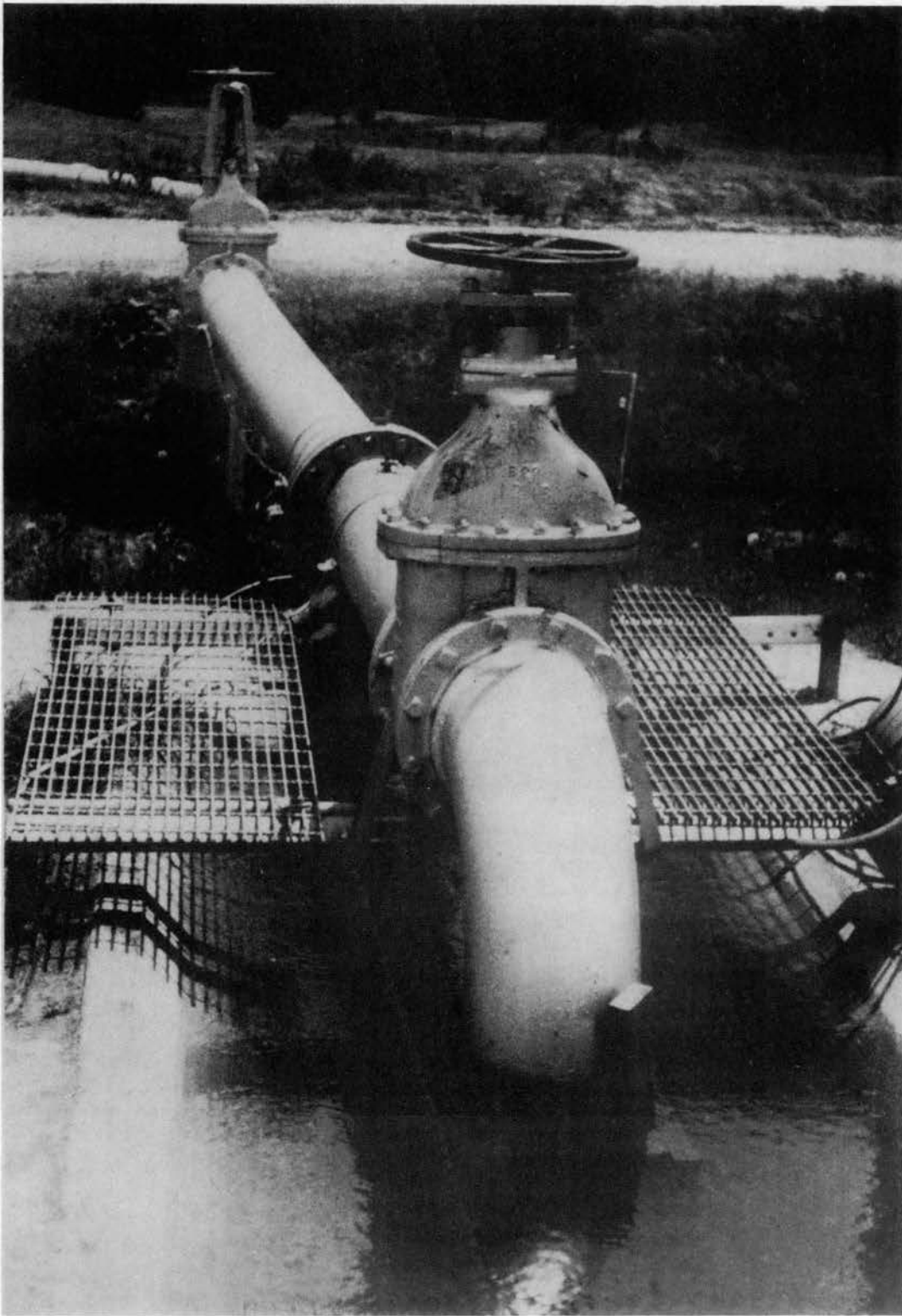


Figure 2. Water Supply System Showing the Control Valves and Orifice Flanges.

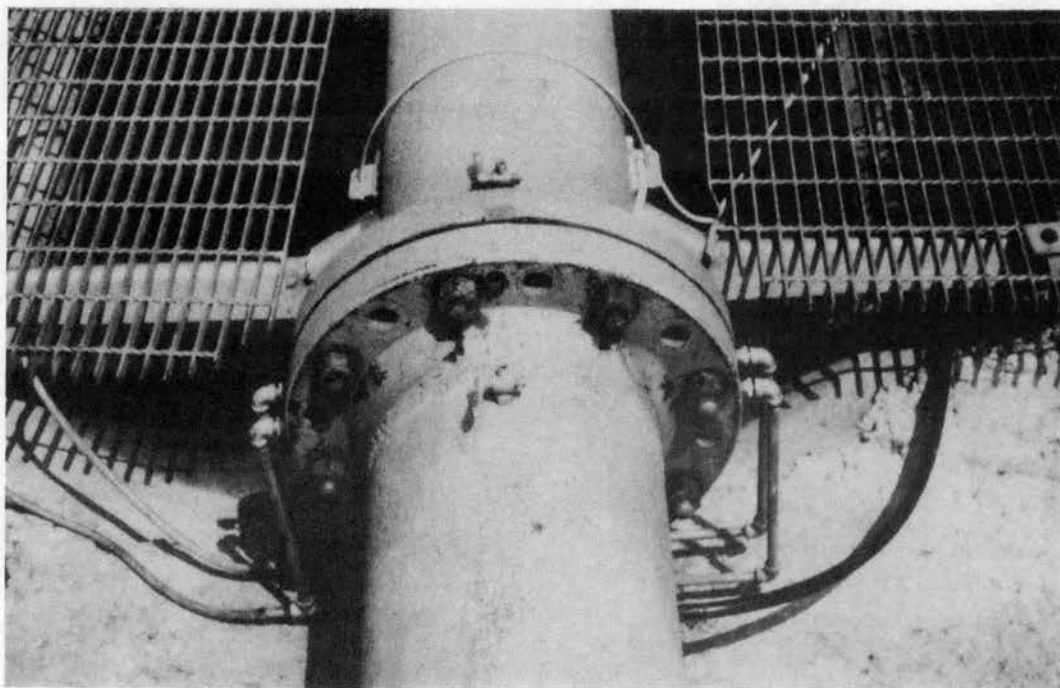


Figure 3. View of the Orifice Flanges, Manometer Pressure Taps, and Air Discharge Valves.

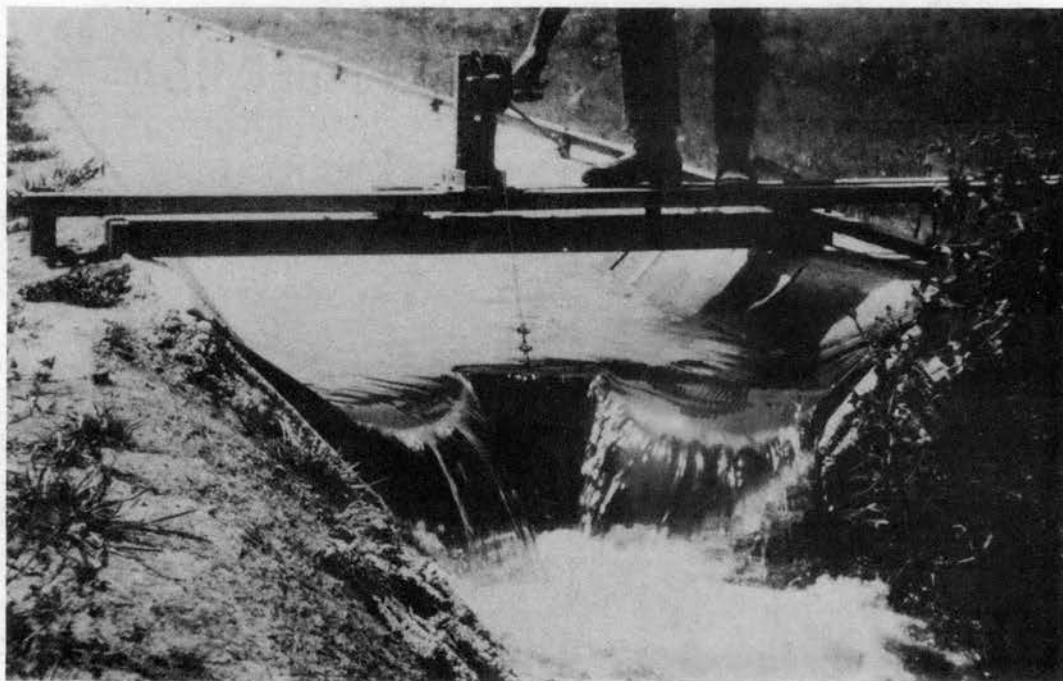


Figure 4. The Check Dam with Cable and Winch Used for Accurate Depth Control.

300 feet long. Nominal dimensions were 24 inches deep with 12 inch bottom width and 1:1 side slopes. Although designed for 0.00 per cent bottom slope, the channel bottom was placed with a resultant adverse slope of 0.022 per cent.

The canvas overfall check dam shown in Figure 4 was located immediately downstream from station 3+00. This dam was raised and lowered by a fine steel cable attached to a small winch. An earthen discharge ditch parallel but opposite in direction to the main channel carried the water away from the test site.

The test reach was subdivided into 11 equally spaced stations. Adjacent to the channel at each station, a gage or stilling well was installed. A small-diameter plastic pipe connected each 10 inch diameter gage well to the channel. A typical station cross-section is shown in Appendix A.

Measurement of water surface elevations at each station was accomplished with point gages mounted in brackets which were bolted near the tops of the gage wells. Both 2 foot and 3 foot Lory gages, readable to 0.001 foot, were the measuring devices utilized. Figure 5 shows a typical gage well and point gage installation.

Siphon Tubes

Spatially varied flow was achieved with primed double-bend plastic siphon tubes with a 5 foot curve length. Sizes selected were 1.0, 1.5, 2.0, and 3.0 inch diameters. These tubes were placed at spacings of 20, 40, 60, and 80 inches. The tubes were representative of the plastic siphon tube population.

The tube outlet elevations, necessary for tube discharge calcula-



Figure 5. Gage Well, Point Gage, and Electrical Outlet at Station 2+40.

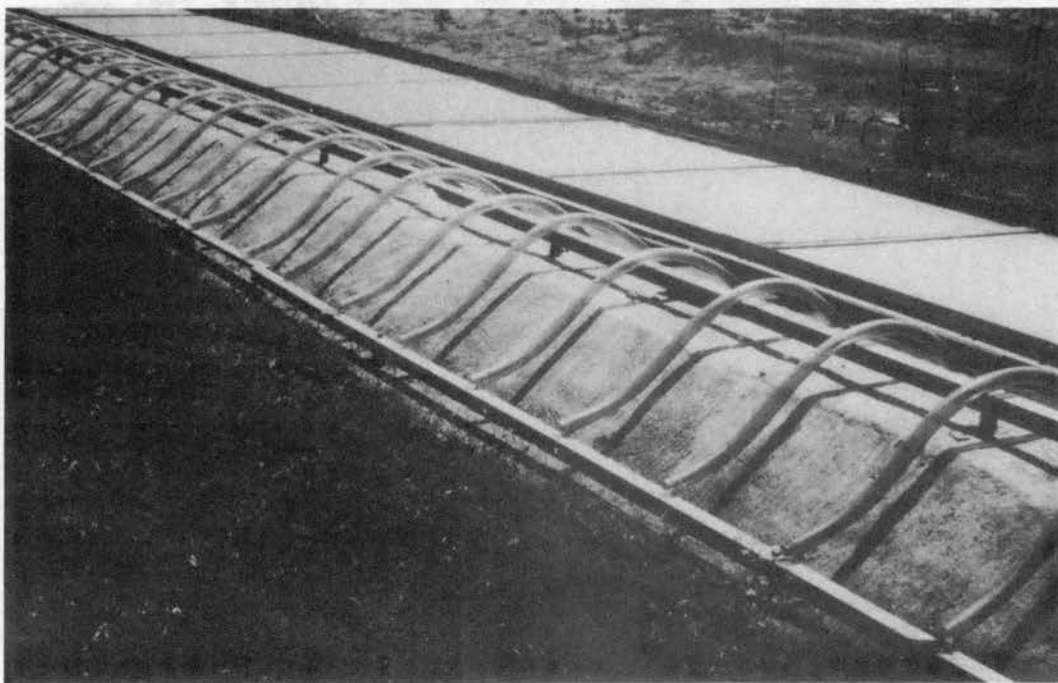


Figure 6. Siphon Tube Outlets Placed at the Reference Elevation, with Wind Panels Installed in the Background.

tions, were standardized on the top surfaces of adjusted structural steel angles as indicated in Figure 6. A detailed drawing of an adjustable siphon tube mount is presented in Appendix A. A Wye level and a Philadelphia rod with target vernier were used to set the reference surfaces at $923.913 \pm .005$ feet. Unevenness of the angle surfaces made shimming necessary at low spots.

For the restrained siphon tube tests, the experiments were performed with the channel or inlet end of each tube fastened to the channel wall as shown in Figure 7. Expandable plastic anchors, $5/16 \times 1$ inch, were imbedded into holes drilled in the concrete lining at 20 inch intervals. Into each anchor was inserted a screw; a 0.025 inch diameter steel wire wrapped around the siphon tube inlet end was tightened by the screws. Location of the siphon tube inlets was 12 inches vertically above the channel bottom.

A limited number of unrestrained siphon tube experiments were conducted in which the inlet ends of the tubes could swing freely with the channel current. The siphon tube outlet ends were loosely tied to the structural steel angles, preventing appreciable lateral movement. The topmost bends in the siphon tubes were lightly wired to the upper row of structural steel angles, leaving the tubes free to rotate. From this method of attachment, the inlet inverts of the siphon tubes lay approximately 11 inches above the plane of the channel bottom and about 1 inch away from the channel wall. The movement of empty, unrestrained siphon tubes due to channel current is illustrated in Figure 8.

Accessory Equipment

Wind played a vital role in the outdoor experimentation. The wind

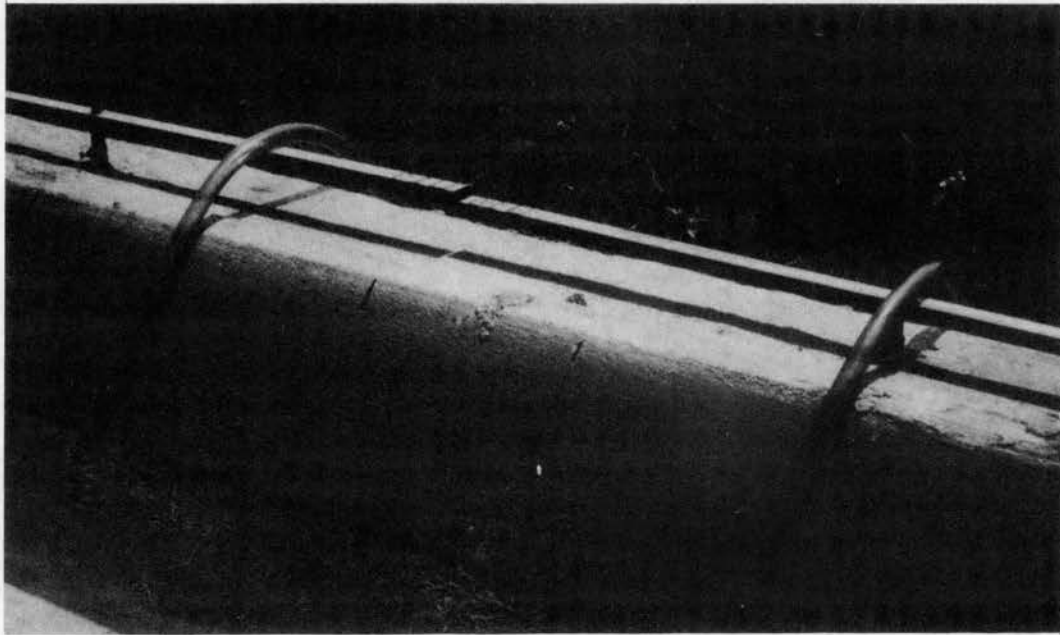


Figure 7. Interior View of Channel Showing Restrained Siphon Tubes.

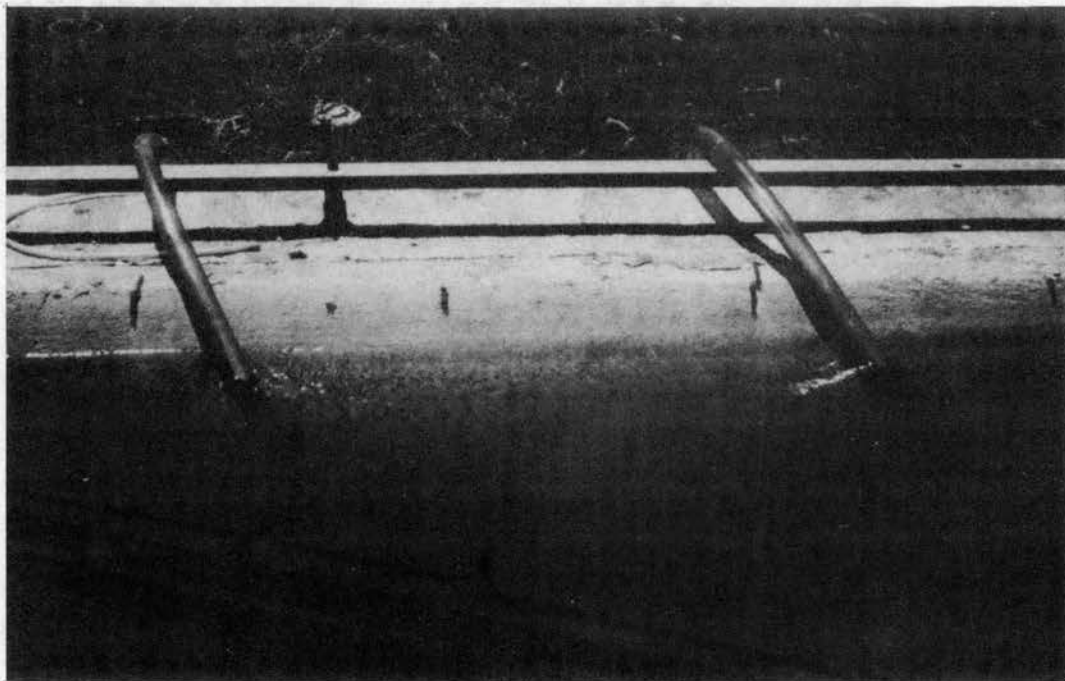


Figure 8. Rotation of Unrestrained Siphon Tubes Due to Channel Current.

effect was magnified by the low flow velocities, and hence low energy losses, inherent in the available range of depths and flow rates. Light, durable covers for the channel were constructed to minimize wind induced waves. The 5 foot wide frames, built in 10 foot lengths, were covered with 20 mil transparent polyethylene. Frame construction was of 2 x 2 inch lumber. The channel covers were placed as shown in Figure 6. Their 10 minute installation and removal times paid off in extra testing days. Execution of experiments at night when wind velocities were lower also proved expedient. Electrical outlets installed at each 30 foot station allowed sufficient lighting to read the point gages and the manometer.

A means for determining water surface stability was needed since all tests were steady flow in nature. An FW-1 stage recorder with a 6 inch float was mounted on the station 0 + 00 gage well. The needle trace was useful for spotting transient flow rates, and water surface response to wind gusts could be observed.

A portable gasoline-powered pump (50 gallon/minute maximum capacity) was used to prime the siphon tubes. Water from the channel was drawn into the pump and ejected into each tube inlet. When the tube outlet end flowed full, the pump ejection hose was guided to the next tube. A bay of 90 tubes could be primed in less than 10 minutes by this method.

Experimental Procedure

Measures were taken to restrict the settling and rising of the channel and gage wells while experimentation was in progress. These measures consisted of supplying adequate moisture to the silt loam soil

underlying the channel (19), and of maintaining this moisture condition between tests. For five weeks prior to testing, the channel was filled so that water could seep through cracks such as expansion joints. The preliminary gradually varied flow experiments without siphon tubes added additional soil moisture before the SVF experiments were started. Between testing days, water was left in the channel except when siphon tubes were being rearranged and the channel was being swept.

Channel Properties

The geometric elements, area, wetted perimeter, and top width, were obtained from the fitted equations that Mink (16) calculated for the same channel. A cross-section boundary traverse at each station yielded the channel property data. The IBM 7040 computer transformed the data into fitted equations of the form:

$$\text{Area} = c_1 y + c_2 y^2$$

$$\text{Wetted perimeter} = c_3 + c_4 y$$

$$\text{Top width} = c_5 + c_6 y$$

where

y = depth of flow, feet

Values for c_1 , c_2 , c_3 , c_4 , c_5 , and c_6 are presented in Table III. These constants were considered to be linearly distributed between stations so that properties could be calculated at any cross-section.

Brass Plug Elevations

At each station, a small brass plug had been placed in the concrete channel bottom to reference the channel to a permanent bench mark.

TABLE III
 CONSTANTS FOR EQUATIONS
 OF CHANNEL GEOMETRY

Station	Area		Wetted Perimeter		Top Width	
	C	C	C	C	C	C
	1	2	3	4	5	6
0 + 00	1.036	1.004	1.031	2.832	1.044	2.005
0 + 30	1.043	1.002	1.032	2.829	1.050	2.000
0 + 60	1.048	1.001	1.037	2.828	1.053	1.999
0 + 90	1.050	1.002	1.043	2.830	1.054	2.002
1 + 20	1.045	1.003	1.036	2.828	1.054	1.998
1 + 50	1.041	1.007	1.036	2.835	1.049	2.008
1 + 80	1.051	0.997	1.047	2.823	1.055	1.992
2 + 10	1.046	1.002	1.041	2.826	1.057	1.995
2 + 40	1.013	1.023	1.041	2.830	1.066	2.001
2 + 70	1.054	1.003	1.048	2.829	1.062	2.000
3 + 00	1.041	1.006	1.039	2.835	1.048	2.007

located about 120 feet from the upstream end. Brass plug elevations, determined by surveys using an engineer's level and a point gage, were taken on three occasions; these elevations are shown in Appendix B. The maximum vertical movement of the channel bottom was 0.007 foot. This magnitude of movement becomes negligible in the energy slope computations (16).

Gage Zeros

A gage zero, determined for a given point gage mounted inside a given gage well, was the elevation of the point gage tip when the zero mark on the point gage shaft coincided with the zero mark on the vernier scale. Surveying with the level and point gage constituted one method of measuring point gage zeros, and this method consisted of the following steps:

1. With the point gage tip resting on a known elevation (bench mark or previous brass plug) a reading was taken where the line of sight of the instrument crosshair intersected the vertical point gage shaft. This backsight subtracted from the known elevation produced rod zero for the instrument setup. Analogous to height of instrument in conventional surveying, rod zero is defined as the elevation of the point gage tip that would occur if the horizontal instrument crosshair were reading 0.000 feet on the point gage shaft. Hence;

$$\text{Rod Zero} = (\text{Elevation of Bench Mark}) -$$

$$(\text{Backsight on Point Gage})$$

2. After moving the point gage to a gage well bracket, a convenient foresight, e.g., 1.000 foot, was established and the

vernier scale was read. Subtracting the foresight from the gage reading produced the distance between the crosshair elevation and the vernier zero mark.

3. The remainder obtained in Step 2 was subtracted from the rod zero and the resulting elevation was the gage zero for the station.

Steps 2 and 3 can be expressed as

$$\text{Gage Zero} = \text{Rod Zero} - (\text{Gage Reading} - \text{Foresight})$$

The foregoing method of gage zero determination was unwieldy for frequent application. In addition, the accumulative surveying errors could have become relatively large compared to SVF surface profile differences.

Fortunately, a simplified method proved more accurate; it was based on the assumption that relative gage zeros are much more important, about 50 times according to Mink (16), than the absolute gage zero elevations. Three replications of the surveying method showed that the gage zero for station 0 + 60 was 921.563 feet, and this reference elevation was assumed constant for the 45 day testing period.

To obtain the same surface elevation in each gage well, water contained by the channel was allowed to reach equilibrium. The gage reading at station 0 + 60 gave the reference water-surface elevation WS_r by the following expression:

$$WS_r = 921.563 + (\text{Gage Reading at station } 0 + 60)$$

By reading the remaining point gages as their tips contacted the water, a gage zero for each station was ascertained. In equation form:

$$\text{Gage Zero} = WS_r - \text{Gage Reading}$$

Gage zero calculations for several consecutive days were grouped

together. An average gage zero (based on 3 to 9 replications of 5 subsamples each) was calculated for each station. The average gage zeros computed by the above method are presented in Appendix B.

Testing Procedure

Essentially the same procedures of measurement were followed for both the spatially varied and gradually varied flow experiments. For the spatially varied flow experiments, the check dam was raised and channel inflow was initiated. The siphon tubes were primed using the portable pump when the channel depth was sufficient to establish siphon tube discharge. As equilibrium between inflow and outflow progressed, the wind panels were positioned and then anchored with loose structural steel angles. Adjustment of the gate valve produced the desired manometer reading. Water-surface stabilization was indicated by a straight line trace on the FW-1 recorder cylinder.

Point gage readings, five subsamples at each station, were taken starting from the upstream channel end. If more than ± 0.001 foot variation from wind effects was observed, the set of subsamples was begun again. When wind induced waves in either channel or gage wells forced new readings at more than two stations, the entire series of readings was postponed until calmer conditions prevailed.

The downstream water-surface elevation was marked for later reference. A planed redwood lath, screwed to one channel wall, was used for this purpose.

Inflow through the orifice plate was measured by two variables: differential manometer head and water temperature. Ten sequential observations of piezometric head were taken from both water columns in

the U-tube manometer and the average head difference was calculated. A thermometer placed three feet downstream from the inflow point permitted water temperature readings in degrees Fahrenheit.

Gradually varied flow experiments involving unprimed siphon tubes were conducted after the SVF tests and before tube size and/or spacing were altered. For each combination of flow rate, tube spacing, and tube diameter, an attempt was made to duplicate the depth from the corresponding SVF experiment to ± 0.005 foot. The reference point was the gage well at station 3 + 00. Initial check gate adjustments were made in accordance with the water surface level recorded in the corresponding SVF test. Finer gate adjustments were based on point gage readings at station 3 + 00. The water surface generally could be controlled well within ± 0.005 foot.

CHAPTER V

PRESENTATION AND ANALYSIS OF DATA

Gradually varied flow (GVF) and decreasing spatially varied flow (SVF) experiments were conducted. The gradually varied flow experiments were aimed at determining hydraulic roughness both with and without siphon tubes. The roughness coefficients from GVF experiments are discussed first.

The most emphasis was placed on spatially varied flow wherein roughness coefficients, flow profiles, and siphon tube discharge uniformity were the topics of major interest. Two methods of siphon tube placement, restrained and unrestrained tubes, were used for gradually varied flow and spatially varied flow experiments. The pilot experiments involving unrestrained siphon tubes were discussed last.

Gradually Varied Flow

Channel Roughness Without Siphon Tubes

A brief series of gradually varied flow experiments was designed to measure the hydraulic resistance of the concrete channel. Three depths were established for each of the three selected flow rates. The energy slope was computed by Equation (11) from the measured discharge and water-surface elevations at Stations 0 + 00 and 3 + 00. At the eleven stations, the product $AR^{2/3}$ was computed from the equations for

area and wetted perimeter; the constants used were previously listed in Table III. The average value of $AR^{2/3}$ was substituted into Equation (12) from which Manning's n was calculated. The values of n for gradually varied flow without siphon tubes are presented in Table IV.

By relating n to the Reynolds number and hydraulic radius, Mink (16) obtained the following equation:

$$n = \frac{R_n R^{1/6}}{218500 + 86.59 R_n}$$

where

n = Manning's roughness coefficient

R = Average hydraulic radius, feet

R_n = Reynolds number

Values of n calculated from this equation slightly exceeded the observed resistance coefficients. The discrepancy was partly attributed to the fact that Mink considered only the upstream 180 feet of the channel. Average values of the hydraulic radius and Reynolds number would have been lower and slightly higher, respectively, had the entire channel been used. Consequently, the n values calculated using a 300 foot channel reach required smaller coefficients in the denominator of the above equation.

The nine experimental n values from Table IV were best represented by the equation,

$$n = \frac{R_n R^{1/6}}{205600 + 81.47 R_n}$$

The observed roughness coefficients lay within five per cent of their mean of 0.01101. In addition, they agreed closely with the average value of 0.01115 which Mink recorded (16).

TABLE IV
 CHANNEL ROUGHNESS WITHOUT SIPHON
 TUBES ($\alpha = 1.00$)

Q (cfs)	Average Depth (ft.)	Hydraulic Radius (ft.)	Reynolds Number	Manning's n
4.285	1.723	0.808	73,165	0.0105
4.294	1.528	0.734	80,830	0.0105
4.331	1.168	0.596	100,508	0.0108
2.995	1.693	0.797	51,876	0.0114
3.002	1.423	0.695	59,822	0.0111
2.999	1.014	0.535	77,314	0.0115
1.997	1.718	0.806	34,189	0.0106
2.000	1.428	0.696	39,751	0.0114
2.000	0.884	0.482	56,941	0.0113

Channel Roughness With Siphon Tubes

Gradually varied flow experiments were designed to measure Manning's n for boundary roughnesses, discharges, and depths which were similar to the spatially varied flow experiments. The chosen spacings were 20, 40, 60, and 80 inches, while the tube diameters were 1.0, 1.5, 2.0, and 3.0 inches. The tube outlets were located 1.0 foot above the channel bottom for each experiment. The data for the experiments involving 1.0, 1.5, and 2.0 inch diameter tubes spaced at 40 inches was contributed by Mink (16).

Values of Manning's n were calculated by substituting the energy slope from Equation (11) into Equation (12). In Equation (11), the areas A_1 and A_2 , and the water-surface elevations WS_1 and WS_2 , were evaluated at the stations bounding the channel reach of length L which contained siphon tubes. For this reach, the mean value of $AR^{2/3}$ was computed for use in Equation (12). Table V summarizes the roughness coefficients for gradually varied flow with siphon tubes.

Spatially Varied Flow

An interdependence existed between entering flow rate, siphon tube head, tube diameter, and number of primed tubes. As a result, for each combination of tube spacing and size the number of experiments was not uniform.

Error Criteria for Selecting Experiments

The flow profiles for some of the experiments involved changes in the water-surface elevations that were similar in magnitude to the

TABLE V
 EXPERIMENTAL CONDITIONS AND MANNING'S n FOR GRADUALLY
 VARIED FLOW WITHOUT SIPHON TUBES

LENGTH OF REACH FT	TUBE SPACING IN.	TUBE DIAM. IN.	Q CFS	AVE. DEPTH FT	REYNOLDS ¹ NUMBER	MANNING'S n ($\alpha=1.00$)
150	20	2.0	4.269	1.845	71,492	0.0170
150	20	2.0	3.302	1.672	59,986	0.0167
150	20	2.0	2.248	1.837	37,768	0.0156
150	20	2.0	1.648	1.632	30,131	0.0165
150	20	1.5	3.856	1.853	66,712	0.0160
150	20	1.5	2.495	1.581	48,627	0.0160
150	20	1.5	2.280	1.852	39,004	0.0176
150	20	1.5	1.508	1.553	29,459	0.0163
150	20	1.0	1.650	1.848	28,277	0.0103
150	20	1.0	1.148	1.576	22,440	0.0105
*300	40	2.0	4.499	1.756	51,383	0.0137
*300	40	2.0	4.524	1.389	62,415	0.0126
*300	40	2.0	4.521	1.146	72,252	0.0112
*300	40	2.0	2.981	1.658	35,695	0.0139
*300	40	2.0	3.019	1.261	44,933	0.0120
*300	40	2.0	1.001	1.365	14,011	0.0094
*300	40	1.5	4.633	1.678	58,589	0.0128
*300	40	1.5	4.659	1.362	69,611	0.0120
*300	40	1.5	4.639	1.175	77,626	0.0113
*300	40	1.5	3.027	1.656	39,895	0.0113
*300	40	1.5	3.010	1.294	48,284	0.0116
*300	40	1.5	1.007	1.466	14,646	0.0073
*300	40	1.5	1.007	1.067	18,718	0.0086
*300	40	1.0	4.492	1.665	57,153	0.0124
*300	40	1.0	4.514	1.341	68,311	0.0114
*300	40	1.0	4.526	1.142	77,409	0.0107
*300	40	1.0	3.002	1.660	37,105	0.0125
*300	40	1.0	2.995	1.254	46,270	0.0112
*300	40	1.0	1.006	1.464	13,541	0.0073
*300	40	1.0	1.000	1.062	17,249	0.0104
300	60	2.0	4.201	1.808	72,424	0.0143
300	60	2.0	3.301	1.633	61,270	0.0140
300	60	2.0	2.242	1.837	37,664	0.0148
300	60	2.0	1.650	1.613	30,439	0.0141
300	60	1.5	2.506	1.816	44,616	0.0147
300	60	1.5	1.650	1.535	33,709	0.0137
300	60	1.0	1.097	1.835	19,364	0.0113
300	80	2.0	3.395	1.857	55,753	0.0141
300	80	2.0	2.491	1.620	46,417	0.0126
300	80	2.0	1.993	1.821	33,272	0.0138
300	80	2.0	1.509	1.617	28,176	0.0141
300	80	1.5	1.892	1.829	33,087	0.0131
300	80	1.5	1.244	1.542	24,735	0.0138

TABLE V (Continued)

LENGTH OF REACH FT	TUBE SPACING IN.	TUBE DIAM. IN.	Q CFS	AVE. DEPTH FT	REYNOLDS ¹ NUMBER	MANNING'S n ($\sigma=1.00$)
90	40	3.0	3.816	1.787	68,869	0.0191
90	40	3.0	3.850	1.379	85,662	0.0152
90	40	3.0	2.999	1.827	53,777	0.0196
90	40	3.0	2.982	1.368	67,596	0.0167
90	40	3.0	2.017	1.823	36,238	0.0222
90	40	3.0	2.014	1.356	45,989	0.0163

¹Reynolds number is defined as:

$$R_n = \frac{Q R}{A U}$$

*Tabulated values were recalculated from the original data of Mink (16).

expected error of measurement. Excessive errors in calculating roughness coefficients were expected for these experiments. Criteria were established to select the experiments which had the least amount of probable error.

The entering velocity head provided a suitable guide to the rise or fall in the flow profiles. The highest velocity head attained was near 0.011 foot as compared to the expected accuracy of point gage readings of 0.001 foot.

The ratio (hereinafter called δ) of the gage reading accuracy to the velocity head was computed for each experiment. For δ greater than 0.50, the maximum rise or fall in the water surface could be misread more than 50 per cent, and experiments in this category were omitted from most analyses. The value of $\delta = 0.30$ formed the upper limit for accepting those experiments whose roughness coefficients possessed the highest degree of certainty. In many cases, the experiments with $0.30 < \delta < 0.50$ were included in the data analyses.

Adjusted \bar{n}

Adjusted \bar{n} was the roughness coefficient which predicted the measured water-surface profile. Values of \bar{n} were derived by incrementing n in Equation (15) until the calculated profile fitted the observed flow profile.

A linear equation for the water-surface profile of the reach containing primed siphon tubes was computed by regression. The downstream water-surface elevation, evaluated from the regression equation, became the starting elevation for calculating the flow profile.

A computer program, written in Fortran IV for the IBM-7040, was

employed in calculating each water-surface profile and the corresponding value of \bar{n} . The energy equation — Equation (15) — was rewritten as:

$$\left(\frac{Q_2^2}{2gA_2^3} + y_2 \right) - \left(\frac{Q_1^2}{2gA_1^3} + y_1 \right) = z_1 - z_2 + \frac{Q_2^2 \bar{n}^2 \Delta x}{2.208 A_{avg}^2 R_{avg}^{4/3}} \quad (23)$$

At any cross-section (denoted by the subscript j) the bottom elevation z_j was known. The geometric elements A_j and R_j could be computed for any depth y_j . Downstream from the last siphon tube where $Q_1 = 0$, y_1 was computed by subtracting z_1 from the reference water-surface elevation. At this point, the solution to Equation (23) was begun. The value of n was assumed from the gradually varied flow experiments. The water-surface elevation at Δx (one siphon tube spacing) upstream was assumed equal to the reference elevation so that,

$$y_2 = y_1 + z_1 - z_2$$

and Q_2 could be calculated by,

$$Q_2 = Q_1 + Q_t$$

where the tube discharge Q_t was defined in Equation (9). Substituting the known values into Equation (23) produced an inequality which required adjustment of y_2 and H_m , in Equation (9). When the inequality had been reduced within ± 0.00001 foot, Equation (23) was solved between the next successive pair of siphon tubes by the same procedure. Calculations proceeded upstream in this manner until the last siphon tube was reached.

The upstream calculated water-surface elevation was compared with the upstream reference elevation calculated from linear regression which was assumed to be the standard. When the profiles differed more than

± 0.0001 foot, n was incremented and the series of calculations was begun again. Usually, several values of n were required before the profile from Equation (23) and the profile from regression matched at their end points. The final water-surface profile and the value of adjusted \bar{n} were recorded.

Effective n

The effective roughness coefficient n_e was derived to predict the total rise or decline of the flow profile, i.e. the change in total energy, between the ends of an irrigation bay. Values of n_e were computed from Equation (17) in which the water-surface elevations WS_i and WS_o were found from the profile regression line. The initial discharge Q_i was measured.

The geometric elements A_i and R_i were defined by three methods representing three degrees of refinement. The inflow depth in each case was obtained by subtracting the bottom elevation at the upstream cross-section from WS_i . In Method I, the actual A_i and R_i were calculated by interpolating, where necessary, the coefficients found in Table III for the geometric element equations. Further improvement in technique was not available.

Method II consisted of summing the areas and hydraulic radii for stations inside or bounding the reach of primed siphon tubes. The average A and R were substituted into Equation (17). For this method, the inflow depth was assumed constant for all stations.

For the least refined technique, Method III, a prismatic channel with bottom width 1.000 foot and 1:1 side slopes was assumed. The quantities A_i and R_i were then computed using the inflow depth.

The various methods of defining A_i and R_i produced nearly identical values of n_e . Equations relating n_{e_I} (n_e from Method I) to $n_{e_{II}}$ and $n_{e_{III}}$ were calculated by linear regression using the experiments where $\delta < 0.50$. These equations were plotted in Figures 9 and 10. Only values of n_{e_I} were considered further in the analysis and the numerical subscript is hereinafter deleted.

Presentation of Roughness Coefficients

The roughness coefficients from all restrained tube SVF experiments are listed in Table VI. Tables VII and VIII, comprised of experiments with error-to-velocity-head-ratios δ less than 0.30 and 0.50, contain values of \bar{n} , n_e , and upstream and downstream water-surface elevations from the profile regression lines.

Nine tests were omitted from the roughness coefficient analyses. Experiments 13, 14, 15, and 16 were deleted because alternate tubes were left unprimed. The two lowest discharges, Experiments 31 and 39, produced erratic results. The roughness condition in Experiments 40, 41, and 42 was unrepresentative of the remaining tests inasmuch as the 3 inch diameter tubes, 6 feet in length, were placed at approximately 45° with the direction of flow.

Experimental Relation of \bar{n} and n_e

The theoretical relationship between \bar{n} and n_e was derived in a previous chapter. Equation (22) can be written as:

$$\bar{n} = 1.732 n_e \quad (22)$$

The experimental values of \bar{n} and n_e were related by regression lines forced through the origin. The use of 33 experiments from Table VI

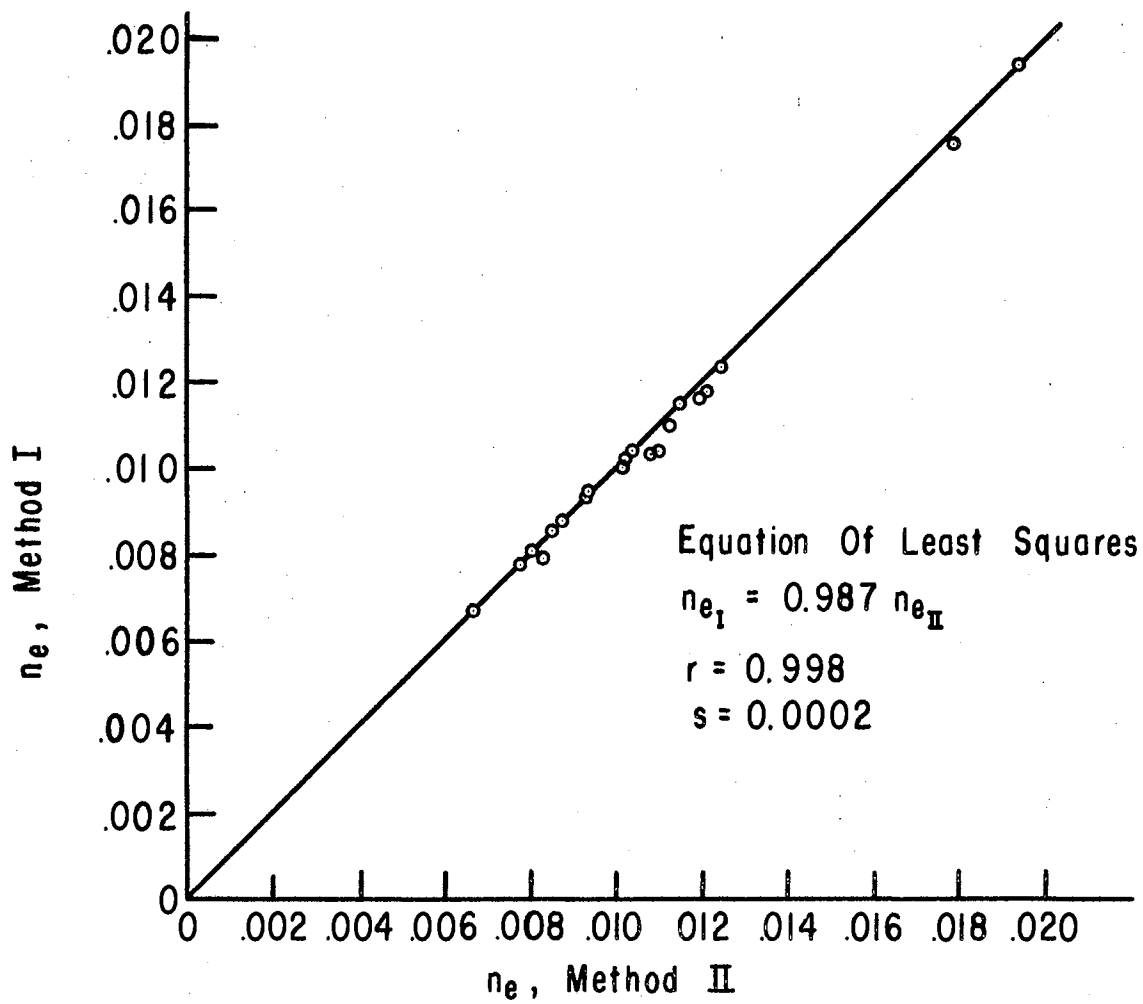


Figure 9. Comparison of n_{e_I} With $n_{e_{II}}$

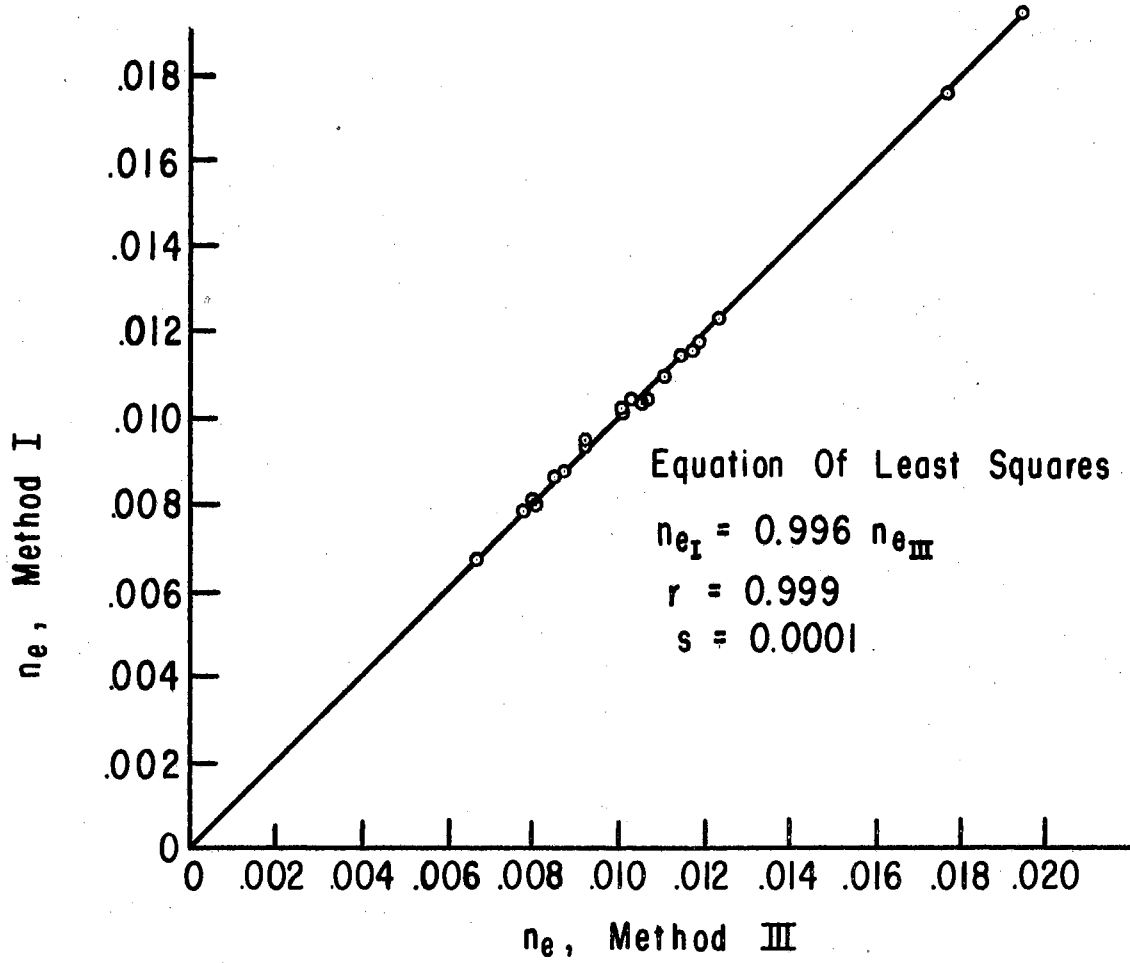


Figure 10. Comparison of n_{eI} With n_{eIII}

TABLE VI
 ROUGHNESS COEFFICIENTS FROM ALL RESTRAINED
 TUBE SPATIALLY VARIED FLOW EXPERIMENTS

EXPER. NO.	TUBE SPACING IN.	TUBE SIZE IN.	Q CFS	AVERAGE DEPTH FT	ADJUSTED \bar{n}	n_e	n_{gvf}
1	20.0	2.0	4.287	1.811	0.01900	0.01157	0.01700
2	20.0	2.0	4.279	1.813	0.01900	0.01174	0.01700
3	20.0	2.0	3.310	1.616	0.01920	0.01093	0.01670
4	20.0	2.0	3.300	1.616	0.02095	0.01228	0.01670
5	20.0	2.0	2.248	1.821	0.02960	0.01757	0.01560
6	20.0	2.0	1.651	1.603	0.03250	0.01943	0.01650
7	20.0	1.5	3.850	1.823	0.01900	0.01150	0.01600
8	20.0	1.5	2.498	1.550	0.01750	0.01004	0.01600
9	20.0	1.5	2.300	1.830	0.01660	0.01040	0.01760
10	20.0	1.5	1.506	1.546	0.01630	0.01032	0.01630
11	20.0	1.0	1.646	1.832	0.01830	0.01374	0.01030
12	20.0	1.0	1.146	1.561	0.01050	0.00776	0.01050
*13	40.0	2.0	3.788	1.908	0.01641	0.00937	0.01291
*14	40.0	2.0	3.318	1.774	0.01687	0.00955	0.01287
*15	40.0	2.0	2.681	1.635	0.01607	0.00908	0.01282
*16	40.0	2.0	2.240	1.547	0.01555	0.00889	0.01280
*17	40.0	1.5	4.226	1.902	0.01847	0.01037	0.01272
*18	40.0	1.5	3.612	1.752	0.01819	0.01020	0.01269
*19	40.0	1.5	2.884	1.609	0.01692	0.00943	0.01267
*20	40.0	1.5	2.137	1.475	0.01519	0.00854	0.01269
*21	40.0	1.0	1.770	1.910	0.01362	0.00947	0.01362
*22	40.0	1.0	1.558	1.774	0.01760	0.01004	0.01360
*23	40.0	1.0	1.303	1.617	0.01718	0.00957	0.01368
*24	40.0	1.0	0.985	1.488	0.01888	0.01074	0.01388
25	60.0	2.0	4.225	1.791	0.01615	0.00928	0.01440
26	60.0	2.0	3.305	1.620	0.01425	0.00804	0.01400
27	60.0	2.0	2.249	1.835	0.01880	0.01144	0.01480
28	60.0	2.0	1.650	1.613	0.01410	0.00794	0.01410
29	60.0	1.5	2.508	1.815	0.01370	0.00779	0.01470
30	60.0	1.5	1.650	1.537	0.01170	0.00671	0.01370
31	60.0	1.0	1.099	1.830		0.00175	0.01130
32	80.0	2.0	3.404	1.847	0.01547	0.00874	0.01410
33	80.0	2.0	2.482	1.619	0.01435	0.00805	0.01260
34	80.0	2.0	1.997	1.818	0.00980	0.00552	0.01380
35	80.0	2.0	1.509	1.617	0.01610	0.00909	0.01410
36	80.0	1.5	1.891	1.824	0.01610	0.00932	0.01310
37	80.0	1.5	1.249	1.544	0.01680	0.00957	0.01380
38	80.0	1.5	1.249	1.544	0.01530	0.00875	0.01380
39	80.0	1.0	0.800	1.809		0.00731	0.01250
40	40.0	3.0	3.809	1.766	0.01835	0.01104	0.01890
41	40.0	3.0	3.528	1.718	0.01710	0.01032	0.01860
42	40.0	3.0	3.095	1.638	0.01960	0.01102	0.01840

* \bar{n} and n_e were recalculated from the original data of Mink (16).

TABLE VII

CHANGE IN WATER-SURFACE ELEVATIONS AND ROUGHNESS COEFFICIENTS
FOR VARIOUS SIPHON TUBE SPACINGS, DIAMETERS,
CHANNEL DISCHARGES AND DEPTHS ($\delta \approx 0.30$)

EXP. NO.	TUBE SPAC. IN.	TUBE SIZE IN.	Q CFS	AVE. DEPTH FT	UPSTREAM SURFACE ELEVATION	DOWNSTREAM SURFACE ELEVATION	ADJUSTED \bar{n}	n_e
1	20.0	2.0	4.287	1.811	924.4819	924.4873	0.01900	0.01157
2	20.0	2.0	4.279	1.813	924.4840	924.4893	0.01900	0.01174
3	20.0	2.0	3.310	1.616	924.2880	924.2924	0.01920	0.01093
4	20.0	2.0	3.300	1.616	924.2888	924.2921	0.02095	0.01228
7	20.0	1.5	3.850	1.823	924.4958	924.4981	0.01900	0.01150
8	20.0	1.5	2.498	1.550	924.2230	924.2250	0.01750	0.01004
17	40.0	1.5	4.226	1.902	924.5771	924.5760	0.01847	0.01037
18	40.0	1.5	3.612	1.752	924.4276	924.4260	0.01819	0.01020
19	40.0	1.5	2.884	1.609	924.2841	924.2833	0.01692	0.00943
20	40.0	1.5	2.137	1.475	924.1496	924.1496	0.01519	0.00854
25	60.0	2.0	4.225	1.791	924.4654	924.4662	0.01615	0.00928
26	60.0	2.0	3.305	1.620	924.2938	924.2956	0.01425	0.00804
29	60.0	1.5	2.508	1.815	924.4891	924.4903	0.01370	0.00779
32	80.0	2.0	3.404	1.847	924.5211	924.5222	0.01547	0.00874
33	80.0	2.0	2.482	1.619	924.2930	924.2940	0.01435	0.00805

TABLE VIII

CHANGE IN WATER-SURFACE ELEVATIONS AND ROUGHNESS COEFFICIENTS
FOR VARIOUS SIPHON TUBE SPACINGS, DIAMETERS,
CHANNEL DISCHARGES AND DEPTHS ($\delta \cong 0.50$)

EXP. NO.	TUBE SPAC. IN.	TUBE SIZE IN.	Q CFS	AVE. DEPTH FT	UPSTREAM SURFACE ELEVATION	DOWNSTREAM SURFACE ELEVATION	ADJUSTED \bar{n}	n_e
1	20.0	2.0	4.287	1.811	924.4819	924.4873	0.01900	0.01157
2	20.0	2.0	4.279	1.813	924.4840	924.4893	0.01900	0.01174
3	20.0	2.0	3.310	1.616	924.2880	924.2924	0.01920	0.01093
4	20.0	2.0	3.300	1.616	924.2888	924.2921	0.02095	0.01228
5	20.0	2.0	2.248	1.821	924.4956	924.4968	0.02960	0.01757
6	20.0	2.0	1.651	1.603	924.2780	924.2785	0.03250	0.01943
7	20.0	1.5	3.850	1.823	924.4958	924.4981	0.01900	0.01150
8	20.0	1.5	2.498	1.550	924.2230	924.2250	0.01750	0.01004
9	20.0	1.5	2.300	1.830	924.5036	924.5054	0.01660	0.01040
10	20.0	1.5	1.506	1.546	924.2194	924.2206	0.01630	0.01032
17	40.0	1.5	4.226	1.902	924.5771	924.5760	0.01847	0.01037
18	40.0	1.5	3.612	1.752	924.4276	924.4260	0.01819	0.01020
19	40.0	1.5	2.884	1.609	924.2841	924.2833	0.01692	0.00943
20	40.0	1.5	2.137	1.475	924.1496	924.1496	0.01519	0.00854
25	60.0	2.0	4.225	1.791	924.4654	924.4662	0.01615	0.00928
26	60.0	2.0	3.305	1.620	924.2938	924.2956	0.01425	0.00804
27	60.0	2.0	2.249	1.835	924.5096	924.5104	0.01880	0.01144
28	60.0	2.0	1.650	1.613	924.2868	924.2881	0.01410	0.00794
29	60.0	1.5	2.508	1.815	924.4891	924.4903	0.01370	0.00779
30	60.0	1.5	1.650	1.537	924.2108	924.2119	0.01170	0.00671
32	80.0	2.0	3.404	1.847	924.5211	924.5222	0.01547	0.00874
33	80.0	2.0	2.482	1.619	924.2930	924.2940	0.01435	0.00805
36	80.0	1.5	1.891	1.824	924.4991	924.4992	0.01610	0.00932

yielded a coefficient of 1.689 for n_e . The standard deviation from regression was $s = 0.0013$ while the correlation coefficient $r = 0.961$ was attained. The 23 experiments for which $\delta < 0.50$ produced:

$$\bar{n} = 1.705 n_e$$

with $r = 0.991$ and $s = 0.0004$.

The 15 values of \bar{n} and n_e from Table VII were plotted in Figure 11. The equation which best fit these points was:

$$\bar{n} = 1.728 n_e$$

The values of r and s accompany the graph. The magnitude of one standard deviation represents an error of 3.5 per cent in the smallest \bar{n} value shown in Figure 11.

Comparison of Manning's n with \bar{n} and n_e

Similar conditions of flow rate and siphon tube placement were created for GVF and SVF experiments which dealt with 20, 60, and 80 inch tube spacings. The analogous experiments had a dual purpose:

1. To determine if the population of Manning's n for gradually varied flow and adjusted \bar{n} for spatially varied flow possessed the same mean.
2. To find the existing relationships between the resistance coefficients from gradually varied flow and spatially varied flow.

Nineteen values of \bar{n} and seventeen values of n_{gvf} (Manning's n from gradually varied flow) were analyzed as a group experiment. The detailed analysis is shown in Appendix C. The calculated $t = 2.326$ was significant at the $\alpha = 0.05$ level. Thus, there is a 95 per cent chance that a difference exists between the mean values of \bar{n} and n_{gvf} .

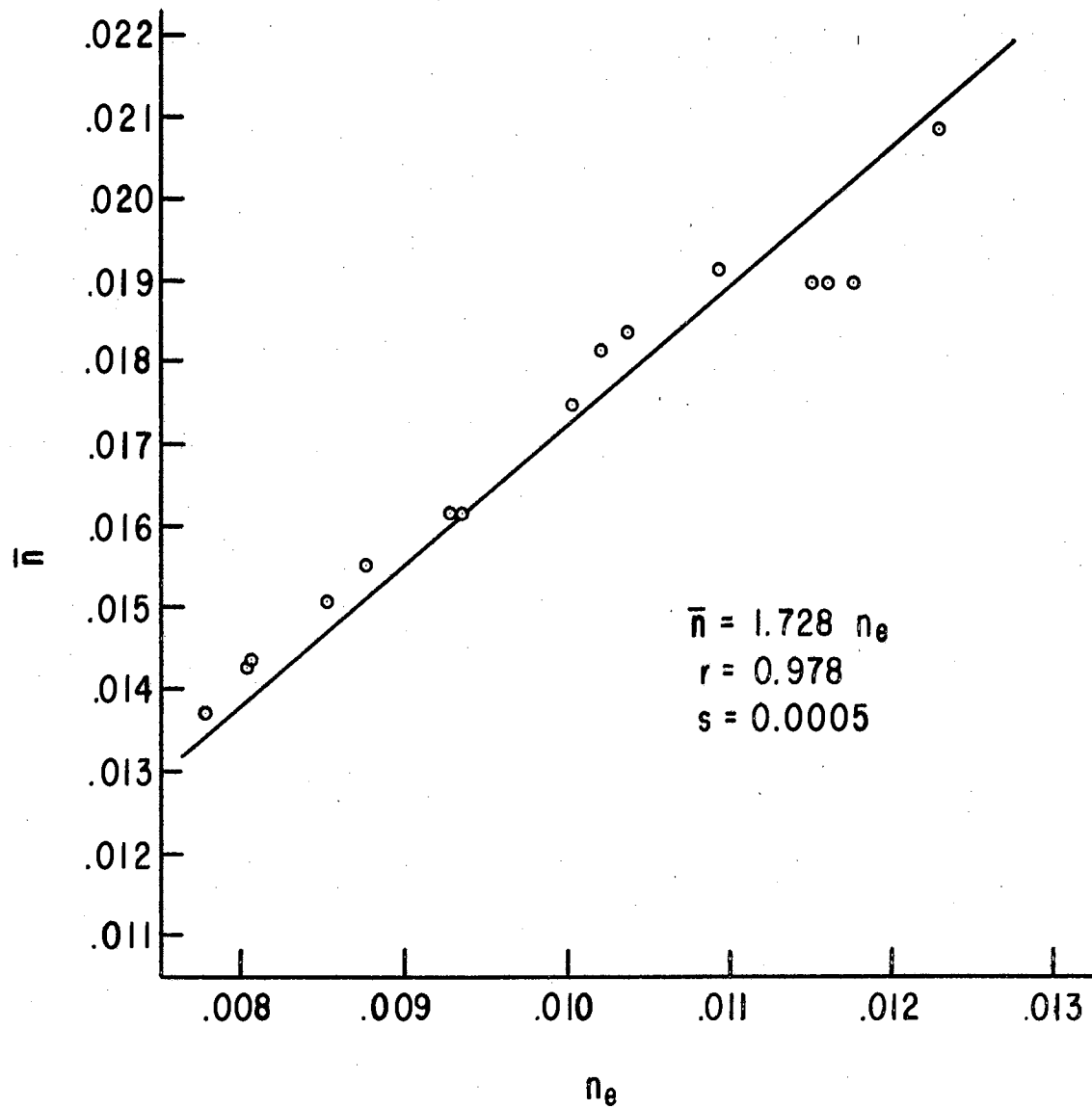


Figure 11. Relationship Between \bar{n} and n_e ($\delta \cong 0.30$)

Regression analysis using polynomials and logarithmic transformations failed to uncover a concrete relationship between \bar{n} and n_{gvf} and between n_e and n_{gvf} . The various trial equations were characterized by low correlation of calculated versus observed roughness coefficients. The simple equation,

$$\bar{n} = 1.164 n_{gvf}$$

best predicted \bar{n} from n_{gvf} , although a correlation coefficient of 0.590 and standard deviation of 0.0018 were produced. Higher correlation and somewhat better precision was found between n_e and n_{gvf} . The calculated equation,

$$n_e = 0.674 n_{gvf}$$

yielded values of r and s of 0.687 and 0.0011.

The inability to confidently relate Manning's n to SVF situations had significance because Manning's n has been defined for many types of channels.

Multivariable Response Surfaces

A direct means of predicting roughness coefficients for spatially varied flow was desirable since n_{gvf} could not be related to SVF experiments. Siphon tube spacing, diameter, and submergence were assumed to exert the most influence on the hydraulic roughness. Multivariable response surfaces involving three independent variables with interactions were calculated for \bar{n} and n_e . The following statistical models were assumed:

Linear

$$Y = C_1 + C_2 X_1 + C_5 X_2 + C_8 X_3 \quad (24)$$

Quadratic

$$Y = C_1 + C_2 X_1 + C_3 X_1^2 + C_5 X_2 + C_6 X_2^2 + C_8 X_3 + C_9 X_3^2 + C_{11} X_1 X_2 + C_{12} X_1 X_3 + C_{13} X_2 X_3 \quad (25)$$

Cubic

$$Y = C_1 + C_2 X_1 + C_3 X_1^2 + C_4 X_1^3 + C_5 X_2 + C_6 X_2^2 + C_7 X_2^3 + C_8 X_3 + C_9 X_3^2 + C_{10} X_3^3 + C_{11} X_1 X_2 + C_{12} X_1 X_3 + C_{13} X_2 X_3 \quad (26)$$

where

C_1, C_2, \dots, C_{13} are experimental coefficients

and

$Y = \bar{n}$ or n_e

$X_1 =$ siphon tube spacing, feet

$X_2 =$ siphon tube diameter, feet

$X_3 =$ siphon tube submergence, feet

From Equations (24), (25), and (26) the best results were attained using $\delta < 0.30$ as the error criterion. Correlation coefficients and standard deviations were evaluated from linear regressions of Y (calculated) versus Y (observed). Values of r , s , and the experimental coefficients are given in Table IX. The equations have the following range of applicability:

$$1.667 \leq \text{Spacing} \leq 6.667$$

$$0.125 \leq \text{Diameter} \leq 0.167$$

$$0.592 \leq \text{Submergence} \leq 0.903$$

Using Equation (26), seventy values of \bar{n} and n_e were calculated by varying X_1 , X_2 , and X_3 within their respective limits. The ratios of \bar{n}

TABLE IX

EXPERIMENTAL COEFFICIENTS, STANDARD DEVIATIONS,
AND CORRELATION COEFFICIENTS OF MULTIVARIABLE
EQUATIONS FOR COMPUTING \bar{n} AND n_e

	\bar{n}			n_e		
	Eqn. (24) r = 0.891 S = 0.0009	Eqn. (25) r = 0.913 S = 0.0009	Eqn. (26) r = 0.983 S = 0.0004	Eqn. (24) r = 0.940 S = 0.0005	Eqn. (25) r = 0.950 S = 0.0005	Eqn. (26) r = 0.981 S = 0.0003
C_1	0.01467	0.02607	0.03329	0.00712	-0.00098	0.02801
C_2	-0.00104	-0.00356	0.01102	-0.00072	-0.00183	0.00474
C_3	_____	0.00001	-0.00414	_____	0.00004	-0.00187
C_4	_____	_____	0.00033	_____	_____	0.00015
C_5	0.02151	-0.16494	0.01650	0.01879	0.13079	0.08794
C_6	_____	0.84375	-1.98242	_____	-0.37500	-2.17188
C_7	_____	_____	11.18750	_____	_____	9.50000
C_8	0.00397	0.02178	-0.09103	.00343	0.00976	-0.08858
C_9	_____	-0.00456	0.19920	_____	-0.00237	0.16323
C_{10}	_____	_____	-0.10686	_____	_____	-0.08398

TABLE IX (Continued)

\bar{n}			n_e		
Eqn. (24)	Eqn. (25)	Eqn. (26)	Eqn. (24)	Eqn. (25)	Eqn. (26)
$r = 0.891$	$r = 0.913$	$r = 0.983$	$r = 0.940$	$r = 0.950$	$r = 0.981$
$S = 0.0009$	$S = 0.0009$	$S = 0.0004$	$S = 0.0005$	$S = 0.0005$	$S = 0.0003$
C_{11}	0.00804	0.01137		0.00400	0.00622
C_{12}	0.00154	0.00203		0.00020	0.00045
C_{13}	-0.11664	-0.20483		-0.02573	-0.08076

to n_e for each combination of the independent variables had a mean of 1.765.

A response surface for n_e was plotted in Figure 12 from Equation (26). Qualitatively, the effect of siphon tube spacing, diameter, and submergence on n_e was revealed. The variation of each factor produced a realistic effect on n_e , although the irregular response from siphon tube spacing is unaccountable. For different regions of the diagram, different factors appear to exert the greatest influence on n_e .

Water-Surface Profiles in Decreasing Spatially Varied Flow

The iterative procedure for solving Equation (23) was discussed in conjunction with adjusted \bar{n} . By this method, flow profiles were calculated using \bar{n} and n_{gvf} .

The observed water-surface elevations were plotted in Figures 13, 14, and 15 for the experiments in which $\delta < 0.30$. Figure 16 contains the experimental profiles from Experiments 40 - 42. The calculated flow profiles are drawn for the channel reach involving spatially varied flow. Experiments 1 - 4 and 40 - 42, which had the highest outflow per unit of channel length, produced the best agreement between observed and calculated flow profiles. The large rise of these profiles as compared to similar discharges and depths in other experiments was attributed to the shorter length of channel in which friction loss occurred.

Flow Profiles Using Entering Velocity

Another method of calculating flow profiles was employed. This method made use of Equation (20) in which the energy losses were

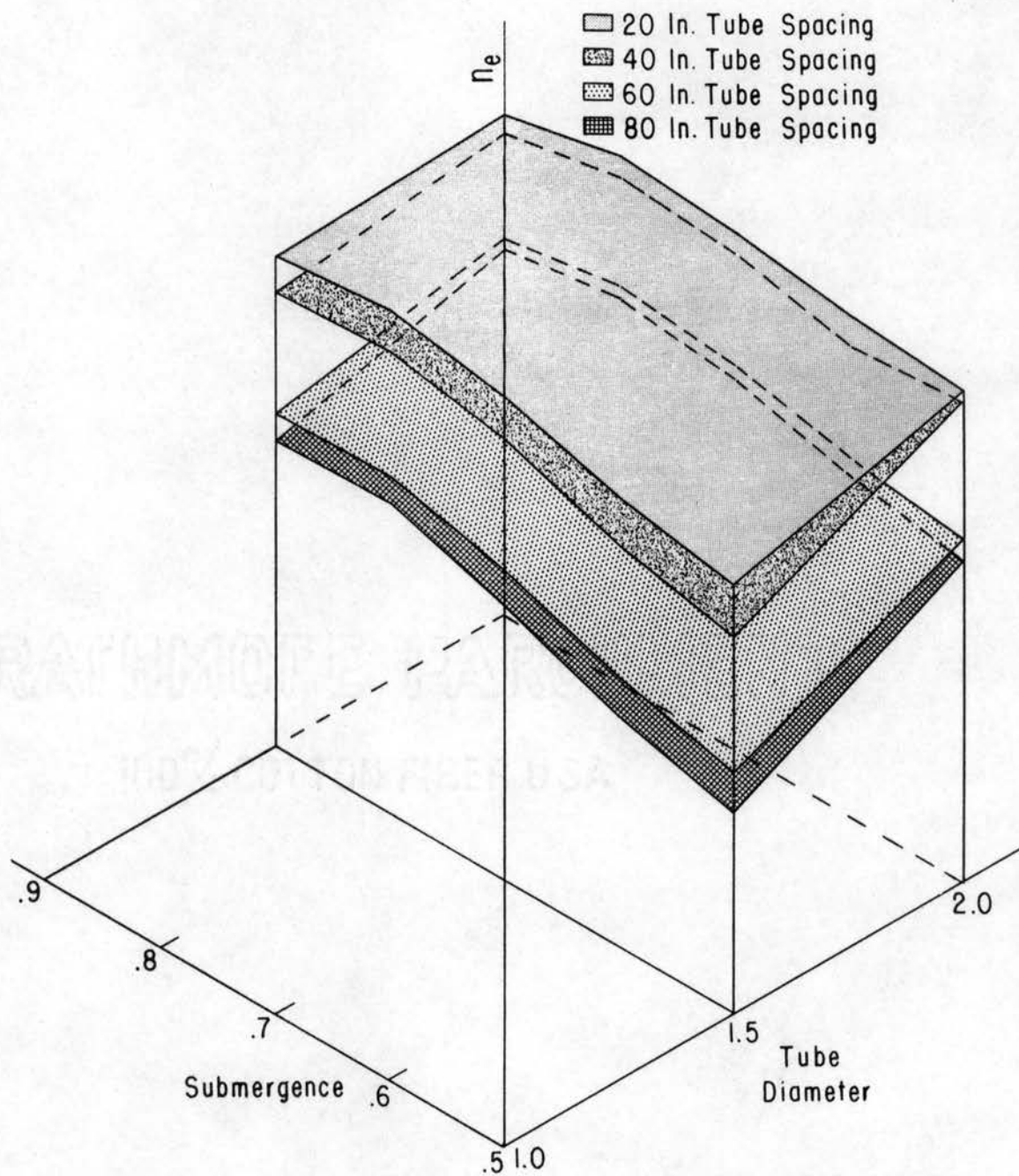


Figure 12. Multivariable Response Surface, Equation (26), Showing the Effects of Siphon Tube Spacing, Diameter, and Submergence on n_e

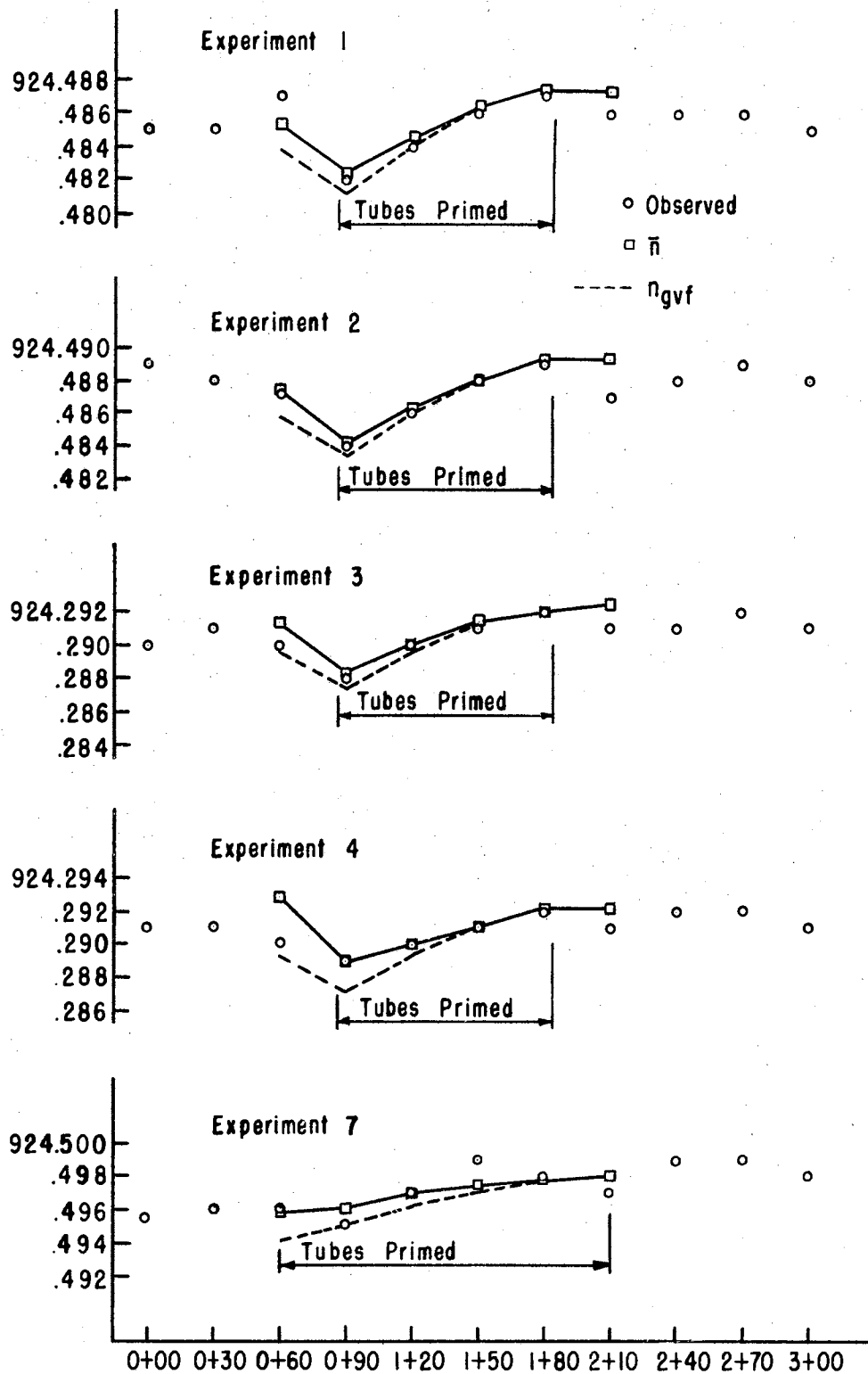


Figure 13. Observed and Calculated Flow Profiles for Experiments Using 1.5 and 2 Inch Siphon Tubes at 20 Inch Spacing

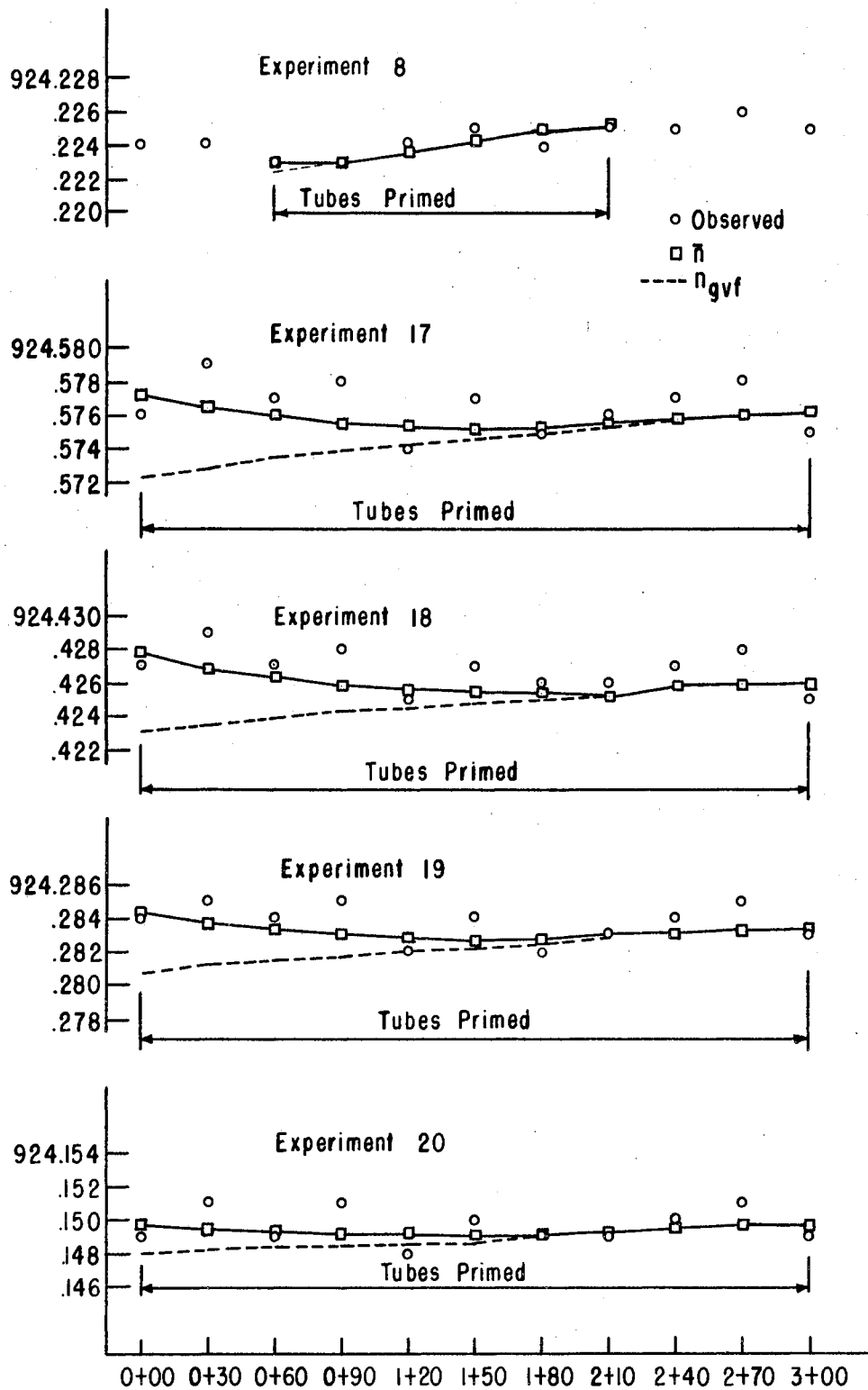


Figure 14. Observed and Calculated Flow Profiles for Experiments Using 1.5 Inch Siphon Tubes at 20 and 40 Inch Spacings

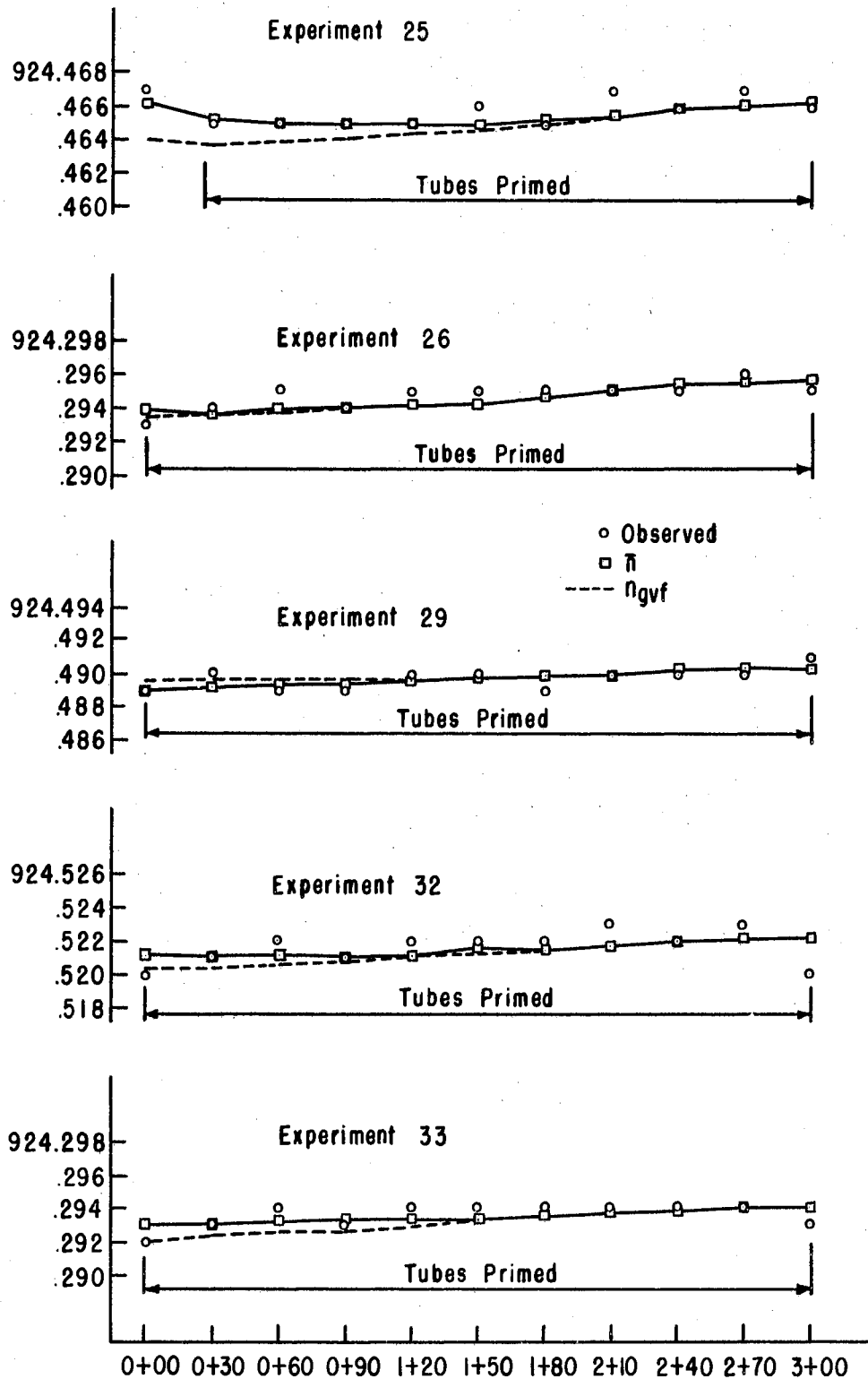


Figure 15. Observed and Calculated Flow Profiles for Experiments Using 1.5 and 2 Inch Siphon Tubes at 60 Inch Spacing, and 2 Inch Tubes at 80 Inch Spacing

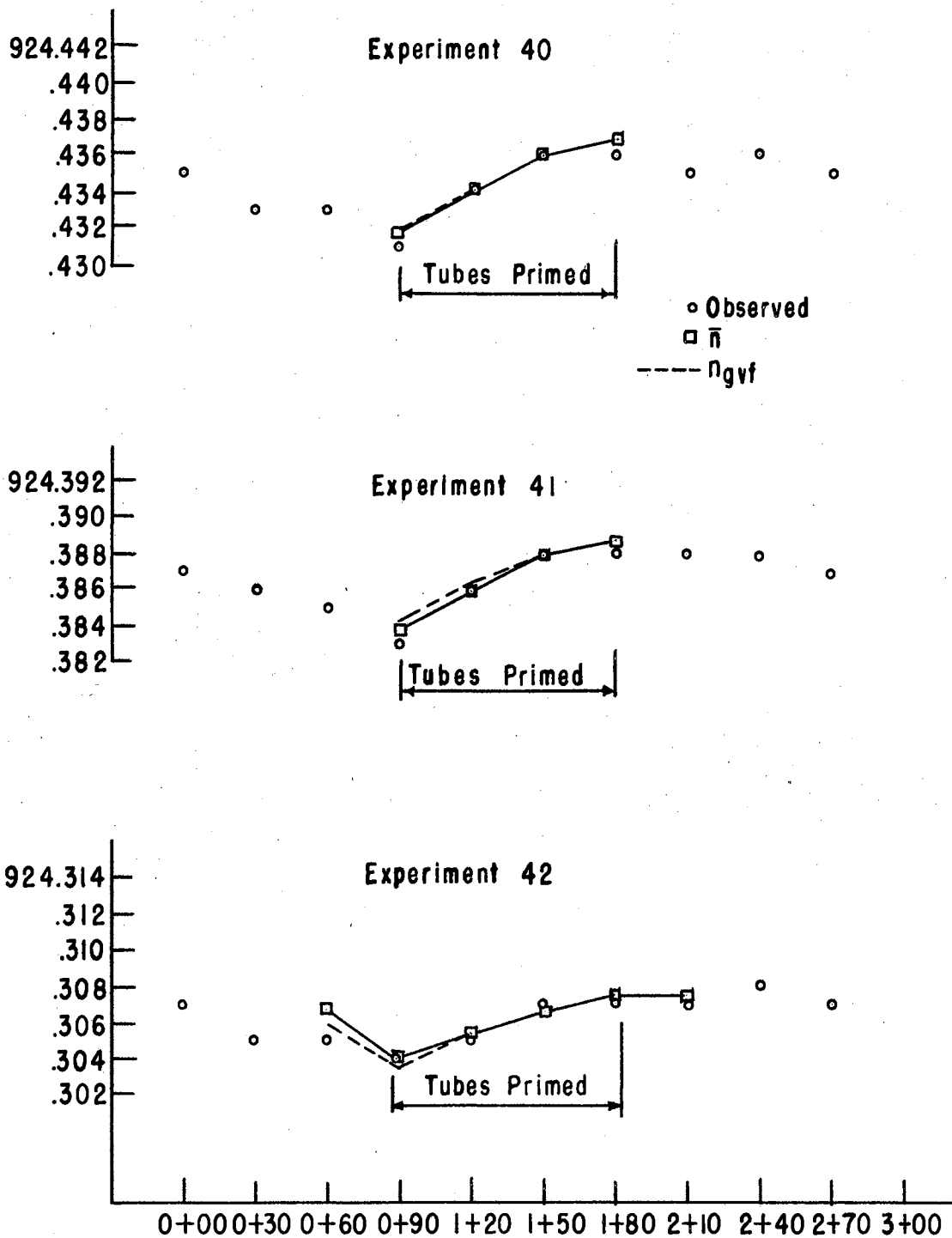


Figure 16. Observed and Calculated Flow Profiles for Experiments Using 3 Inch Siphon Tubes at 40 Inch Spacing

subtracted from the velocity head gained. From Equation (20), the water-surface elevation at any channel section could be calculated with reference to the upstream water-surface elevation.

A program entitled Delta-WS was written to solve Equation (20). The following items from the program which solved Equation (23) were read into the Delta-WS program: WS_i , V_i , \bar{n} , L , x_j , and R_j , where the upstream cross-section is denoted by the subscript i and j refers to each tube location. A horizontal channel was assumed. For each x_j , the calculated value of ΔWS from Equation (20) was added algebraically to WS_i to give the water-surface elevation.

Typical flow profiles from Equation (20) are plotted in Figure 17. The velocity head line shows the potential energy gain due to the diminishing velocity. The offsetting friction energy losses are also portrayed. The observed water-surface elevations were included for comparison.

Equations (20) and (23) produced flow profiles that were practically identical. The largest difference at any location was 0.0005 foot. These results were somewhat expected since both equations were solved with the same values of \bar{n} and hydraulic radius. However, three conclusions can be deduced from the sameness of the profiles:

1. The mean velocity varies approximately linearly with distance in the irrigation bay.
2. The integral method of calculating the mean energy slope is valid.
3. Equation (20) provides a direct method of calculating flow profiles for decreasing spatially varied flow in a horizontal irrigation channel where \bar{n} is known.

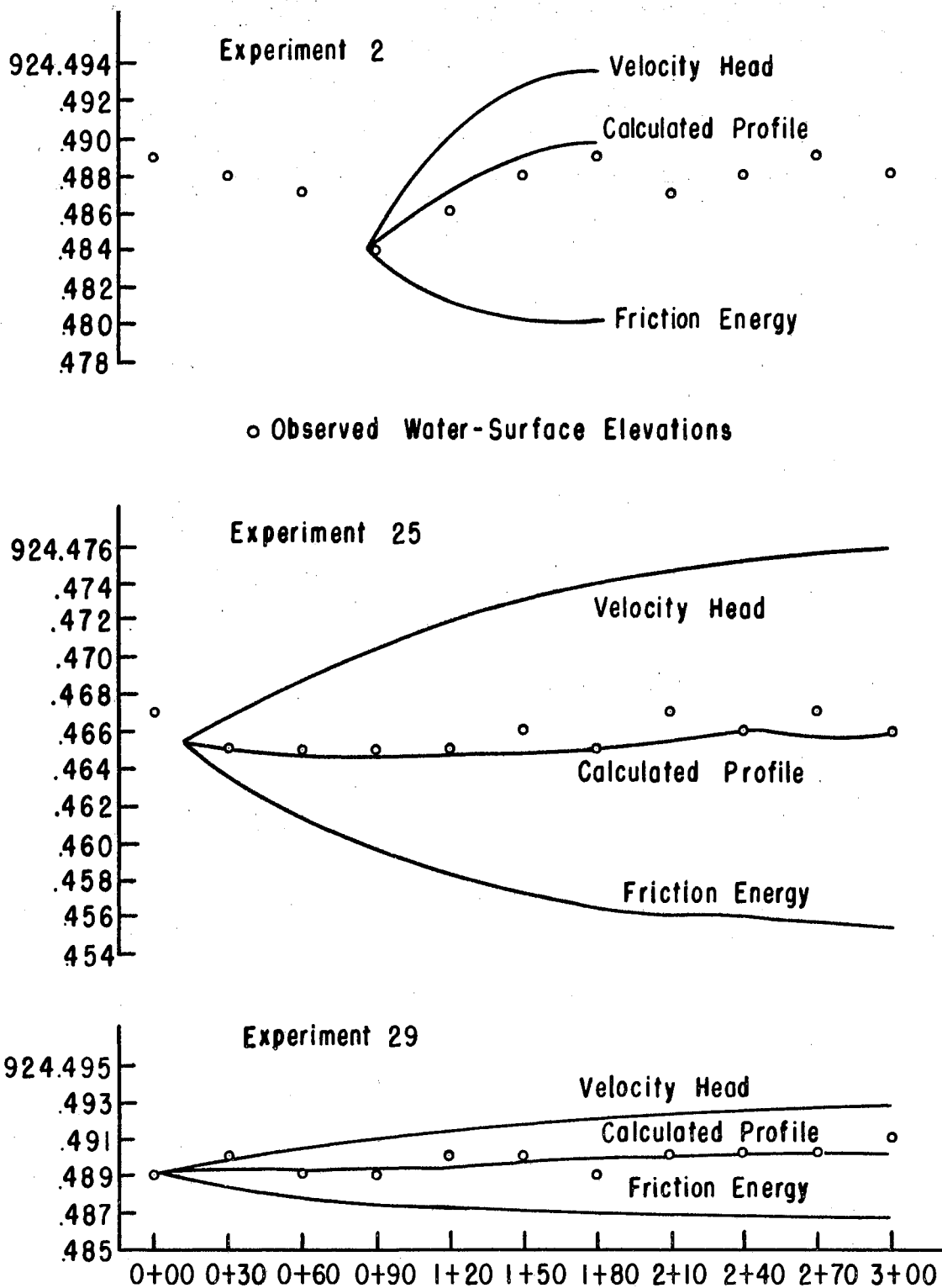


Figure 17. Comparison of Observed Water-Surface Elevations to Velocity Head Recoveries, Friction Losses, and Resultant Flow Profiles

Depth Required for Level Water Surface

Equation (20) can be solved at the downstream end of the irrigation bay, i.e. at $x = L$, to produce Equation (21). For a profile having the same upstream and downstream elevations, $\Delta WS_L = 0$ so that Equation (21) can be written as:

$$V_i^2 \left(\frac{1}{2g} - \frac{\bar{n}^2 L}{6.624 R^{4/3}} \right) = 0$$

solving for R produces,

$$R = \left(\frac{2g \bar{n}^2 L}{6.624} \right)^{3/4} = (9.705 \bar{n}^2 L)^{3/4} \quad (27)$$

In a prismatic trapezoidal channel with a 1.000 foot base width and 1:1 side slopes, the hydraulic radius for any depth y is:

$$R = \frac{y + y^2}{1 + 2.828 y}$$

Solving this equation for y by rearranging and completing the square yields,

$$y = \sqrt{R + \left(\frac{1 - 2.828 R}{2} \right)^2} - \frac{1}{2} (1 - 2.828 R) \quad (28)$$

The flow depth required for equal upstream and downstream water-surface elevations can be found by substituting Equation (27) into Equation (28). The positive sign preceding the radical should be chosen. The resulting equation will be a function of \bar{n} and L only.

Equations (27) and (28) were solved by incrementing \bar{n} from 0.010 to 0.020 and L from 50 to 500 feet. Curves of y versus \bar{n} for constant values of L were drawn in Figure 18. From these curves, the entering depth at which the net rise or fall in the flow profile will be zero

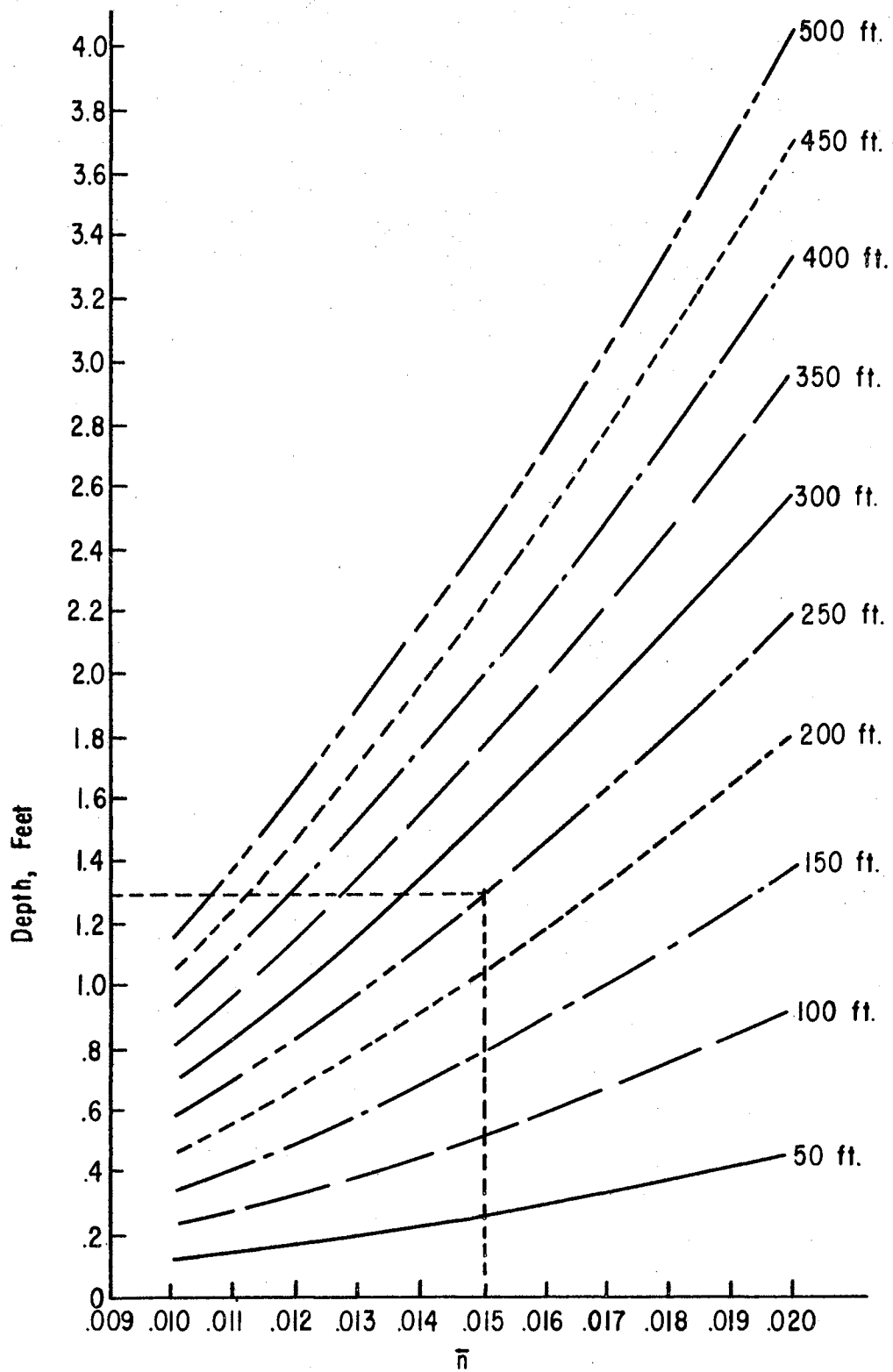


Figure 18. Depth for Level Water Surface as a Function of Roughness and Length of Horizontal Irrigation Bay

can be read for typical values of \bar{n} and L.

Graphical Solution to Flow Profiles

The change in the water-surface elevation between the upstream and downstream ends of an irrigation bay can be computed by Equation (21) using \bar{n} . The same result can be obtained by rearranging Equation (17) and solving for $WS_i - WS_o$. However, the solution to such problems is expedited by the use of nomographs such as Figures 19 and 20. The nomographs were designed to solve Equation (21) in the following manner:

$$\Delta WS_L = \Delta H_v - H_f$$

where

ΔH_v = kinetic energy of flow converted to potential energy

H_f = kinetic energy lost due to hydraulic resistance

A direct graphical solution requires that Q_i , L, depth, and either \bar{n} or n_e be known.

The procedure for finding the rise or fall of the flow profile can be illustrated by a realistic example in which the following quantities are given:

Length of irrigation bay = 300 feet

Desired depth y = 1.50 feet

Number of siphon tubes = 60

Design tube discharge = 22.5 gallons/minute

$\bar{n} = 0.018$

The solution can be initiated by determining that an entering flow rate of 1350 gallons/minute, or 3.01 cfs, will be required. From Figure 19 using $Q_i = 3.01$ cfs and $y = 1.50$ feet, the gain in velocity head will be

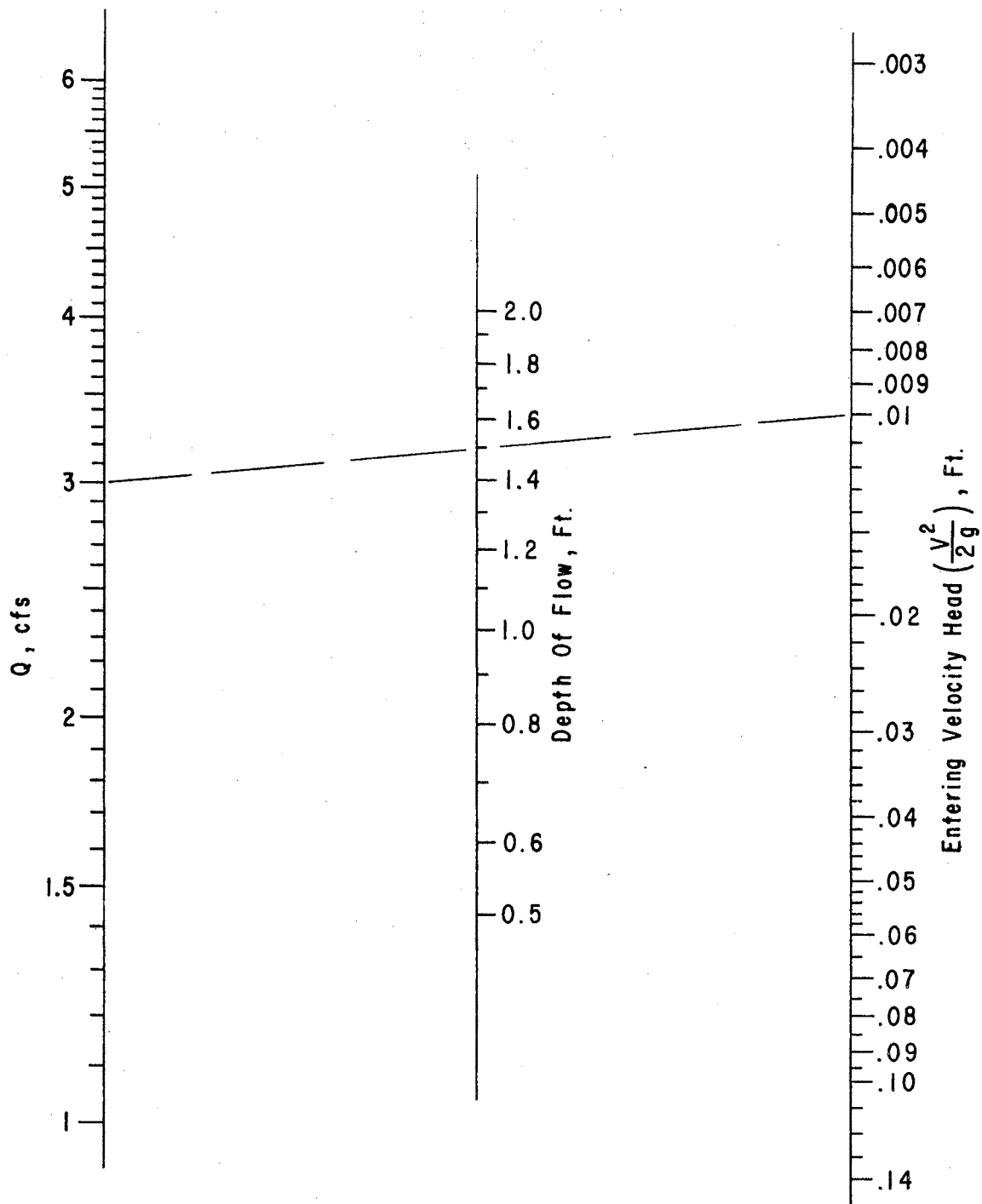


Figure 19. Nomograph for Finding Velocity Head Recovery

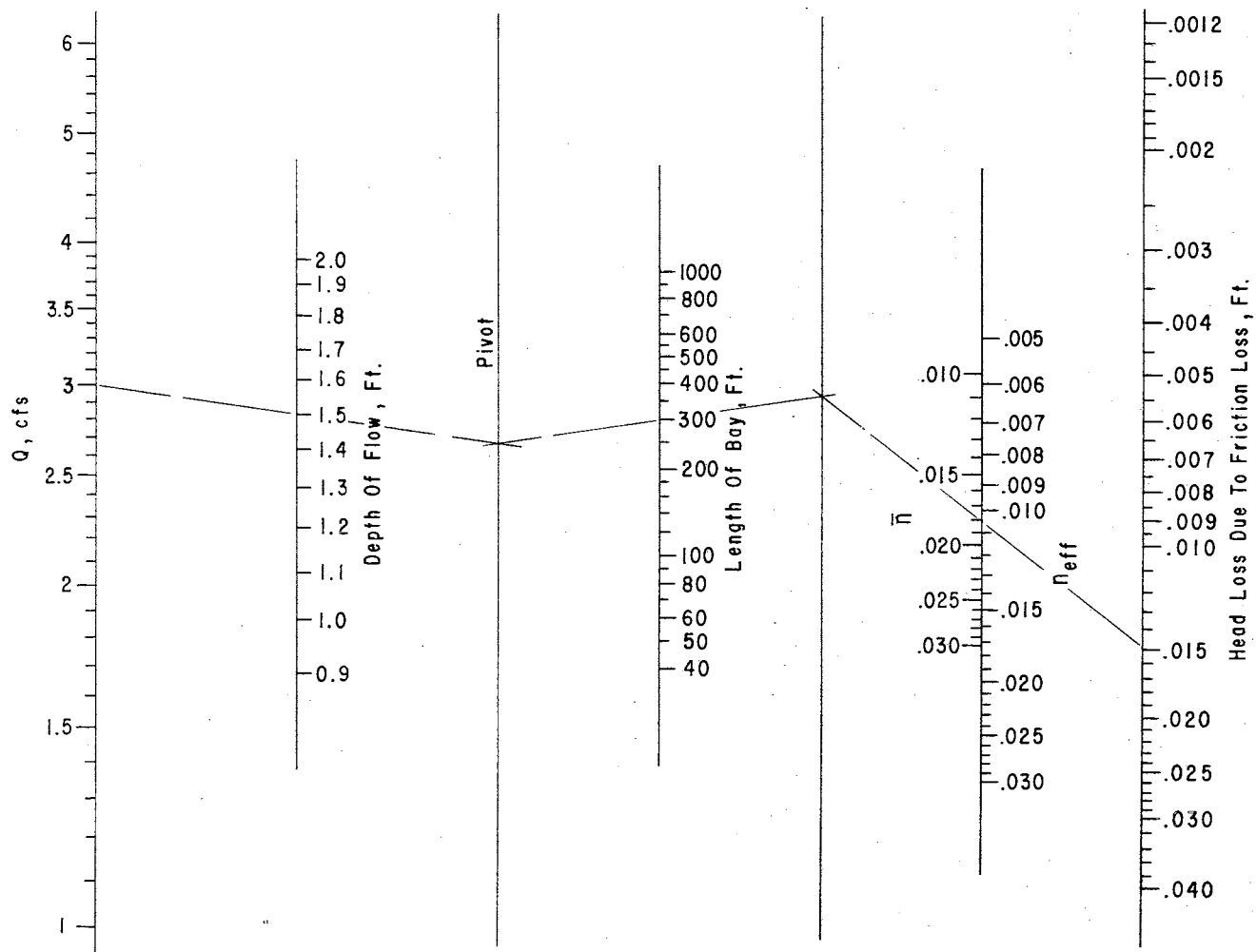


Figure 20. Nomograph for Finding Friction Head Loss

0.0099 foot. The friction energy loss from Figure 20 will be 0.0148 foot. Thus,

$$\Delta WS_L = 0.0099 - 0.0148 = -0.0049 \text{ foot}$$

where the negative sign denotes a declining flow profile.

The graphical result can be checked by calculations using n_e .

Equation (17) can be written as:

$$n_e = \frac{1.486 A_i R_i^{2/3} \frac{H_f}{L}^{1/2}}{Q_i}$$

where

$$\frac{H_f}{L} = \text{effective energy line slope}$$

Solving for H_f gives:

$$H_f = \frac{n_e^2 Q_i^2 L}{2.208 A_i^2 R_i^{4/3}}$$

The product $A_i^2 R_i^{4/3}$ can be obtained from Figure 21, which produces:

$$A_i^2 R_i^{4/3} = 9.00$$

Also,

$$n_e = \frac{\bar{n}}{\sqrt{3}} = 0.0104$$

Substituting for the known quantities and evaluating,

$$H_f = 0.0148 \text{ foot}$$

The entering velocity head is:

$$\Delta H_v = \frac{Q_i^2}{2gA_i^2} = 0.0100 \text{ foot}$$

By subtraction, $\Delta WS_L = -0.0048$ foot which agrees closely with the flow profile decline obtained from the nomographs. Essentially the same result could have been obtained from Equation (21) using \bar{n} as the roughness coefficient.

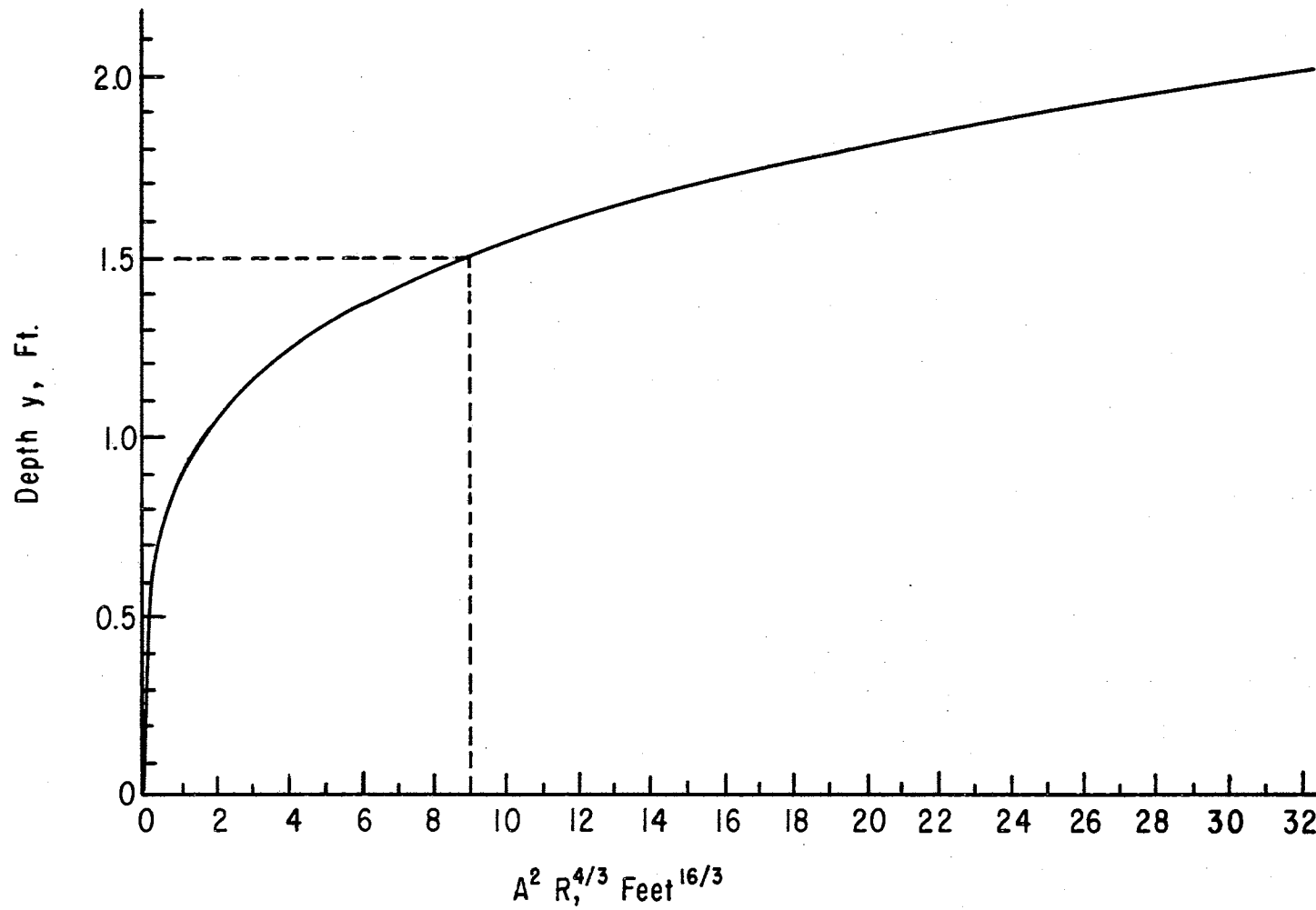


Figure 21. Depth Versus $A^2 R$ for a Trapezoidal Channel With 1 Foot Bottom and 1:1 Side Slopes

Uniformity of Siphon Tube Discharge

Profiles Calculated with \bar{n}

The discharge of every siphon tube was ascertained from the flow profiles calculated with \bar{n} . The tube outlets rested on a standard elevation of 923.913 feet. The head on each tube was obtained by subtracting the outlet elevation from the water-surface in the ditch and the individual tube discharges were computed by Equation (9).

The per cent variation in tube discharge within each experiment was studied. The flow rate of the siphon tube farthest upstream served as the reference value. The calculated variations were positive in sign for rising profiles and negative for declining profiles. Experiments 40 - 42 with 3 inch diameter tubes produced the highest deviations. In Experiment 41 the quantity ΔWS_L was 0.005 feet and a difference in siphon tube discharge between the ends of the bay was 0.89 per cent. For Experiments 1 - 39 using 1.0, 1.5, and 2.0 inch tubes, the maximum discharge variation was 0.75 per cent. This value occurred in Experiment 3 in which $Q = 3.310$ cfs. The largest negative digression -0.33 per cent was found in Experiment 18. Table X lists the change in the water-surface, the upstream tube flow rate, the maximum deviation and the per cent deviation in siphon tube discharge for those experiments producing the largest variations.

The Effect of Roughness

The channel roughness by influencing the flow profile affects the uniformity of siphon tube discharge. The change in tube discharge with controlled variations in the roughness coefficient was evaluated for

TABLE X

PER CENT VARIATION IN TUBE DISCHARGE, BASED
ON THE UPSTREAM SIPHON TUBE, FOR
FLOW PROFILES CALCULATED WITH \bar{n}

Exper. No.	Tube Size inches	$\Delta W S_L$ (Using \bar{n}) feet	Discharge of Upstream Tube		Max. Deviation		Per Cent Deviation
			cfs	gpm	cfs	gpm	
1	2.0	0.0054	0.07353	33.00	0.00045	0.202	0.61
3	2.0	0.0044	0.05596	25.11	0.00042	0.188	0.75
40	3.0	0.0051	0.1399	62.79	0.00114	0.512	0.81
41	3.0	0.0051	0.1288	57.81	0.00114	0.512	0.89
42	3.0	0.0037	0.1099	49.32	0.00088	0.395	0.80

those experiments where $\delta < 0.30$. The initial flow rates and the upstream water-surface elevations from the actual experiments were assumed. Also unchanged were the tube spacings, diameters, inlet locations, and outlet elevations. A horizontal channel was assumed.

The value of the SVF roughness coefficient was varied in 5 per cent increments from 75 per cent to 125 per cent of \bar{n} . From Equation (20), the water-surface elevations at six points in the channel were calculated for each value of \bar{n}_p , where the subscript p refers to the fractional value of the actual \bar{n} . Typical profiles for $p = 0.75, 0.90, 1.00, 1.10, \text{ and } 1.25$ were plotted in Figure 22. The maximum rise for any flow profile was 0.0073 foot, recorded using $\bar{n}_{.75}$ in Experiments 1 and 2. The maximum drop in any profile was 0.0082 foot in Experiment 18.

As expected the calculated variations in tube discharge were largest in magnitude for the maximum and minimum roughness conditions. The most pronounced deviations, regardless of sign, were produced by two groups of experiments:

1. 2 inch tubes at 20 inch spacing (Experiments 1 - 4)
2. 1.5 inch tubes at 40 inch spacing (Experiments 17 - 20)

The greatest positive variation in tube discharge, based on the upstream siphon tube, was 1.10 per cent calculated in Experiment 3 for the roughness coefficient $\bar{n}_{.75} = 0.0144$. On the other hand, a difference of -1.06 per cent was produced for $\bar{n}_{1.25} = 0.0212$ in Experiment 19.

The least value assumed for the roughness coefficient was 0.0103 while the highest was 0.0262. These two values produced tube discharge deviations of 0.23 per cent and 0.08 per cent respectively, in

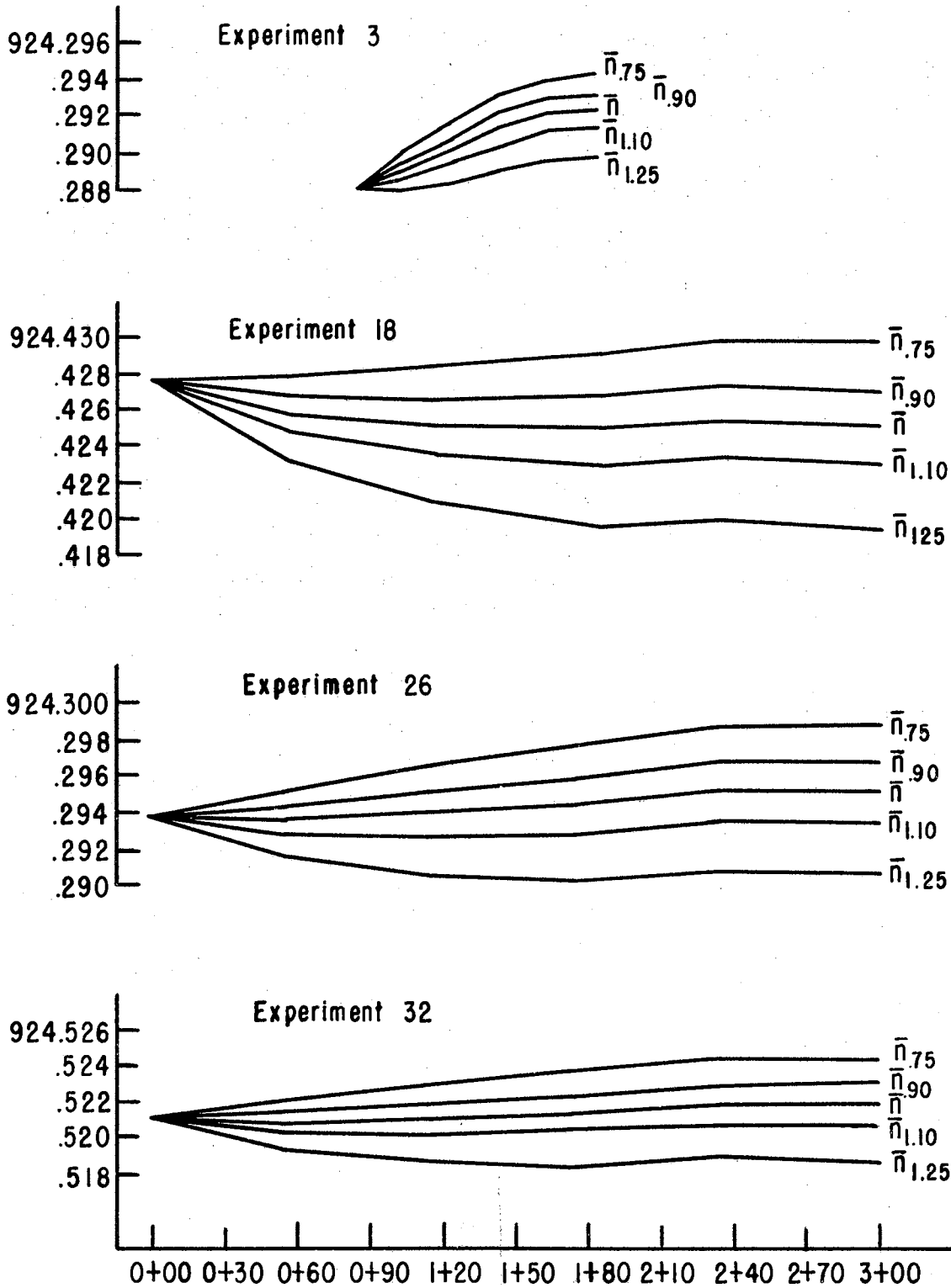


Figure 22. Flow Profiles Calculated From Equation (20) for 0, ± 10 , and ± 25 Per Cent Variation in Roughness

Experiments 29 and 4.

The calculated variations in siphon tube discharge were insignificant when compared to the other factors influencing the operation of a furrow irrigation system. Assuming that the tube outlets have equal elevations, the roughness of a horizontal irrigation channel has a minor effect on the siphon tube discharge uniformity. This conclusion applies to values of \bar{n} within the range 0.0103 -.0262. The actual design, more variation would likely be caused from inaccurate placement of the siphon tube outlets than from choosing an incorrect roughness coefficient.

Unrestrained Siphon Tubes

Experiments were performed in which the inlet ends of the siphon tubes were free to move with the current. The roughness coefficients were desired for both gradually varied and spatially varied flows. For both types of flow 3.25 and 2.50 cfs were the flow rates used. The tube size and spacing selected were 1.5 and 40 inches, respectively. The tube outlet elevation was 923.913 feet while the inlets averaged about 1.0 foot above the channel bottom. In general, the same quantities were measured as compared to the restrained tube experiments.

Gradually Varied Flow

The energy slope was calculated from Equation (11) using water surface and flow rate measurements. Manning's n was then evaluated using Equation (12).

The basis for comparing n values for restrained and unrestrained siphon tubes was a prediction equation that Mink (16) had calculated for restrained siphon tubes spaced at 40 inches. This equation was:

$$n = 0.00510 + R^{1/6} \left[(0.00319 + 0.00821 \frac{TS}{R}) \frac{Su}{R} + \frac{0.44175 R_n}{218500 + 85.61 R_n} \right] \quad (29)$$

where

TS = tube diameter, feet

Su = submergence, feet

R = hydraulic radius, feet

Also, the Reynolds number R_n was defined as:

$$R_n = \frac{VR}{\nu}$$

in which

V = mean velocity of flow, feet/second

ν = kinematic viscosity, ft²/sec.

and R was previously defined.

The values of n calculated from Equation (29) are compared in Table XI with values of n_{gvf} computed for the unrestrained siphon tube experiments. In general, the experimental n values slightly exceeded the values predicted from Equation (29). The opposite result was expected since the inlet ends of the unrestrained siphon tubes were swept downstream.

However, in contrast to the restrained tubes held adjacent to the channel wall, the unrestrained siphon tubes protruded about 1 inch into the stream. The higher flow velocities away from the boundary could have caused the slightly greater energy losses observed for unrestrained siphon tubes.

Further analysis revealed that the current caused the siphon tubes to rotate a maximum of 10° from the channel cross-sectional plane.

TABLE XI

EXPERIMENTAL AND CALCULATED n VALUES
 FROM GVF EXPERIMENTS USING
 UNRESTRAINED SIPHON TUBES

Tube Spacing inches	Tube Size inches	Inflow Q cfs	Average Depth feet	Hydraulic Radius feet	Reynolds Number	Experimental n_{gvf}	Calculated n Eqn. (29)
40	1.5	3.241	1.874	0.865	59230	0.0143	0.0143
40	1.5	3.236	1.798	0.836	68570	0.0138	0.0140
40	1.5	3.255	1.723	0.808	63527	0.0146	0.0137
40	1.5	3.278	1.541	0.739	71888	0.0140	0.0130
40	1.5	2.480	1.814	0.842	44717	0.0148	0.0140
40	1.5	2.508	1.654	0.782	48825	0.0138	0.0134
40	1.5	2.491	1.561	0.747	50830	0.0137	0.0130

(The angles were measured on full tubes with blocked outlets.) For this angle, the submergence would be decreased by only 0.02 foot.

The narrow range of observed n_{gvf} values are adequately represented by their mean of 0.01414. The largest deviation from this value was 4.7 per cent.

Spatially Varied Flow

Six experiments were conducted to ascertain the degree of roughness caused by unrestrained siphon tubes under conditions of decreasing spatially varied flow. Measurements of water-surface elevation allowed the calculation of \bar{n} and n_e using procedures from the restrained tube experiments. These roughness coefficients together with resistances computed using the multivariable model Equation (24) are summarized in Table XII. Equation (24), as compared to Equations (25) and (26), resulted in values of \bar{n} and n_e most representative of the observed roughness coefficients. The average ratio of \bar{n} (calculated) to n_e (calculated) was 1.755 while the experimental values of \bar{n} and n_e produced the average ratio of 1.743. The narrow range of the roughness coefficients made regression analysis of experimental versus calculated n_e and \bar{n} values practically meaningless.

Slight rises (about 0.001 foot) in the observed flow profiles were noted in four experiments:

1. $Q \approx 3.25$ cfs at all three depths
2. $Q = 2.480$ cfs at a depth of 1.813 feet.

The remaining two experiments produced less than 0.001 foot deviation between the upstream and downstream ends of the bay.

TABLE XII

ROUGHNESS COEFFICIENTS FROM SVF EXPERIMENTS
USING UNRESTRAINED SIPHON TUBES

Tube Spacing inches	Tube Size inches	Q cfs	Average Depth feet	\bar{n}	n_e	Roughness Coefficients from Multivariable Equation (24)	
						\bar{n}	n_e
40	1.5	3.262	1.713	0.0157	0.00891	0.0167	0.00952
40	1.5	3.242	1.793	0.0162	0.00924	0.0170	0.00979
40	1.5	3.247	1.859	0.0172	0.00983	0.0173	0.01002
40	1.5	2.484	1.553	0.0157	0.00969	0.0161	0.00896
40	1.5	2.505	1.646	0.0177	0.00967	0.0165	0.00928
40	1.5	2.480	1.813	0.0172	0.00988	0.0171	0.00986

Tube discharges calculated from the water-surface elevations varied a maximum of 0.14 per cent which could be termed excellent discharge control.

CHAPTER VI

SUMMARY AND CONCLUSIONS

Summary

Hydraulic experiments pertaining to siphon tube irrigation were conducted in a horizontal concrete-lined irrigation channel. The hydraulic resistance of the channel was determined for gradually varied flow and decreasing spatially varied flow using various siphon tube spacings, tube diameters, entering discharges, and flow depths.

Values of Manning's n were determined for gradually varied flow in the channel both with and without siphon tubes. Two roughness coefficients were computed for the spatially varied flow experiments. Adjusted \bar{n} was determined by calculating the flow profile which best fitted the measured water-surface elevations. Effective n (or n_e) predicted the total energy change between the ends of the reach containing primed siphon tubes (assuming that $\alpha = 1.00$).

A theoretical relationship between \bar{n} and n_e was derived and was verified by experimental results. Values of \bar{n} and n_e were related to siphon tube spacing, diameter and submergence by linear, quadratic, and cubic multivariable equations. The roughness coefficients for spatially varied and gradually varied flows could not be related with confidence.

Flow profiles for decreasing spatially varied flow were calculated by two procedures, both using \bar{n} , which produced practically equivalent

results. For the first method, a Bernoulli-type energy equation was solved between successive pairs of siphon tubes by incrementing the flow depth. Secondly, profiles based on the upstream water-surface elevation were directly calculated by subtracting the friction energy lost from the velocity head recovered, both components being computed as functions of the entering velocity.

The observed and calculated flow profiles for spatially varied flow were found to have three possible shapes: rising, descending, or level. In general, rising profiles were associated with close siphon tube spacings and large discharges per tube. The maximum observed rise for any profile was 0.005 foot. Declining profiles were associated with (1) small, widely spaced tubes, and (2) moderate siphon tube spacings and tube discharges. The greatest water-surface decline was 0.002 foot.

Siphon tube discharge variations were evaluated for the observed experimental conditions using correct and assumed values of \bar{n} for calculating the flow profiles. For an actual experiment, the highest discharge variation was 0.89 per cent. When \bar{n} was altered ± 25 per cent from its experimental value, the resulting flow profiles produced less than 1.2 per cent deviation in tube discharge.

Pilot experiments involving unrestrained siphon tubes were conducted for both gradually varied flow and spatially varied flow. The roughness coefficients from restrained and unrestrained siphon tube experiments were of similar magnitudes.

Conclusions

The following conclusions are based on the analysis and interpretation of the experimental results:

1. Hydraulic roughness increases with closer siphon tube spacing, larger tube diameter, and greater submergence.
2. Equation (22) is a valid relationship between \bar{n} and n_e .
3. Water-surface profiles for spatially varied flow can be predicted more accurately using \bar{n} than with Manning's n from gradually varied flow.
4. The water-surface elevation at any cross-section in a horizontal prismatic irrigation bay containing primed siphon tubes can be calculated from Equation (20).
5. For the type of channel used in this study, the total energy change between the ends of a reach containing primed siphon tubes can be accurately predicted from the Manning formula using n_e , the entering velocity and flow depth.
6. Variations in siphon tube discharge in a horizontal channel can be expected to be less than 1.5 per cent, provided that the tube outlets have the same elevation.
7. Based on limited observations, unrestrained siphon tubes appear to produce hydraulic roughnesses similar to restrained tubes for equivalent conditions of flow, tube size, and tube spacing.

Suggestions For Future Research

1. The roughness coefficients for gradually varied flow and decreasing spatially varied flow are probably related. A definition of this relationship would be beneficial since roughness coefficients for gradually varied flow are more easily obtained.
2. The hydraulic resistance caused by unrestrained siphon tubes needs more positive definition, especially for spatially varied flow.
3. Automatic cut-back furrow irrigation systems will likely increase in popularity as labor costs rise. Therefore, experiments should be conducted to determine the proper roughness coefficients for these systems.
4. Automatic furrow irrigation could be accomplished from notches formed in the side of a concrete channel producing multiple side weir discharge. An extensive study of the hydraulic phenomena encountered in this form of decreasing spatially varied flow might contribute significantly to hydraulic and irrigation knowledge.

SELECTED BIBLIOGRAPHY

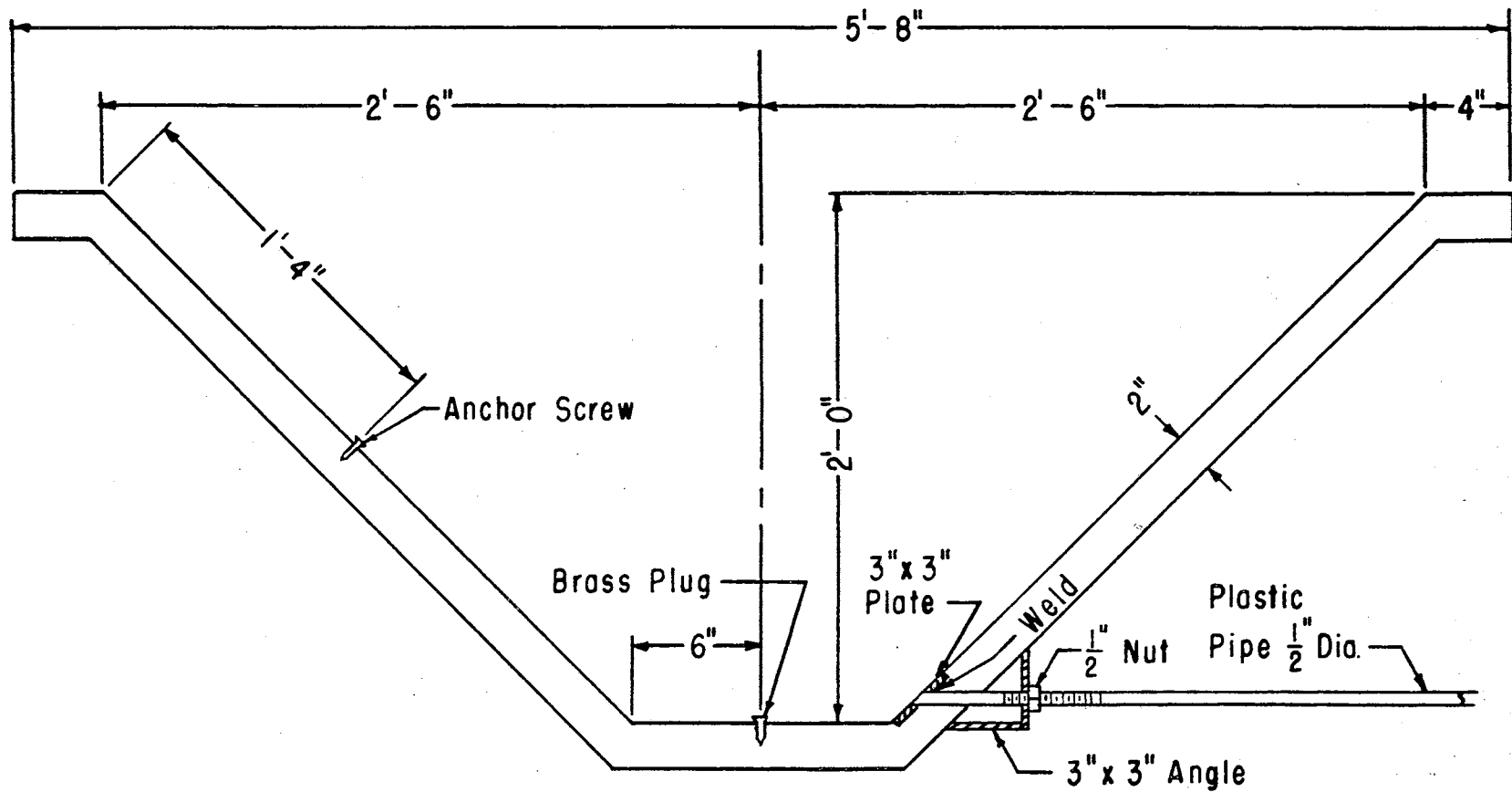
1. Argyropoulos, Praxitelis. Discussion of "Side Channel Spillway Design" by Harold S. Farney and Adolfs Markus. Proceedings of the American Society of Civil Engineers, Journal of the Hydraulics Division. 88:225-226, No. HY6, November, 1962.
2. Carter, R. W., et al. "Friction Factors in Open Channels." Proceedings of the American Society of Civil Engineers, Journal of the Hydraulics Division. 89:97-143, No. HY2, March, 1963.
3. Chow, Ven Te. Open Channel Hydraulics. New York: McGraw-Hill Book Company, Inc., 1959.
4. Collinge, Vincent K. "The Discharge Capacity of Side Weirs." Proceedings of the Institution of Civil Engineers, London. 6:288-304, February, 1957.
5. Farney, Harold S. and Adolfs Markus. "Side Channel Spillway Design." Proceedings of the American Society of Civil Engineers, Journal of the Hydraulics Division. 88:131-154, No. HY3, May, 1962.
6. Farney, Harold S. and Adolfs Markus. Closure to "Side Channel Spillway Design" by Harold S. Farney and Adolfs Markus. Proceedings of the American Society of Civil Engineers, Journal of the Hydraulics Division. 89:223-228, No. HY6, November, 1963.
7. Garton, James E. and Albert L. Mink. "Spatially Varied Flow in an Irrigation Distribution Ditch." Transactions of the American Society of Agricultural Engineers. 8:530-531, No. 4, 1965.
8. Hansen, Vaughn E. "The Importance of Hydraulics of Surface Irrigation." Proceedings of the American Society of Civil Engineers, Journal of the Irrigation and Drainage Division. 84:1788.1-1788.8, No. 1, September, 1958.
9. Hinds, Julian. "Side Channel Spillways: Hydraulic Theory, Erosion Factors, and Experimental Determination of Losses." Transactions of the American Society of Civil Engineers. 89:881-927, 1926.

10. Israelsen, Orson W. and Vaughn E. Hansen. Irrigation Principles and Practices. 3rd ed. New York: John Wiley and Sons, Inc., 1962.
11. Keflemariam, Joseph. "Flow Through Plastic Siphon Tubes." Special Report, Agricultural Engineering Department, Oklahoma State University, 1966.
12. Keller, Jack. "Effect of Irrigation Method on Water Conservation." Proceedings of the American Society of Civil Engineers, Journal of the Irrigation and Drainage Division. 91:61-72, No. IR2, June, 1965.
13. King, Horace W. and Ernest F. Brater. Handbook of Hydraulics. 5th ed. New York: McGraw-Hill Book Company, Inc., 1963.
14. Li, Wen-Hsiung. "Open Channels with Nonuniform Discharge." Transactions of the American Society of Civil Engineers, 120:255-274, 1955.
15. McCool, Don K. "Spatially Varied Steady Flow in a Vegetated Channel." Unpublished Ph.D. dissertation, Oklahoma State University, 1965.
16. Mink, Albert L. "The Hydraulics of an Irrigation Distribution Channel." Unpublished Ph.D. dissertation, Oklahoma State University, 1967.
17. Murphy, Glenn. Similitude in Engineering. New York: The Ronald Press Company, 1950.
18. Nimmo, W. H. R. "Side Spillways for Regulating Diversion Canals." Transactions of the American Society of Civil Engineers. 92:1561-1584, 1928.
19. Rhoades, Edd D. "The Effect of the Moldboard Plowshare Condition on the Formation of 'Plow Sole'." Unpublished M.S. thesis, Oklahoma Agricultural and Mechanical College, 1951.
20. Rouse, Hunter. Elementary Mechanics of Fluids. New York: John Wiley and Sons, Inc., 1946.
21. "Small, Low - Cost Hydraulic Structures for Conveyance and Distribution Systems." Panel Discussion. Proceedings of the American Society of Civil Engineers, Journal of the Irrigation and Drainage Division. 90:63-72, No. IR4, December, 1964.
22. Steel, Robert G. D. and James H. Torrie. Principles and Procedures of Statistics. New York: McGraw-Hill Book Company, Inc., 1960.
23. Streeter, Victor L. Fluid Mechanics. New York: McGraw-Hill Book Company, Inc., 1962.

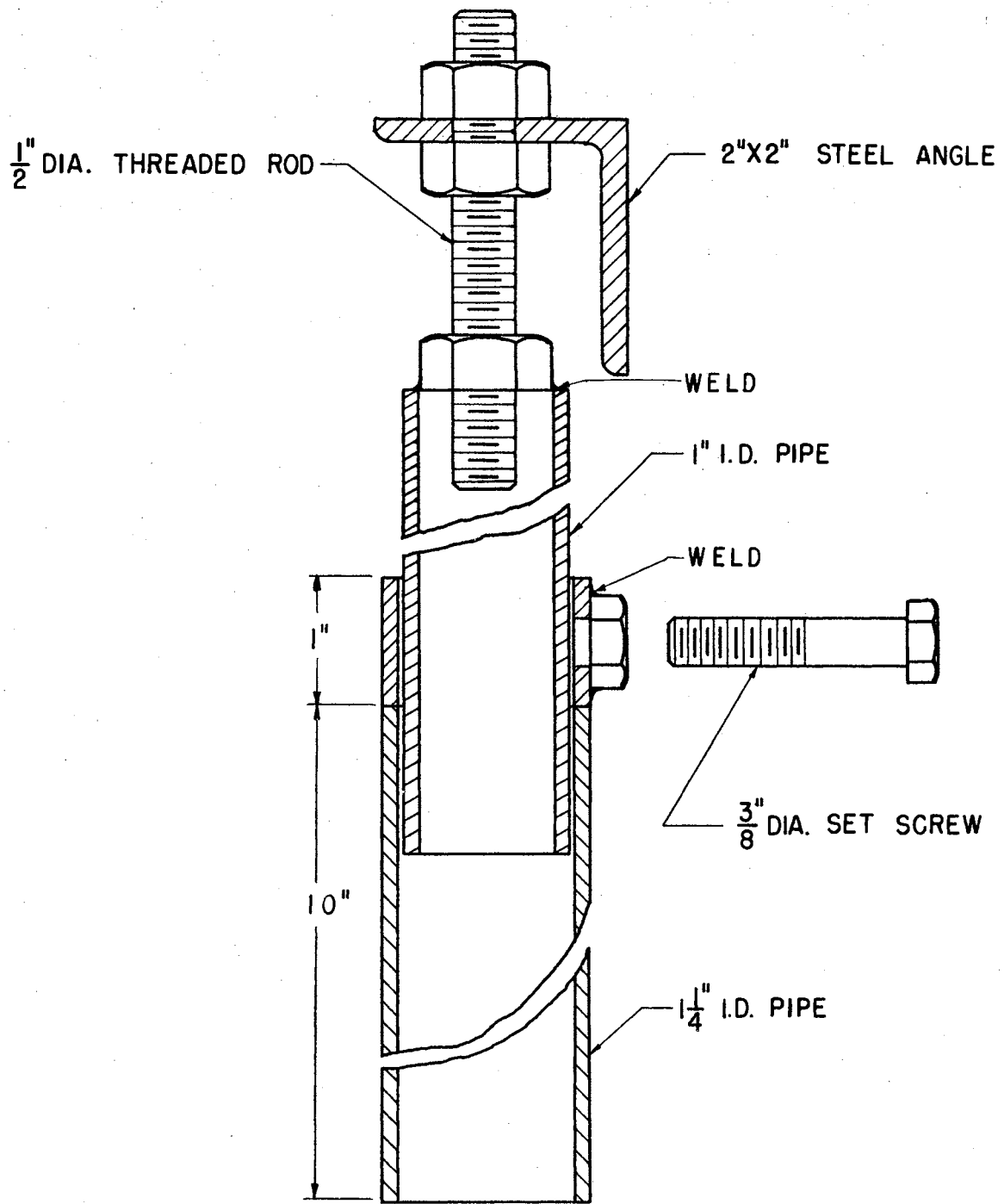
24. Tilp, Paul J. "Capacity Tests in Large Concrete-Lined Canals." Proceedings of the American Society of Civil Engineers, Journal of the Hydraulics Division. 91:189-216, No. HY3, May, 1965.
25. Vennard, John K. Elementary Fluid Mechanics. 4th ed. New York: John Wiley and Sons, Inc., 1961.
26. Woodward, Sherman M. and Chesley J. Posey. Hydraulics of Steady Flow in Open Channels. New York: John Wiley and Sons, Inc., 1941.

APPENDIX A

CROSS-SECTIONS OF CHANNEL,
GAGE WELL, AND SIPHON
TUBE MOUNT



Experimental Channel Cross-Section at a Gaging Station

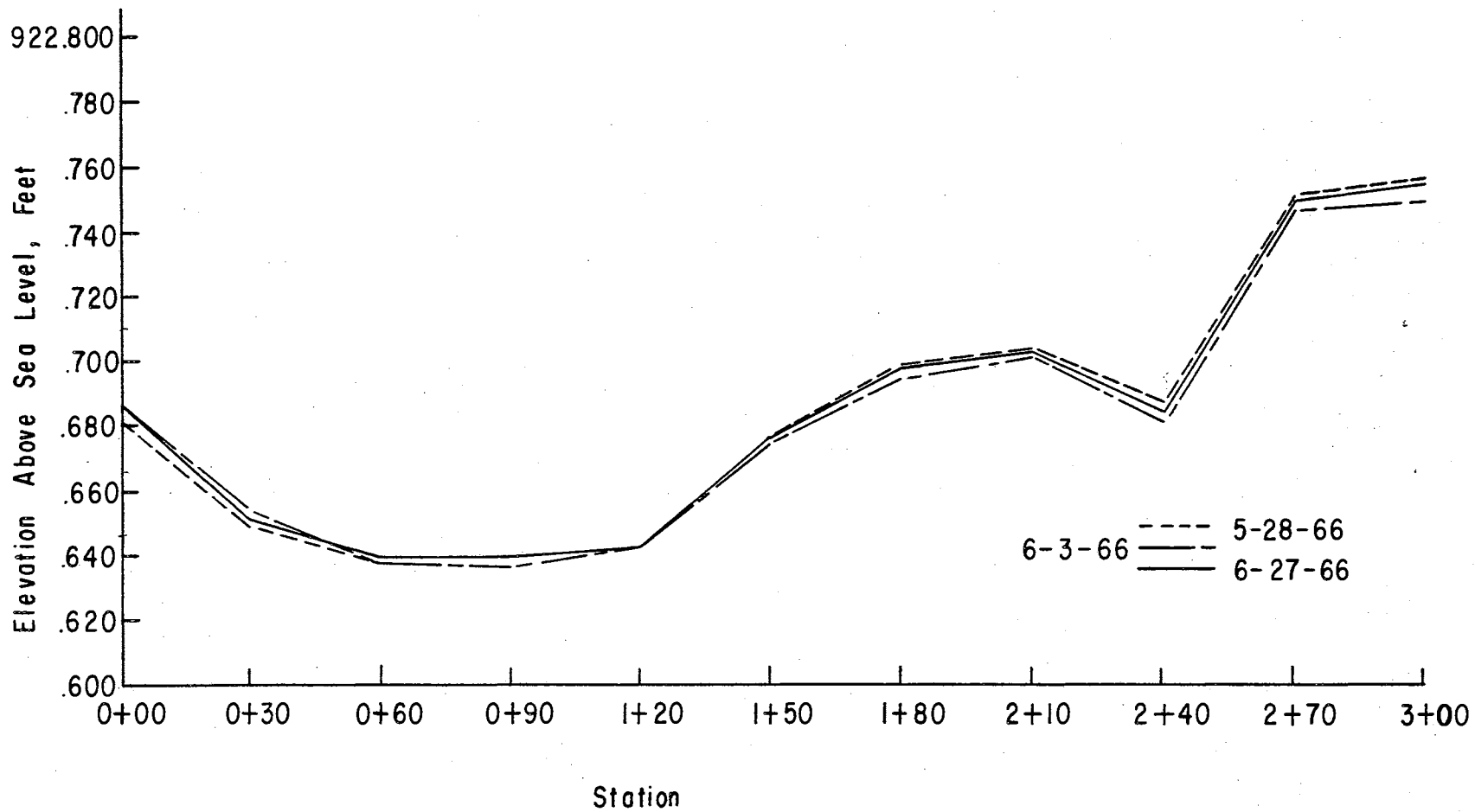


Cross-Section of a Typical Siphon Tube Mount

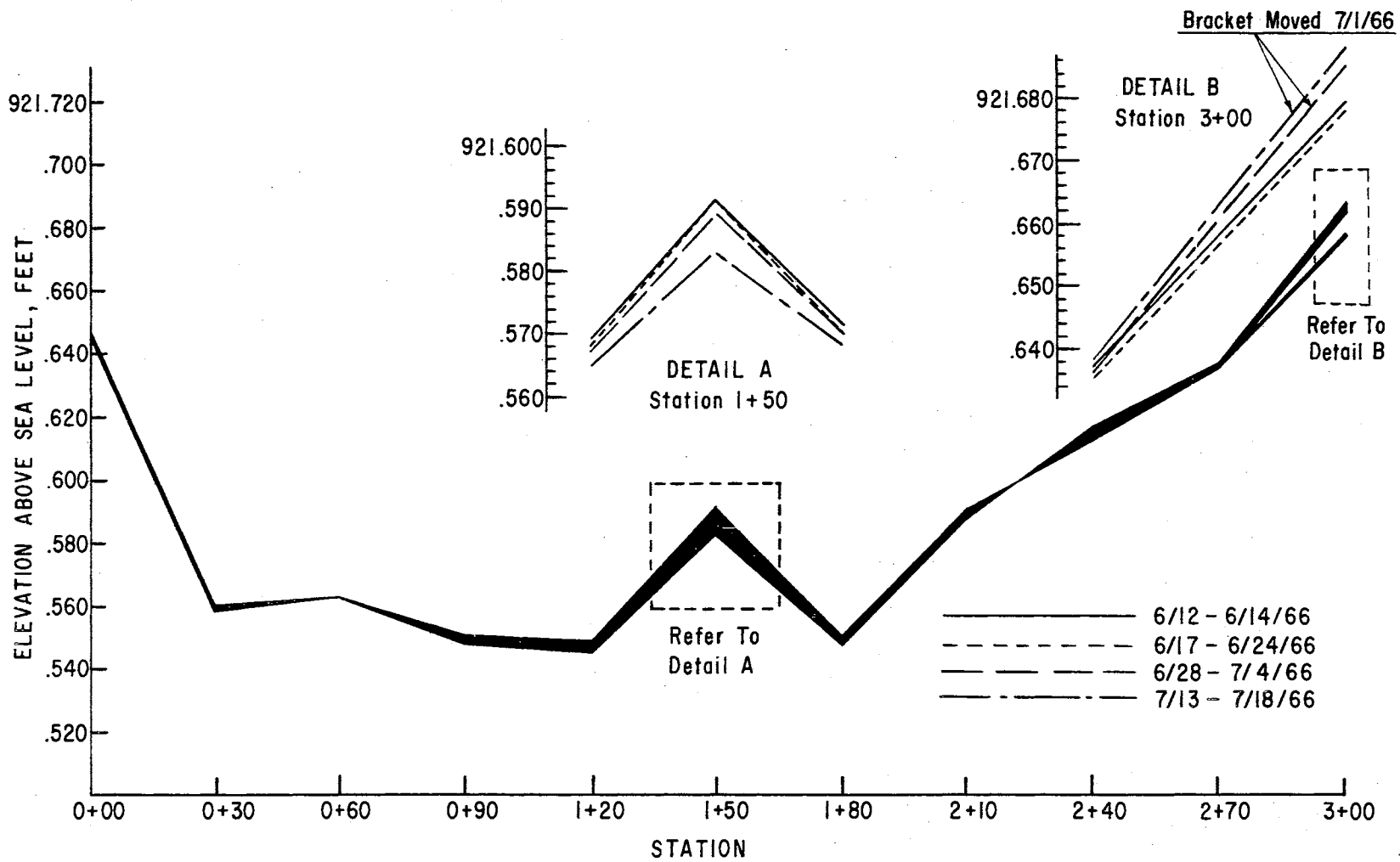
APPENDIX B

BRASS PLUG AND GAGE

ZERO ELEVATIONS



Elevations of the Brass Plugs Which Were Embedded in the Concrete Channel Bottom



Gage Zero Elevations for Referencing Water-Surface Measurements

APPENDIX C

STATISTICAL COMPARISON OF \bar{n} AND n_{gvf}

GROUP EXPERIMENT COMPARISON (22) OF \bar{n} AND n_{gvf}
 FROM SVF AND GVF EXPERIMENTS ($\delta \cong 0.50$)
 HAVING SIMILAR DEPTHS, DISCHARGES,
 SIPHON TUBE SPACINGS AND
 DIAMETERS

Tube Spacing	Tube Diameter	Discharge Q	Roughness Coefficients	
			$\bar{n} (= X_1)$	$n_{gvf} (= X_2)$
inches	inches	cfs		
20	2.0	4.3	0.0190	0.0170
20	2.0	4.3	0.0190	
20	2.0	3.3	0.0192	0.0167
20	2.0	3.3	0.0210	
20	2.0	2.25	0.0296	0.0156
20	2.0	1.65	0.0325	0.0165
20	1.5	3.85	0.0190	0.0160
20	1.5	2.5	0.0175	0.0160
20	1.5	2.3	0.0166	0.0176
20	1.5	1.5	0.0163	0.0163
60	2.0	4.2	0.0162	0.0143
60	2.0	3.3	0.0143	0.0140
60	2.0	2.25	0.0188	0.0148
60	2.0	1.65	0.0141	0.0141
60	1.5	2.5	0.0137	0.0147
60	1.5	1.65	0.0117	0.0137
80	2.0	3.4	0.0155	0.0141
80	2.0	2.5	0.0144	0.0126
80	1.5	1.9	0.0161	0.0131

$$\Sigma X_1 = 0.3445$$

$$\Sigma X_1^2 = 0.0067231$$

$$\bar{X}_1 = 0.01813$$

$$\Sigma X_2 = 0.2571$$

$$\Sigma X_2^2 = 0.0039223$$

$$\bar{X}_2 = 0.01512$$

Sums of Squares:

$$\Sigma x_1^2 = \Sigma X_1^2 - (\Sigma X_1)^2 / m_1 = (6.7231 - 6.6243) \times 10^{-3}$$

$$\Sigma x_1^2 = 4.768 \times 10^{-4}$$

$$\Sigma x_2^2 = \Sigma X_2^2 - (\Sigma X_2)^2 / m_2 = (3.9223 - 3.8883) \times 10^{-3}$$

$$\Sigma x_2^2 = 0.340 \times 10^{-4}$$

Weighted Average of the Sample Variances:

$$s_p^2 = \frac{\Sigma x_1^2 + \Sigma x_2^2}{m_1 + m_2 - 2} = 1.5024 \times 10^{-4}$$

Standard Deviation of the Difference Between Means:

$$s_d = \sqrt{s_p^2 \left(\frac{m_1 + m_2}{m_1 m_2} \right)} = 1.2940 \times 10^{-3}$$

Hypothesis:

$$\mu_{\bar{n}} = \mu_{n_{\text{gvf}}}$$

Alternate Hypothesis:

$$\mu_{\bar{n}} \neq \mu_{n_{\text{gvf}}}$$

Test of Hypothesis:

$$\text{Degrees of freedom} = m_1 + m_2 - 2 = 34$$

$$\text{Calculated Student's } t = \frac{\bar{X}_1 - \bar{X}_2}{s_d} = 2.326$$

$$\text{Tabulated } t_{(.05)} = 2.033$$

Conclusion - Reject Hypothesis

APPENDIX D

EXPERIMENTAL DATA , ROUGHNESS COEFFICIENTS , AND
CALCULATED FLOW PROFILES FOR SPATIALLY
VARIED FLOW EXPERIMENTS

EXPERIMENT 1
 Q= 4.287 CFS SPACING= 20 IN. DIAMETER= 2.0 IN.
 N-BAR= 0.01900 N-EFF= 0.01157
 VERTICAL TUBE SUBMERGENCE= 0.811 FT.

LINEAR REGRESSION ELEVATIONS (SVF)
 UPSTREAM= 924.4819 DOWNSTREAM= 924.4873

STATIONS	OBSERVED WATER-SURFACE ELEVATIONS	PROFILE CALCULATED WITH N-BAR	PROFILE CALCULATED WITH N-GVF
0+00	924.485		
0+30	924.485		
0+60	924.487		
0+90	924.482	924.4822	924.4814
1+20	924.484	924.4844	924.4842
1+50	924.486	924.4863	924.4863
1+80	924.487	924.4873	924.4873
2+10	924.486		
2+40	924.486		
2+70	924.486		
3+00	924.485		

EXPERIMENT 2
 Q= 4.279 CFS SPACING= 20 IN. DIAMETER= 2.0 IN.
 N-BAR= 0.01900 N-EFF= 0.01174
 VERTICAL TUBE SUBMERGENCE= 0.813 FT.

LINEAR REGRESSION ELEVATIONS (SVF)
 UPSTREAM= 924.4840 DOWNSTREAM= 924.4893

STATIONS	OBSERVED WATER-SURFACE ELEVATIONS	PROFILE CALCULATED WITH N-BAR	PROFILE CALCULATED WITH N-GVF
0+00	924.489		
0+30	924.488		
0+60	924.487		
0+90	924.484	924.4842	924.4834
1+20	924.486	924.4864	924.4862
1+50	924.488	924.4883	924.4883
1+80	924.489	924.4893	924.4893
2+10	924.487		
2+40	924.488		
2+70	924.489		
3+00	924.488		

EXPERIMENT 3
 Q= 3.310 CFS SPACING= 20 IN. DIAMETER= 2.0 IN.
 N-BAR= 0.01920 N-EFF= 0.01093
 VERTICAL TUBE SUBMERGENCE= 0.616 FT.

LINEAR REGRESSION ELEVATIONS (SVF)
 UPSTREAM= 924.2880 DOWNSTREAM= 924.2924

STATIONS	OBSERVED WATER-SURFACE ELEVATIONS	PROFILE CALCULATED WITH N-BAR	PROFILE CALCULATED WITH N-GVF
0+00	924.290		
0+30	924.291		
0+60	924.290		
0+90	924.288	924.2882	924.2874
1+20	924.290	924.2899	924.2896
1+50	924.291	924.2914	924.2914
1+80	924.292	924.2923	924.2923
2+10	924.291		
2+40	924.291		
2+70	924.292		
3+00	924.291		

EXPERIMENT 4
 Q= 3.300 CFS SPACING= 20 IN. DIAMETER= 2.0 IN.
 N-BAR= 0.02095 N-EFF= 0.01228
 VERTICAL TUBE SUBMERGENCE= 0.616 FT.

LINEAR REGRESSION ELEVATIONS (SVF)
 UPSTREAM= 924.2888 DOWNSTREAM= 924.2921

STATIONS	OBSERVED WATER-SURFACE ELEVATIONS	PROFILE CALCULATED WITH N-BAR	PROFILE CALCULATED WITH N-GVF
0+00	924.291		
0+30	924.291		
0+60	924.290		
0+90	924.289	924.2889	924.2871
1+20	924.290	924.2900	924.2894
1+50	924.291	924.2912	924.2911
1+80	924.292	924.2921	924.2921
2+10	924.291		
2+40	924.292		
2+70	924.292		
3+00	924.291		

EXPERIMENT 5
 Q= 2.248 CFS SPACING= 20 IN. DIAMETER= 2.0 IN.
 N-BAR= 0.02960 N-EFF= 0.01757
 VERTICAL TUBE SUBMERGENCE= 0.821 FT.

LINEAR REGRESSION ELEVATIONS (SVF)
 UPSTREAM= 924.4956 DOWNSTREAM= 924.4968

STATIONS	OBSERVED WATER-SURFACE ELEVATIONS	PROFILE CALCULATED WITH N-BAR	PROFILE CALCULATED WITH N-GVF
0+00	924.496		
0+30	924.495		
0+60	924.496		
0+90	924.495	924.4974	924.4949
1+20	924.496	924.4959	924.4953
1+50	924.497	924.4967	924.4967
1+80	924.497	924.4968	924.4968
2+10	924.496		
2+40	924.496		
2+70	924.497		
3+00	924.497		

EXPERIMENT 6
 Q= 1.651 CFS SPACING= 20 IN. DIAMETER= 2.0 IN.
 N-BAR= 0.03250 N-EFF= 0.01943
 VERTICAL TUBE SUBMERGENCE= 0.603 FT.

LINEAR REGRESSION ELEVATIONS (SVF)
 UPSTREAM= 924.2780 DOWNSTREAM= 924.2785

STATIONS	OBSERVED WATER-SURFACE ELEVATIONS	PROFILE CALCULATED WITH N-BAR	PROFILE CALCULATED WITH N-GVF
0+00	924.278		
0+30	924.278		
0+60	924.278		
0+90	924.278	924.2798	924.2771
1+20	924.278	924.2779	924.2773
1+50	924.278	924.2784	924.2784
1+80	924.279	924.2785	924.2785
2+10	924.278		
2+40	924.278		
2+70	924.279		
3+00	924.278		

EXPERIMENT 7
 Q= 3.850 CFS SPACING= 20 IN. DIAMETER= 1.5 IN.
 N-BAR= 0.01900 N-EFF= 0.01150
 VERTICAL TUBE SUBMERGENCE= 0.823 FT.

LINEAR REGRESSION ELEVATIONS (SVF)
 UPSTREAM= 924.4958 DOWNSTREAM= 924.4981

STATIONS	OBSERVED WATER-SURFACE ELEVATIONS	PROFILE CALCULATED WITH N-BAR	PROFILE CALCULATED WITH N-GVF
0+00	924.496		
0+30	924.496		
0+60	924.496	924.4958	924.4941
0+90	924.495	924.4961	924.4952
1+20	924.497	924.4967	924.4963
1+50	924.499	924.4973	924.4971
1+80	924.498	924.4978	924.4978
2+10	924.497	924.4981	924.4981
2+40	924.499		
2+70	924.499		
3+00	924.498		

EXPERIMENT 8
 Q= 2.498 CFS SPACING= 20 IN. DIAMETER= 1.5 IN.
 N-BAR= 0.01750 N-EFF= 0.01004
 VERTICAL TUBE SUBMERGENCE= 0.550 FT.

LINEAR REGRESSION ELEVATIONS (SVF)
 UPSTREAM= 924.2230 DOWNSTREAM= 924.2250

STATIONS	OBSERVED WATER-SURFACE ELEVATIONS	PROFILE CALCULATED WITH N-BAR	PROFILE CALCULATED WITH N-GVF
0+00	924.224		
0+30	924.224		
0+60	924.223	924.2229	924.2225
0+90	924.223	924.2231	924.2231
1+20	924.224	924.2237	924.2237
1+50	924.225	924.2242	924.2242
1+80	924.224	924.2248	924.2248
2+10	924.225	924.2250	924.2250
2+40	924.225		
2+70	924.226		
3+00	924.225		

EXPERIMENT 9
 Q= 2.300 CFS SPACING= 20 IN. DIAMETER= 1.5 IN.
 N-BAR= 0.01660 N-EFF= 0.01040
 VERTICAL TUBE SUBMERGENCE= 0.830 FT.

LINEAR REGRESSION ELEVATIONS (SVF)
 UPSTREAM= 924.5036 DOWNSTREAM= 924.5054

STATIONS	OBSERVED WATER-SURFACE ELEVATIONS	PROFILE CALCULATED WITH N-BAR	PROFILE CALCULATED WITH N-GVF
0+00	924.505		
0+30	924.506		
0+60	924.504		
0+90	924.503	924.5036	924.5037
1+20	924.505	924.5045	924.5045
1+50	924.505	924.5051	924.5051
1+80	924.505	924.5054	924.5054
2+10	924.505		
2+40	924.506		
2+70	924.505		
3+00	924.505		

EXPERIMENT 10
 Q= 1.506 CFS SPACING= 20 IN. DIAMETER= 1.5 IN.
 N-BAR= 0.01630 N-EFF= 0.01032
 VERTICAL TUBE SUBMERGENCE= 0.546 FT.

LINEAR REGRESSION ELEVATIONS (SVF)
 UPSTREAM= 924.2194 DOWNSTREAM= 924.2206

STATIONS	OBSERVED WATER-SURFACE ELEVATIONS	PROFILE CALCULATED WITH N-BAR	PROFILE CALCULATED WITH N-GVF
0+00	924.221		
0+30	924.221		
0+60	924.220		
0+90	924.219	924.2193	924.2193
1+20	924.220	924.2199	924.2199
1+50	924.221	924.2204	924.2204
1+80	924.220	924.2206	924.2206
2+10	924.220		
2+40	924.221		
2+70	924.221		
3+00	924.221		

EXPERIMENT 11
 Q= 1.646 CFS SPACING= 20 IN. DIAMETER= 1.0 IN.
 N-BAR= 0.01830 N-EFF= 0.01374
 VERTICAL TUBE SUBMERGENCE= 0.832 FT.

LINEAR REGRESSION ELEVATIONS (SVF)
 UPSTREAM= 924.5063 DOWNSTREAM= 924.5063

STATIONS	OBSERVED WATER-SURFACE ELEVATIONS	PROFILE CALCULATED WITH N-BAR	PROFILE CALCULATED WITH N-GVF
0+00	924.506		
0+30	924.506		
0+60	924.506	924.5063	924.5052
0+90	924.506	924.5063	924.5057
1+20	924.507	924.5063	924.5059
1+50	924.507	924.5063	924.5062
1+80	924.506	924.5063	924.5063
2+10	924.506	924.5063	924.5063
2+40	924.507		
2+70	924.506		
3+00	924.506		

EXPERIMENT 12
 Q= 1.146 CFS SPACING= 20 IN. DIAMETER= 1.0 IN.
 N-BAR= 0.01050 N-EFF= 0.00776
 VERTICAL TUBE SUBMERGENCE= 0.561 FT.

LINEAR REGRESSION ELEVATIONS (SVF)
 UPSTREAM= 924.2355 DOWNSTREAM= 924.2362

STATIONS	OBSERVED WATER-SURFACE ELEVATIONS	PROFILE CALCULATED WITH N-BAR	PROFILE CALCULATED WITH N-GVF
0+00	924.235		
0+30	924.235		
0+60	924.235	924.2355	924.2355
0+90	924.236	924.2358	924.2358
1+20	924.236	924.2361	924.2361
1+50	924.236	924.2362	924.2362
1+80	924.236	924.2362	924.2362
2+10	924.236	924.2362	924.2362
2+40	924.236		
2+70	924.236		
3+00	924.236		

EXPERIMENT 13
 Q= 3.788 CFS SPACING= 40 IN. DIAMETER= 2.0 IN.
 N-BAR= 0.01641 N-EFF= 0.00937
 VERTICAL TUBE SUBMERGENCE= 0.908 FT.

LINEAR REGRESSION ELEVATIONS (SVF)
 UPSTREAM= 924.5827 DOWNSTREAM= 924.5833

STATIONS	OBSERVED WATER-SURFACE ELEVATIONS	PROFILE CALCULATED WITH N-BAR	PROFILE CALCULATED WITH N-GVF
0+00	924.583	924.5826	924.5802
0+30	924.584	924.5823	924.5806
0+60	924.583	924.5824	924.5811
0+90	924.583	924.5822	924.5814
1+20	924.581	924.5823	924.5818
1+50	924.583	924.5823	924.5820
1+80	924.582	924.5826	924.5824
2+10	924.582	924.5827	924.5826
2+40	924.584	924.5830	924.5830
2+70	924.585	924.5832	924.5832
3+00	924.583	924.5833	924.5833

EXPERIMENT 14
 Q= 3.318 CFS SPACING= 40 IN. DIAMETER= 2.0 IN.
 N-BAR= 0.01687 N-EFF= 0.00955
 VERTICAL TUBE SUBMERGENCE= 0.774 FT.

LINEAR REGRESSION ELEVATIONS (SVF)
 UPSTREAM= 924.4487 DOWNSTREAM= 924.4485

STATIONS	OBSERVED WATER-SURFACE ELEVATIONS	PROFILE CALCULATED WITH N-BAR	PROFILE CALCULATED WITH N-GVF
0+00	924.449	924.4488	924.4459
0+30	924.450	924.4483	924.4462
0+60	924.448	924.4482	924.4467
0+90	924.449	924.4479	924.4468
1+20	924.447	924.4479	924.4472
1+50	924.449	924.4478	924.4473
1+80	924.448	924.4479	924.4477
2+10	924.447	924.4481	924.4479
2+40	924.450	924.4483	924.4483
2+70	924.450	924.4484	924.4484
3+00	924.448	924.4485	924.4485

EXPERIMENT 15
 Q= 2.681 CFS SPACING= 40 IN. DIAMETER= 2.0 IN.
 N-BAR= 0.01607 N-EFF= 0.00908
 VERTICAL TUBE SUBMERGENCE= 0.635 FT.

LINEAR REGRESSION ELEVATIONS (SVF)
 UPSTREAM= 924.3101 DOWNSTREAM= 924.3100

STATIONS	OBSERVED WATER-SURFACE ELEVATIONS	PROFILE CALCULATED WITH N-BAR	PROFILE CALCULATED WITH N-GVF
0+00	924.310	924.3102	924.3079
0+30	924.311	924.3098	924.3081
0+60	924.310	924.3097	924.3085
0+90	924.311	924.3095	924.3086
1+20	924.309	924.3095	924.3089
1+50	924.310	924.3094	924.3090
1+80	924.309	924.3095	924.3093
2+10	924.309	924.3096	924.3095
2+40	924.311	924.3099	924.3098
2+70	924.311	924.3100	924.3099
3+00	924.310	924.3100	924.3100

EXPERIMENT 16
 Q= 2.240 CFS SPACING= 40 IN. DIAMETER= 2.0 IN.
 N-BAR= 0.01555 N-EFF= 0.00889
 VERTICAL TUBE SUBMERGENCE= 0.547 FT.

LINEAR REGRESSION ELEVATIONS (SVF)
 UPSTREAM= 924.2223 DOWNSTREAM= 924.2221

STATIONS	OBSERVED WATER-SURFACE ELEVATIONS	PROFILE CALCULATED WITH N-BAR	PROFILE CALCULATED WITH N-GVF
0+00	924.222	924.2222	924.2206
0+30	924.223	924.2217	924.2206
0+60	924.222	924.2216	924.2209
0+90	924.223	924.2214	924.2209
1+20	924.221	924.2215	924.2212
1+50	924.223	924.2214	924.2212
1+80	924.221	924.2216	924.2214
2+10	924.221	924.2217	924.2216
2+40	924.223	924.2219	924.2219
2+70	924.224	924.2220	924.2220
3+00	924.221	924.2221	924.2221

EXPERIMENT 17
 Q= 4.226 CFS SPACING= 40 IN. DIAMETER= 1.5 IN.
 N-BAR= 0.01847 N-EFF= 0.01037
 VERTICAL TUBE SUBMERGENCE= 0.902 FT.

LINEAR REGRESSION ELEVATIONS (SVF)
 UPSTREAM= 924.5771 DOWNSTREAM= 924.5760

STATIONS	OBSERVED WATER-SURFACE ELEVATIONS	PROFILE CALCULATED WITH N-BAR	PROFILE CALCULATED WITH N-GVF
0+00	924.576	924.5771	924.5721
0+30	924.579	924.5764	924.5728
0+60	924.577	924.5759	924.5734
0+90	924.578	924.5755	924.5738
1+20	924.574	924.5753	924.5742
1+50	924.577	924.5752	924.5745
1+80	924.575	924.5752	924.5749
2+10	924.576	924.5755	924.5753
2+40	924.577	924.5758	924.5757
2+70	924.578	924.5759	924.5759
3+00	924.575	924.5760	924.5760

EXPERIMENT 18
 Q= 3.612 CFS SPACING= 40 IN. DIAMETER= 1.5 IN.
 N-BAR= 0.01819 N-EFF= 0.01020
 VERTICAL TUBE SUBMERGENCE= 0.752 FT.

LINEAR REGRESSION ELEVATIONS (SVF)
 UPSTREAM= 924.4276 DOWNSTREAM= 924.4260

STATIONS	OBSERVED WATER-SURFACE ELEVATIONS	PROFILE CALCULATED WITH N-BAR	PROFILE CALCULATED WITH N-GVF
0+00	924.427	924.4277	924.4229
0+30	924.429	924.4268	924.4235
0+60	924.427	924.4263	924.4239
0+90	924.428	924.4258	924.4242
1+20	924.425	924.4256	924.4245
1+50	924.427	924.4254	924.4248
1+80	924.426	924.4254	924.4251
2+10	924.426	924.4255	924.4255
2+40	924.427	924.4258	924.4258
2+70	924.428	924.4260	924.4260
3+00	924.425	924.4260	924.4260

EXPERIMENT 19
 Q= 2.884 CFS SPACING= 40 IN. DIAMETER= 1.5 IN.
 N-BAR= 0.01692 N-EFF= 0.00943
 VERTICAL TUBE SUBMERGENCE= 0.609 FT.

LINEAR REGRESSION ELEVATIONS (SVF)
 UPSTREAM= 924.2841 DOWNSTREAM= 924.2833

STATIONS	OBSERVED WATER-SURFACE ELEVATIONS	PROFILE CALCULATED WITH N-BAR	PROFILE CALCULATED WITH N-GVF
0+00	924.284	924.2842	924.2807
0+30	924.285	924.2837	924.2812
0+60	924.284	924.2833	924.2814
0+90	924.285	924.2830	924.2817
1+20	924.282	924.2828	924.2820
1+50	924.284	924.2827	924.2822
1+80	924.282	924.2827	924.2825
2+10	924.283	924.2828	924.2828
2+40	924.284	924.2831	924.2831
2+70	924.285	924.2832	924.2832
3+00	924.283	924.2833	924.2833

EXPERIMENT 20
 Q= 2.137 CFS SPACING= 40 IN. DIAMETER= 1.5 IN.
 N-BAR= 0.01519 N-EFF= 0.00854
 VERTICAL TUBE SUBMERGENCE= 0.475 FT.

LINEAR REGRESSION ELEVATIONS (SVF)
 UPSTREAM= 924.1496 DOWNSTREAM= 924.1496

STATIONS	OBSERVED WATER-SURFACE ELEVATIONS	PROFILE CALCULATED WITH N-BAR	PROFILE CALCULATED WITH N-GVF
0+00	924.149	924.1497	924.1480
0+30	924.151	924.1494	924.1482
0+60	924.149	924.1492	924.1484
0+90	924.151	924.1491	924.1485
1+20	924.148	924.1491	924.1486
1+50	924.150	924.1491	924.1487
1+80	924.149	924.1491	924.1489
2+10	924.149	924.1492	924.1492
2+40	924.150	924.1495	924.1494
2+70	924.151	924.1496	924.1496
3+00	924.149	924.1496	924.1496

EXPERIMENT 21
 Q= 1.770 CFS SPACING= 40 IN. DIAMETER= 1.0 IN.
 N-BAR= 0.01362 N-EFF= 0.00947
 VERTICAL TUBE SUBMERGENCE= 0.910 FT.

LINEAR REGRESSION ELEVATIONS (SVF)
 UPSTREAM= 924.5843 DOWNSTREAM= 924.5844

STATIONS	OBSERVED WATER-SURFACE ELEVATIONS	PROFILE CALCULATED WITH N-BAR	PROFILE CALCULATED WITH N-GVF
0+00	924.583	924.5843	924.5843
0+30	924.585	924.5844	924.5844
0+60	924.584	924.5844	924.5844
0+90	924.585	924.5844	924.5844
1+20	924.586	924.5844	924.5844
1+50	924.584	924.5844	924.5844
1+80	924.584	924.5844	924.5844
2+10	924.583	924.5844	924.5844
2+40	924.585	924.5844	924.5844
2+70	924.585	924.5844	924.5844
3+00	924.584	924.5844	924.5844

EXPERIMENT 22
 Q= 1.558 CFS SPACING= 40 IN. DIAMETER= 1.0 IN.
 N-BAR= 0.01760 N-EFF= 0.01004
 VERTICAL TUBE SUBMERGENCE= 0.774 FT.

LINEAR REGRESSION ELEVATIONS (SVF)
 UPSTREAM= 924.4492 DOWNSTREAM= 924.4490

STATIONS	OBSERVED WATER-SURFACE ELEVATIONS	PROFILE CALCULATED WITH N-BAR	PROFILE CALCULATED WITH N-GVF
0+00	924.448	924.4492	924.4490
0+30	924.450	924.4490	924.4490
0+60	924.449	924.4490	924.4490
0+90	924.449	924.4490	924.4490
1+20	924.451	924.4490	924.4490
1+50	924.449	924.4490	924.4490
1+80	924.448	924.4490	924.4490
2+10	924.448	924.4490	924.4490
2+40	924.450	924.4490	924.4490
2+70	924.450	924.4490	924.4490
3+00	924.448	924.4490	924.4490

EXPERIMENT 23
 Q= 1.303 CFS SPACING= 40 IN. DIAMETER= 1.0 IN.
 N-BAR= 0.01718 N-EFF= 0.00957
 VERTICAL TUBE SUBMERGENCE= 0.617 FT.

LINEAR REGRESSION ELEVATIONS (SVF)
 UPSTREAM= 924.2922 DOWNSTREAM= 924.2920

STATIONS	OBSERVED WATER-SURFACE ELEVATIONS	PROFILE CALCULATED WITH N-BAR	PROFILE CALCULATED WITH N-GVF
0+00	924.291	924.2922	924.2920
0+30	924.293	924.2921	924.2920
0+60	924.292	924.2920	924.2920
0+90	924.292	924.2920	924.2920
1+20	924.294	924.2920	924.2920
1+50	924.292	924.2920	924.2920
1+80	924.291	924.2920	924.2920
2+10	924.291	924.2920	924.2920
2+40	924.293	924.2920	924.2920
2+70	924.293	924.2920	924.2920
3+00	924.291	924.2920	924.2920

EXPERIMENT 24
 Q= 0.985 CFS SPACING= 40 IN. DIAMETER= 1.0 IN.
 N-BAR= 0.01888 N-EFF= 0.01074
 VERTICAL TUBE SUBMERGENCE= 0.488 FT.

LINEAR REGRESSION ELEVATIONS (SVF)
 UPSTREAM= 924.1631 DOWNSTREAM= 924.1625

STATIONS	OBSERVED WATER-SURFACE ELEVATIONS	PROFILE CALCULATED WITH N-BAR	PROFILE CALCULATED WITH N-GVF
0+00	924.161	924.1631	924.1625
0+30	924.164	924.1628	924.1625
0+60	924.162	924.1627	924.1625
0+90	924.165	924.1626	924.1625
1+20	924.165	924.1625	924.1625
1+50	924.162	924.1625	924.1625
1+80	924.162	924.1625	924.1625
2+10	924.162	924.1625	924.1625
2+40	924.163	924.1625	924.1625
2+70	924.164	924.1625	924.1625
3+00	924.161	924.1625	924.1625

EXPERIMENT 25
 Q= 4.225 CFS SPACING= 60 IN. DIAMETER= 2.0 IN.
 N-BAR= 0.01615 N-EFF= 0.00928
 VERTICAL TUBE SUBMERGENCE= 0.791 FT.

LINEAR REGRESSION ELEVATIONS (SVF)
 UPSTREAM= 924.4654 DOWNSTREAM= 924.4662

STATIONS	OBSERVED WATER-SURFACE ELEVATIONS	PROFILE CALCULATED WITH N-BAR	PROFILE CALCULATED WITH N-GVF
0+00	924.467	924.4662	924.4640
0+30	924.465	924.4652	924.4636
0+60	924.465	924.4650	924.4639
0+90	924.465	924.4649	924.4641
1+20	924.465	924.4649	924.4644
1+50	924.466	924.4649	924.4646
1+80	924.465	924.4652	924.4650
2+10	924.467	924.4655	924.4655
2+40	924.466	924.4659	924.4659
2+70	924.467	924.4661	924.4661
3+00	924.466	924.4662	924.4662

EXPERIMENT 26
 Q= 3.305 CFS SPACING= 60 IN. DIAMETER= 2.0 IN.
 N-BAR= 0.01425 N-EFF= 0.00804
 VERTICAL TUBE SUBMERGENCE= 0.620 FT.

LINEAR REGRESSION ELEVATIONS (SVF)
 UPSTREAM= 924.2938 DOWNSTREAM= 924.2956

STATIONS	OBSERVED WATER-SURFACE ELEVATIONS	PROFILE CALCULATED WITH N-BAR	PROFILE CALCULATED WITH N-GVF
0+00	924.293	924.2937	924.2935
0+30	924.294	924.2938	924.2937
0+60	924.295	924.2940	924.2938
0+90	924.294	924.2940	924.2940
1+20	924.295	924.2942	924.2942
1+50	924.295	924.2943	924.2943
1+80	924.295	924.2946	924.2946
2+10	924.295	924.2950	924.2950
2+40	924.295	924.2953	924.2953
2+70	924.296	924.2955	924.2955
3+00	924.295	924.2956	924.2956

EXPERIMENT 27
 Q= 2.249 CFS SPACING= 60 IN. DIAMETER= 2.0 IN.
 N-BAR= 0.01880 N-EFF= 0.01144
 VERTICAL TUBE SUBMERGENCE= 0.835 FT.

LINEAR REGRESSION ELEVATIONS (SVF)
 UPSTREAM= 924.5096 DOWNSTREAM= 924.5104

STATIONS	OBSERVED WATER-SURFACE ELEVATIONS	PROFILE CALCULATED WITH N-BAR	PROFILE CALCULATED WITH N-GVF
0+00	924.509		
0+30	924.509		
0+60	924.509	924.5096	924.5089
0+90	924.510	924.5097	924.5093
1+20	924.510	924.5099	924.5097
1+50	924.511	924.5101	924.5101
1+80	924.510	924.5103	924.5103
2+10	924.510	924.5104	924.5104
2+40	924.510		
2+70	924.510		
3+00	924.509		

EXPERIMENT 28
 Q= 1.650 CFS SPACING= 60 IN. DIAMETER= 2.0 IN.
 N-BAR= 0.01410 N-EFF= 0.00794
 VERTICAL TUBE SUBMERGENCE= 0.613 FT.

LINEAR REGRESSION ELEVATIONS (SVF)
 UPSTREAM= 924.2868 DOWNSTREAM= 924.2881

STATIONS	OBSERVED WATER-SURFACE ELEVATIONS	PROFILE CALCULATED WITH N-BAR	PROFILE CALCULATED WITH N-GVF
0+00	924.287		
0+30	924.287		
0+60	924.287	924.2868	924.2868
0+90	924.287	924.2872	924.2872
1+20	924.287	924.2875	924.2876
1+50	924.288	924.2878	924.2878
1+80	924.288	924.2880	924.2880
2+10	924.288	924.2881	924.2881
2+40	924.288		
2+70	924.288		
3+00	924.288		

EXPERIMENT 29
 Q= 2.508 CFS SPACING= 60 IN. DIAMETER= 1.5 IN.
 N-BAR= 0.01370 N-EFF= 0.00779
 VERTICAL TUBE SUBMERGENCE= 0.815 FT.

LINEAR REGRESSION ELEVATIONS (SVF)
 UPSTREAM= 924.4891 DOWNSTREAM= 924.4903

STATIONS	OBSERVED WATER-SURFACE ELEVATIONS	PROFILE CALCULATED WITH N-BAR	PROFILE CALCULATED WITH N-GVF
0+00	924.489	924.4891	924.4895
0+30	924.490	924.4893	924.4896
0+60	924.489	924.4894	924.4896
0+90	924.489	924.4895	924.4897
1+20	924.490	924.4896	924.4897
1+50	924.490	924.4897	924.4898
1+80	924.489	924.4899	924.4899
2+10	924.490	924.4901	924.4901
2+40	924.490	924.4902	924.4902
2+70	924.490	924.4903	924.4903
3+00	924.491	924.4903	924.4903

EXPERIMENT 30
 Q= 1.650 CFS SPACING= 60 IN. DIAMETER= 1.5 IN.
 N-BAR= 0.01170 N-EFF= 0.00671
 VERTICAL TUBE SUBMERGENCE= 0.537 FT.

LINEAR REGRESSION ELEVATIONS (SVF)
 UPSTREAM= 924.2108 DOWNSTREAM= 924.2119

STATIONS	OBSERVED WATER-SURFACE ELEVATIONS	PROFILE CALCULATED WITH N-BAR	PROFILE CALCULATED WITH N-GVF
0+00	924.210	924.2108	924.2115
0+30	924.212	924.2110	924.2116
0+60	924.211	924.2112	924.2116
0+90	924.211	924.2113	924.2116
1+20	924.212	924.2114	924.2116
1+50	924.211	924.2115	924.2116
1+80	924.211	924.2116	924.2117
2+10	924.211	924.2117	924.2118
2+40	924.212	924.2118	924.2119
2+70	924.212	924.2119	924.2119
3+00	924.212	924.2119	924.2119

EXPERIMENT 31
 Q= 1.099 CFS SPACING= 60 IN. DIAMETER= 1.0 IN.
 N-BAR= N-EFF= 0.00175
 VERTICAL TUBE SUBMERGENCE= 0.830 FT.

LINEAR REGRESSION ELEVATIONS (SVF)
 UPSTREAM= 924.5041 DOWNSTREAM= 924.5048

STATIONS	OBSERVED WATER-SURFACE ELEVATIONS	PROFILE CALCULATED WITH N-BAR	PROFILE CALCULATED WITH N-GVF
0+00	924.503		924.5047
0+30	924.504		924.5047
0+60	924.504		924.5047
0+90	924.505		924.5047
1+20	924.506		924.5047
1+50	924.505		924.5047
1+80	924.504		924.5047
2+10	924.505		924.5047
2+40	924.504		924.5047
2+70	924.505		924.5048
3+00	924.504		924.5048

EXPERIMENT 32
 Q= 3.404 CFS SPACING= 80 IN. DIAMETER= 2.0 IN.
 N-BAR= 0.01547 N-EFF= 0.00874
 VERTICAL TUBE SUBMERGENCE= 0.847 FT.

LINEAR REGRESSION ELEVATIONS (SVF)
 UPSTREAM= 924.5211 DOWNSTREAM= 924.5222

STATIONS	OBSERVED WATER-SURFACE ELEVATIONS	PROFILE CALCULATED WITH N-BAR	PROFILE CALCULATED WITH N-GVF
0+00	924.520	924.5211	924.5202
0+30	924.521	924.5211	924.5204
0+60	924.522	924.5211	924.5206
0+90	924.521	924.5211	924.5208
1+20	924.522	924.5212	924.5210
1+50	924.522	924.5214	924.5212
1+80	924.522	924.5215	924.5214
2+10	924.523	924.5217	924.5217
2+40	924.522	924.5220	924.5219
2+70	924.523	924.5221	924.5221
3+00	924.520	924.5222	924.5222

EXPERIMENT 33
 Q= 2.482 CFS SPACING= 80 IN. DIAMETER= 2.0 IN.
 N-BAR= 0.01435 N-EFF= 0.00805
 VERTICAL TUBE SUBMERGENCE= 0.619 FT.

LINEAR REGRESSION ELEVATIONS (SVF)
 UPSTREAM= 924.2930 DOWNSTREAM= 924.2940

STATIONS	OBSERVED WATER-SURFACE ELEVATIONS	PROFILE CALCULATED WITH N-BAR	PROFILE CALCULATED WITH N-GVF
0+00	924.292	924.2931	924.2921
0+30	924.293	924.2931	924.2924
0+60	924.294	924.2931	924.2926
0+90	924.293	924.2932	924.2928
1+20	924.294	924.2933	924.2930
1+50	924.294	924.2933	924.2932
1+80	924.294	924.2935	924.2934
2+10	924.294	924.2937	924.2936
2+40	924.294	924.2939	924.2938
2+70	924.294	924.2940	924.2940
3+00	924.293	924.2940	924.2940

EXPERIMENT 34
 Q= 1.997 CFS SPACING= 80 IN. DIAMETER= 2.0 IN.
 N-BAR= 0.00980 N-EFF= 0.00552
 VERTICAL TUBE SUBMERGENCE= 0.818 FT.

LINEAR REGRESSION ELEVATIONS (SVF)
 UPSTREAM= 924.4920 DOWNSTREAM= 924.4937

STATIONS	OBSERVED WATER-SURFACE ELEVATIONS	PROFILE CALCULATED WITH N-BAR	PROFILE CALCULATED WITH N-GVF
0+00	924.493		
0+30	924.492		
0+60	924.492	924.4921	924.4925
0+90	924.492	924.4926	924.4928
1+20	924.493	924.4929	924.4931
1+50	924.493	924.4932	924.4933
1+80	924.493	924.4935	924.4935
2+10	924.493	924.4937	924.4937
2+40	924.494	924.4937	924.4937
2+70	924.493		
3+00	924.493		

EXPERIMENT 35
 Q= 1.509 CFS SPACING= 80 IN. DIAMETER= 2.0 IN.
 N-BAR= 0.01610 N-EFF= 0.00909
 VERTICAL TUBE SUBMERGENCE= 0.617 FT.

LINEAR REGRESSION ELEVATIONS (SVF)
 UPSTREAM= 924.2915 DOWNSTREAM= 924.2922

STATIONS	OBSERVED WATER-SURFACE ELEVATIONS	PROFILE CALCULATED WITH N-BAR	PROFILE CALCULATED WITH N-GVF
0+00	924.292		
0+30	924.292		
0+60	924.291	924.2916	924.2914
0+90	924.292	924.2916	924.2915
1+20	924.292	924.2917	924.2917
1+50	924.292	924.2919	924.2919
1+80	924.292	924.2920	924.2920
2+10	924.292	924.2921	924.2921
2+40	924.292	924.2922	924.2922
2+70	924.292		
3+00	924.292		

EXPERIMENT 36
 Q= 1.891 CFS SPACING= 80 IN. DIAMETER= 1.5 IN.
 N-BAR= 0.01610 N-EFF= 0.00932
 VERTICAL TUBE SUBMERGENCE= 0.824 FT.

LINEAR REGRESSION ELEVATIONS (SVF)
 UPSTREAM= 924.4991 DOWNSTREAM= 924.4992

STATIONS	OBSERVED WATER-SURFACE ELEVATIONS	PROFILE CALCULATED WITH N-BAR	PROFILE CALCULATED WITH N-GVF
0+00	924.498	924.4991	924.4985
0+30	924.499	924.4991	924.4986
0+60	924.500	924.4991	924.4988
0+90	924.499	924.4991	924.4988
1+20	924.500	924.4991	924.4989
1+50	924.500	924.4991	924.4990
1+80	924.499	924.4991	924.4990
2+10	924.499	924.4991	924.4991
2+40	924.499	924.4992	924.4992
2+70	924.499	924.4992	924.4992
3+00	924.499	924.4992	924.4992

EXPERIMENT 37
 Q= 1.249 CFS SPACING= 80 IN. DIAMETER= 1.5 IN.
 N-BAR= 0.01680 N-EFF= 0.00957
 VERTICAL TUBE SUBMERGENCE= 0.544 FT.

LINEAR REGRESSION ELEVATIONS (SVF)
 UPSTREAM= 924.2185 DOWNSTREAM= 924.2182

STATIONS	OBSERVED WATER-SURFACE ELEVATIONS	PROFILE CALCULATED WITH N-BAR	PROFILE CALCULATED WITH N-GVF
0+00	924.217	924.2186	924.2181
0+30	924.218	924.2184	924.2181
0+60	924.220	924.2183	924.2181
0+90	924.219	924.2182	924.2181
1+20	924.219	924.2182	924.2181
1+50	924.219	924.2182	924.2181
1+80	924.217	924.2182	924.2181
2+10	924.219	924.2182	924.2181
2+40	924.218	924.2182	924.2182
2+70	924.218	924.2182	924.2182
3+00	924.218	924.2182	924.2182

EXPERIMENT 38
 Q= 1.249 CFS SPACING= 80 IN. DIAMETER= 1.5 IN.
 N-BAR= 0.01530 N-EFF= 0.00875
 VERTICAL TUBE SUBMERGENCE= 0.544 FT.

LINEAR REGRESSION ELEVATIONS (SVF)
 UPSTREAM= 924.2183 DOWNSTREAM= 924.2183

STATIONS	OBSERVED WATER-SURFACE ELEVATIONS	PROFILE CALCULATED WITH N-BAR	PROFILE CALCULATED WITH N-GVF
0+00	924.217	924.2182	924.2181
0+30	924.219	924.2182	924.2181
0+60	924.219	924.2182	924.2181
0+90	924.218	924.2182	924.2181
1+22	924.219	924.2182	924.2181
1+50	924.218	924.2182	924.2181
1+80	924.218	924.2182	924.2181
2+10	924.218	924.2182	924.2182
2+40	924.219	924.2183	924.2183
2+70	924.218	924.2183	924.2183
3+00	924.218	924.2183	924.2183

EXPERIMENT 39
 Q= 0.800 CFS SPACING= 80 IN. DIAMETER= 1.0 IN.
 N-BAR= N-EFF= 0.00731
 VERTICAL TUBE SUBMERGENCE= 0.809 FT.

LINEAR REGRESSION ELEVATIONS (SVF)
 UPSTREAM= 924.4830 DOWNSTREAM= 924.4836

STATIONS	OBSERVED WATER-SURFACE ELEVATIONS	PROFILE CALCULATED WITH N-BAR	PROFILE CALCULATED WITH N-GVF
0+00	924.482		924.4836
0+30	924.483		924.4836
0+60	924.483		924.4836
0+90	924.484		924.4836
1+20	924.484		924.4836
1+50	924.484		924.4836
1+80	924.483		924.4836
2+10	924.484		924.4836
2+40	924.484		924.4836
2+70	924.483		924.4836
3+00	924.483		924.4836

EXPERIMENT 40
 Q= 3.809 CFS SPACING= 40 IN. DIAMETER= 3.0 IN.
 N-BAR= 0.01835 N-EFF= 0.01104
 VERTICAL TUBE SUBMERGENCE= 0.766 FT.

LINEAR REGRESSION ELEVATIONS (SVF)
 UPSTREAM= 924.4317 DOWNSTREAM= 924.4368

STATIONS	OBSERVED WATER-SURFACE ELEVATIONS	PROFILE CALCULATED WITH N-BAR	PROFILE CALCULATED WITH N-GVF
0+00	924.435		
0+30	924.433		
0+60	924.433		
0+90	924.431	924.4317	924.4319
1+20	924.434	924.4341	924.4341
1+50	924.436	924.4359	924.4359
1+80	924.436	924.4368	924.4368
2+10	924.435		
2+40	924.436		
2+70	924.435		

EXPERIMENT 41
 Q= 3.528 CFS SPACING= 40 IN. DIAMETER= 3.0 IN.
 N-BAR= 0.01710 N-EFF= 0.01032
 VERTICAL TUBE SUBMERGENCE= 0.718 FT.

LINEAR REGRESSION ELEVATIONS (SVF)
 UPSTREAM= 924.3837 DOWNSTREAM= 924.3888

STATIONS	OBSERVED WATER-SURFACE ELEVATIONS	PROFILE CALCULATED WITH N-BAR	PROFILE CALCULATED WITH N-GVF
0+00	924.387		
0+30	924.386		
0+60	924.385		
0+90	924.383	924.3837	924.3842
1+20	924.386	924.3861	924.3863
1+50	924.388	924.3880	924.3880
1+80	924.388	924.3888	924.3888
2+10	924.388		
2+40	924.388		
2+70	924.387		

EXPERIMENT 42
 Q= 3.095 CFS SPACING= 40 IN. DIAMETER= 3.0 IN.
 N-BAR= 0.01960 N-EFF= 0.01102
 VERTICAL TUBE SUBMERGENCE= 0.638 FT.

LINEAR REGRESSION ELEVATIONS (SVF)
 UPSTREAM= 924.3038 DOWNSTREAM= 924.3075

STATIONS	OBSERVED WATER-SURFACE ELEVATIONS	PROFILE CALCULATED WITH N-BAR	PROFILE CALCULATED WITH N-GVF
0+00	924.307		
0+30	924.305		
0+60	924.305		
0+90	924.304	924.3040	924.3036
1+20	924.305	924.3054	924.3052
1+50	924.307	924.3067	924.3067
1+80	924.307	924.3075	924.3075
2+10	924.307		
2+40	924.308		
2+70	924.307		

UNRESTRAINED 1
 Q= 3.262 CFS SPACING= 40 IN. DIAMETER= 1.5 IN.
 N-BAR= 0.01570 N-EFF= 0.00891
 VERTICAL TUBE SUBMERGENCE= 0.713 FT.

LINEAR REGRESSION ELEVATIONS (SVF)
 UPSTREAM= 924.3877 DOWNSTREAM= 924.3883

STATIONS	OBSERVED WATER-SURFACE ELEVATIONS	PROFILE CALCULATED WITH N-BAR	PROFILE CALCULATED WITH N-GVF
0+00	924.388	924.3876	924.3864
0+30	924.388	924.3875	924.3866
0+60	924.387	924.3874	924.3868
0+90	924.387	924.3874	924.3869
1+20	924.389	924.3874	924.3871
1+50	924.388	924.3874	924.3873
1+80	924.389	924.3876	924.3876
2+10	924.388	924.3878	924.3878
2+40	924.388	924.3881	924.3881
2+70	924.388	924.3883	924.3883
3+00	924.388	924.3883	924.3883

UNRESTRAINED 2
 Q= 3.242 CFS SPACING= 40 IN. DIAMETER= 1.5 IN.
 N-BAR= 0.01620 N-EFF= 0.00924
 VERTICAL TUBE SUBMERGENCE= 0.793 FT.

LINEAR REGRESSION ELEVATIONS (SVF)
 UPSTREAM= 924.4669 DOWNSTREAM= 924.4679

STATIONS	OBSERVED WATER-SURFACE ELEVATIONS	PROFILE CALCULATED WITH N-BAR	PROFILE CALCULATED WITH N-GVF
0+00	924.468		
0+30	924.466	924.4669	924.4659
0+60	924.467	924.4669	924.4662
0+90	924.467	924.4669	924.4664
1+20	924.468	924.4670	924.4667
1+50	924.468	924.4671	924.4670
1+80	924.469	924.4673	924.4672
2+10	924.468	924.4676	924.4675
2+40	924.467	924.4678	924.4678
2+70	924.467	924.4679	924.4679
3+00	924.467		

UNRESTRAINED 3
 Q= 3.247 CFS SPACING= 40 IN. DIAMETER= 1.5 IN.
 N-BAR= 0.01720 N-EFF= 0.00983
 VERTICAL TUBE SUBMERGENCE= 0.859 FT.

LINEAR REGRESSION ELEVATIONS (SVF)
 UPSTREAM= 924.5335 DOWNSTREAM= 924.5343

STATIONS	OBSERVED WATER-SURFACE ELEVATIONS	PROFILE CALCULATED WITH N-BAR	PROFILE CALCULATED WITH N-GVF
0+00	924.533		
0+30	924.533	924.5335	924.5323
0+60	924.533	924.5334	924.5326
0+90	924.533	924.5334	924.5328
1+20	924.535	924.5334	924.5331
1+50	924.535	924.5335	924.5334
1+80	924.535	924.5337	924.5337
2+10	924.534	924.5340	924.5340
2+40	924.533	924.5342	924.5342
2+70	924.534	924.5343	924.5343
3+00	924.534		

UNRESTRAINED 4
 Q= 2.484 CFS SPACING= 40 IN. DIAMETER= 1.5 IN.
 N-BAR= 0.01595 N-EFF= 0.00969
 VERTICAL TUBE SUBMERGENCE= 0.553 FT.

LINEAR REGRESSION ELEVATIONS (SVF)
 UPSTREAM= 924.2274 DOWNSTREAM= 924.2273

STATIONS	OBSERVED WATER-SURFACE ELEVATIONS	PROFILE CALCULATED WITH N-BAR	PROFILE CALCULATED WITH N-GVF
0+00	924.227	924.2274	924.2264
0+30	924.228	924.2271	924.2264
0+60	924.227	924.2269	924.2265
0+90	924.227	924.2268	924.2265
1+20	924.228	924.2267	924.2265
1+50	924.227	924.2267	924.2266
1+80	924.227	924.2268	924.2267
2+10	924.228	924.2269	924.2270
2+40	924.228	924.2272	924.2273
2+70	924.227	924.2273	924.2274
3+00	924.227	924.2273	924.2274

UNRESTRAINED 5
 Q= 2.505 CFS SPACING= 40 IN. DIAMETER= 1.5 IN.
 N-BAR= 0.01670 N-EFF= 0.00967
 VERTICAL TUBE SUBMERGENCE= 0.646 FT.

LINEAR REGRESSION ELEVATIONS (SVF)
 UPSTREAM= 924.3205 DOWNSTREAM= 924.3202

STATIONS	OBSERVED WATER-SURFACE ELEVATIONS	PROFILE CALCULATED WITH N-BAR	PROFILE CALCULATED WITH N-GVF
0+00	924.321		
0+30	924.320	924.3204	924.3186
0+60	924.320	924.3200	924.3188
0+90	924.321	924.3198	924.3189
1+20	924.321	924.3198	924.3192
1+50	924.320	924.3198	924.3194
1+80	924.320	924.3199	924.3196
2+10	924.321	924.3200	924.3199
2+40	924.321	924.3201	924.3201
2+70	924.319	924.3202	924.3202
3+00	924.320		

UNRESTRAINED 6
 Q= 2.480 CFS SPACING= 40 IN. DIAMETER= 1.5 IN.
 N-BAR= 0.01720 N-EFF= 0.00988
 VERTICAL TUBE SUBMERGENCE= 0.813 FT.

LINEAR REGRESSION ELEVATIONS (SVF)
 UPSTREAM= 924.4869 DOWNSTREAM= 924.4879

STATIONS	OBSERVED WATER-SURFACE ELEVATIONS	PROFILE CALCULATED WITH N-BAR	PROFILE CALCULATED WITH N-GVF
0+00	924.487		
0+30	924.488		
0+60	924.487	924.4870	924.4864
0+90	924.487	924.4870	924.4867
1+20	924.488	924.4871	924.4870
1+50	924.487	924.4873	924.4872
1+80	924.487	924.4876	924.4875
2+10	924.488	924.4878	924.4878
2+40	924.488	924.4879	924.4879
2+70	924.487		
3+00	924.487		

VITA

John Marbrooks Sweeten, Jr.

Candidate for the Degree of

Master of Science

Thesis: THE HYDRAULIC ROUGHNESS OF AN IRRIGATION CHANNEL WITH
DECREASING SPATIALLY VARIED FLOW

Major Field: Agricultural Engineering

Biographical:

Personal Data: Born at Rocksprings, Texas, January 11, 1944,
the son of John M. and Johnnie R. Sweeten.

Education: Graduated from Rocksprings High School in Rocksprings,
Texas, in 1961 as valedictorian of his class; attended Austin
College (Sherman, Texas), the University of Texas, and grad-
uated from Texas Technological College in 1965 with a Bach-
elor of Science in Agricultural Engineering; completed the
requirements for the Master of Science degree in May, 1967.

Professional Experience: Worked as Student Trainee - Agricultural
Engineer for the Soil Conservation Service in the Summer of
1964; Graduate Research Assistant from September, 1965 -
September, 1966 and from February, 1967 - May, 1967, and
Graduate Teaching Assistant from September, 1966 - January,
1967 for the Agricultural Engineering Department of the Okla-
homa State University.

Professional and Honorary Organizations: Corporate member of the
American Society of Agricultural Engineers; member of Alpha
Zeta.